Cintia Bagne Ueta

Papel do hormônio tiroideano no metabolismo

Tese apresentada ao Programa de Pós-Graduação em Endocrinologia Clínica da Escola Paulista de Medicina- Universidade Federal de São Paulo, para a obtenção do Título de Doutor em Ciências

São Paulo
2013

Cintia Bagne Ueta

Papel do hormônio tiroideano no metabolismo

Tese apresentada ao Programa de Pós-Graduação em Endocrinologia Clínica da Escola Paulista de Medicina- Universidade Federal de São Paulo, para a obtenção do Título de Doutor em Ciências

Orientador:
Prof. Dr. Antonio Carlos Bianco

Coordenador do Programa de Pós-Graduação
Profa. Regina Célia Mello Santiago Moisé

Pró-Reitor de Pesquisa e Pós-Graduação
Prof. Reinaldo Salomão

São Paulo
2013

DEDICATÓRIA

Dedico esta tese aos meus pais com todo carinho e amor incondicional, por serem meus exemplos de vida, coragem, luta e determinação.

AGRADECIMENTOS

Finalizada uma etapa particularmente importante da minha vida, não poderia deixar de expressar o mais profundo agradecimento a todos aqueles que fizeram parte dela durante esses quase quatro anos nos Estados Unidos. Obrigada a todos os amigos que conheci mundo afora, a todos os que me apoiaram nesta longa caminhada, bem como aos que contribuíram para a realização deste trabalho.

A Deus, pois o que seria de mim sem a Tua presença diária na minha vida, me protegendo e guiando.

Ao meu orientador, Antonio Carlos Bianco, que teve um papel fundamental na realização desse trabalho. Obrigada pela dedicação, paciência, ensinamentos e, acima de tudo, por compreender minhas limitações. Agradeço sua presença constante, orientando minha vida acadêmica e profissional e me incentivando durante meu doutorado. Aqui expresso meu maior agradecimento pela oportunidade de trabalhar com o senhor a quem declaro a minha admiração.

To the professor and friend, Dr. Brian Kim, with I worked with in the last year of my phD. Thanks for the lessons, teachings, advice and suggestions that were so important for me.

Aos meus pais, Ademar e Elizabeth, pela educação baseada na simplicidade, no amor e no conceito de família, cujos princípios e valores me transformaram em tudo o que sou. Sem o apoio de vocês nada disso seria possível. Amo muito vocês!!!

À minha irmã, Gizela, pelos conselhos, risadas, apoio e incentivo. Obrigada por ser essa irmã maravilhosa com quem eu posso contar todas as horas.

Ao meu namorado, João Bosco, pelo carinho, amizade, amor e apoio.

À professora Miriam Oliveira Ribeiro, cujos ensinamentos, conselhos e apoio, durante meu mestrado, foram fundamentais para meu amadurecimento na fase do doutorado.

To a great friend I had the pleasure to meet, Gordana. Thanks for the talk, coffee and for been with me always.

To my co-workers in lab and in the University of Miami: Jessica Hall, Matt Rosene, Emerson Olivares, Melany Castillo, Liping Dong, SungRo Jo, Latoya, Tatiana Fonseca, Joel Jundi, Barry Hudson, João Pedro, Behzad Oskouie, José Renato.

À secretária da Pós-Graduação em Endocrinologia Clínica, Yeda, que me ajudou muito.

À minha querida amiga Suelena por ter cuidadosamente revisado esta tese.

EPÍGRAFE

“Tenho a impressão de ter sido uma criança brincando à beira-mar, divertindo-me em descobrir uma pedrinha mais lisa ou uma concha mais bonita que as outras, enquanto o imenso oceano da verdade continua misterioso diante de meus olhos”
Isaac Newton

“A imaginação é mais importante que a ciência, porque a ciência é limitada, ao passo que a imaginação abrange o mundo inteiro”
Albert Einstein

RESUMO

Um conceito bem estabelecido da ação do hormônio tiroideano é que as desiodases controlam a sinalização do hormônio tiroideano de forma tecido-específico, independente das concentrações plasmáticas do hormônio. As desiodases (D1, D2 e D3) são selenoproteínas, cuja síntese requer um tRNA específico (sec-tRNA) e sua isoprenilação, i.e., a incorporação de selenocisteínas necessária para a função normal dessas proteínas. As estatinas, inibidores da hidroxi-metil-glutaril CoA redutase, diminuem a síntese das selenoproteínas via interrupção da isoprenilação, porém pouco é sabido sobre seus efeitos na síntese da D2, a desiodase que ativa o T4 em T3. Mostramos que o tratamento de células ou animais com estatinas ou inibidores da isoprenil transferase aumenta a atividade da D2; os efeitos dos inibidores da isoprenil transferase são através de mecanismos pós-transcricionais. O T3, que é ativado pela D2, desempenha um importante papel no gasto energético. Para definir o papel metabólico desempenhado pelo T3, na dissipação de calorias da dieta, camundongos hipotiroideos, foram estudados por 60 dias num sistema metabólico. Na temperatura ambiente, camundongos hipotiroideos diminuem o programa termogênico do músculo esquelético, mas não do BAT, sem afetar o gasto energético. Somente à termoneutralidade, camundongos hipotiroideos exibem menor gasto energético. O subproduto desse mecanismo compensatório é que, à temperatura ambiente, camundongos hipotiroideos estão protegidos da obesidade induzida pela dieta, um mecanismo que é perdido à termoneutralidade. Em contraste, a ação do T3 é inibida pela D3, como no caso do infarto do miocárdio. Sendo que o gene da D3 (*Dio3*) é “imprinted”, mostramos aqui que camundongos heterozigotos knockout para *Dio3* (HtzD3KO) são eutiroideos e constituem um modelo de inativação isolada da D3 cardíaca. HtzD3KO adultos desenvolvem cardiomiopatia restritiva, incluindo fibrose, prejuízo na contração do miocárdio e disfunção diastólica. O tratamento com isoproterenol (ISO) induz a atividade da D3 no miocárdio, com remodelamento e dilatação cardíaca nos animais controle. Entretanto, camundongos HtzD3KO tratados com ISO apresentam remodelação cardíaca patológica, resultando em insuficiência cardíaca congestiva e aumento da mortalidade. Portanto, esta tese apresenta dados para compreender os mecanismos que regulam a expressão da D2 e sua relevância biológica no fornecimento de T3 para os tecidos, bem como entender o papel da D3 na função e remodelamento cardíaco, que pode ter implicações patofisiológicas para a cardiomiopatia de humanos.

ABSTRACT

A well-established concept of thyroid hormone action holds that deiodinases control tissue-specific thyroid hormone signaling, regardless of plasma hormone concentration. Deiodinases (D1, D2 and D3) are selenoproteins that require a specific tRNA (sec-tRNA) and isoprenilation, selenocysteine incorporation for their synthesis. Statins, inhibitors of the hydroxyl-methyl-glutaryl-coenzyme A reductase have been shown to down-regulate selenoproteins via interruption of isoprenilation. However, little is known about the effect of statins on D2. We report that cells and animals treated with statins and isoprenyl transferase inhibitors increase D2 activity; the effects of isoprenyl transferase inhibitors are via posttranscriptional mechanism. D2-generated T3 plays an important role in the energy expenditure (EE). To define the metabolic role played by T3 in the dissipation of calories from diet, hypothyroid mice were studied for 60 days in a metabolic system. At room temperature, hypothyroid mice decreased skeletal muscle, but not BAT thermogenic programs, without affecting EE. Only at thermoneutrality did hypothyroid mice exhibit slower EE. A byproduct of this mechanism is that at room temperature, hypothyroid mice are protected against diet-induced obesity, i.e. at thermoneutrality they become obese. Cardiac injury induces myocardial expression of D3, which in turn dampens local T3 signaling. Since D3 gene (*Dio3*) is an imprinted gene, here we show that heterozygous D3 knockout (HtzD3KO) mice are euthyroid and constitute a model of cardiac D3 inactivation. Adult HtzD3KO developed restrictive cardiomyopathy, including myocardial fibrosis, impaired myocardial contractility, and diastolic dysfunction. In wild-type littermates, treatment with isoproterenol (ISO)-induced myocardial D3 activity, with cardiac remodeling and dilation. Remarkable, ISO treated HtzD3KO mice exhibited a worse diastolic dysfunction and restrictive cardiomyopathy, resulting in congestive heart failure and increased mortality. The data presented in this thesis helps to better understand the mechanisms that regulate D2 expression and it biological relevance as source of T3 for the tissues and to understand the crucial roles for D3 in the heart function and remodeling, which may have pathophysiologic implication for human restrictive cardiomyopathy.

SUMÁRIO

CAPÍTULO 1

I. Introdução Geral

A tiroxina (T4) é o principal produto secretado pela glândula tiróide enquanto que a forma biologicamente ativa, 5,3,3'-triiodotironina (T3), é secretada em menor quantidade, sendo produzida em grande parte através do metabolismo extratiroideano do T4. O T3 é uma molécula metabolicamente ativa que acelera a oxidação dos substratos através de inúmeros processos celulares que são relevantes para a homeostase energética. Além do papel energético, o hormônio tiroideano também exerce papel fundamental no coração, músculo esquelético, sistema nervoso central e em outros tecidos.

1. Desiodases

Um conceito bem estabelecido da ação do hormônio tiroideano é que sua sinalização é controlada de maneira tecido-específico pelas desiodases, independentemente das concentrações plasmáticas dos mesmos (1). O T4 é considerado um pró-hormônio e deve ser ativado a T3, através da remoção do iodo na posição 5' do anel fenólico ou externo da molécula. Essa reação é catalizada pelas desiodases de iodotironina do tipo 1 (D1) e do tipo 2 (D2), entretanto a D2 tem ~1.000 vezes maior afinidade pelo T4 que a D1 (2) (Figura 1). Ao mesmo tempo, tanto o T4 quanto o T3 podem ser inativados através de um processo onde ocorre a remoção do iodo da posição 5' do anel interno tirosil, resultando em 3,5'3'-triiodotironina (rT3) e 3,3'-diiodotironina (T2), respectivamente. Essa reação é catalizada pela desiodase de iodotironina do tipo 3 (D3) e D1 (Figura 1) (2).

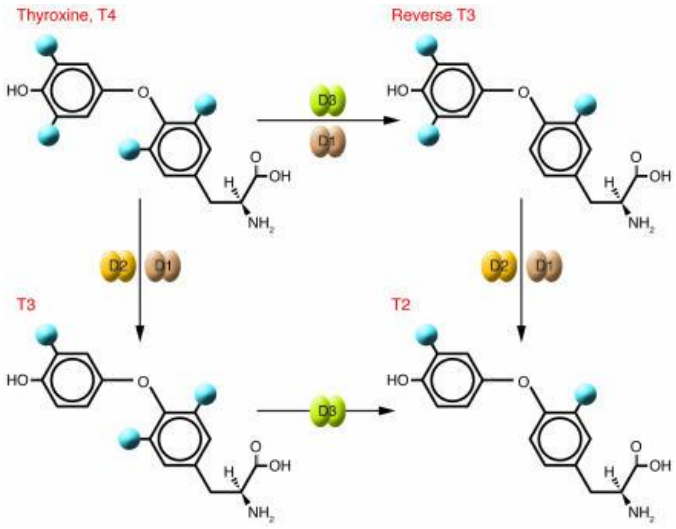

Figura 1. Mecanismo de ação das Desiodases. As reações catalisadas pelas desiodases removem o iodo (círculo azul) dos anéis fenólicos (anel externo) ou tirosil (anel interno) das iodotironinas. Estas vias podem ativar o T4 pela transformação deste a T3 (via D1 ou D2) ou prevenindo este de ser ativado pela conversão deste à forma metabolicamente inativa, reverso T3 (via D1 ou D3). T2 é um produto inativo comum para ambas as vias que é rapidamente metabolizado pela desiodação adicional (3).

As desiodases são selenoproteínas que tem um aminoácido raro, a selenocisteína, no seu centro ativo (2). O códon UGA, que normalmente funciona como STOP códon, é interpretado como selenocisteína graças ao *loop*, uma estrutura chamada sequência de inserção de selenocisteína (do inglês: *Selenoprotein Insertion Sequence*, SECIS) localizada na terminação 3' do mRNA da D2. Essa sequência associa-se à proteína ligadora da SECIS (do inglês: *SECIS Binding Protein 2*, SBP-2) (4), a qual interage com um tRNA (sec-tRNA) carregado com selenocisteína. A síntese de selenoproteínas é dependente da entrega deste sec-tRNA para seu respectivo códon na região ribossomal pelos fatores de alongamento, EF1 e EF2, formando um complexo tRNA-EF (5). A presença dos complexos *stem loop* e tRNA-EF no códon UGA faz com que este codifique para a incorporação de selenocisteínas nas células de mamíferos (Figura 2) (6). A substituição da selenocisteína por cisteína diminui de 2 a 3 ordens de magnitude a afinidade da D2 pelo T4 e da D3 pelo T3 (2).

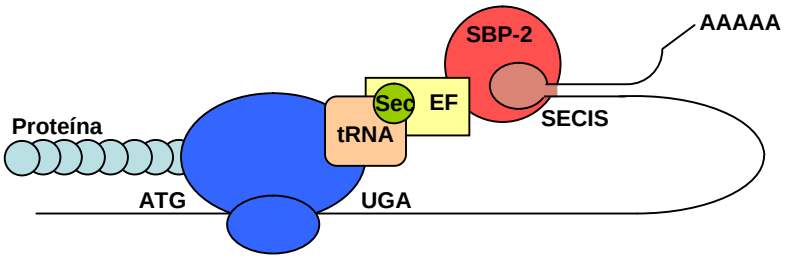

Figura 2. Esquema da síntese de Selenoproteínas. A fim de que UGA codifique selenocisteína e não para o término da tradução, o RNAm da selenoproteína exige uma estrutura *stem loop* na SECIS. O SBP-2 interage com o EF, que interage com o sec-tRNA e promove a incorporação da selenocisteína na proteína de alongamento pelo ribossomo no códon UGA. Modificado de (4).

Para a sua função normal, o sec-tRNA deve ser isoprenilado, isto é, deve receber um radical isoprenil no nucleotídeo adenina vizinho da terminação 3' do anticódon, na posição 37, criando isopreniladenina (7, 8). A isoprenilação deficiente do sec-tRNA em camundongos diminui a síntese de selenoproteínas (9, 10). Em 1980, estudos da biosíntese de colesterol levaram a descoberta de um componente derivado do ácido mavalônico, diferente do colesterol, que é incorporado dentro de uma proteína específica contendo cisteína ligada aos grupos farnesil e geranilgeranil (11) A isoprenilação enzimática do sec-tRNA exige a síntese de pirofosfato de isopentenil (IPP) (12), um metabólito gerado pelo mevalonato (MLL) na via de síntese do colesterol. Em seguida, o IPP é transformado em pirofosfato de farnesil (FPP) e em pirofosfato de geranil (GPP), sendo que ambos podem ser utilizados na isoprenilação. O IPP é um substrato limitante da farnesil pirofosfato sintetase (envolvido com a biosíntese de esteróides) e da tRNA isoprenil transferase (13, 14) (Figura 3).

As estatinas são inibem a enzima chave hidroxi-metil-glutaril-CoA (HMG-CoA) redutase, responsável pela conversão da HMG-CoA a mevalonato e o IPP (15, 16), um precursor da via de síntese de colesterol. Muitos estudos tem realçado os efeitos das estatinas, além da redução dos riscos de doenças cardiovasculares, também podem ter efeitos antiinflamatórios. Recentemente, tem crescido o interesse nos benefícios clínicos das estatinas não diretamente relacionados com a ação hipolipemiantes. Considerando-se essas evidências, poderia-se assumir que as estatinas interferem com a isoprenilação do Sec-tRNA pela redução do IPP, consequentemente levando à redução das selenoproteínas. Entretanto, mostramos que as estatinas e os inibidores da isoprenil transferase, na verdade, aumentam a atividade da D2 em células que expressam D2 endógena e no BAT de camundongos. Apesar de aumentar a

atividade da D2, os inibidores da isoprenil transferase não aumentaram os níveis de RNAm da D2, indicando um possível mecanismo pós-transcricional (17).

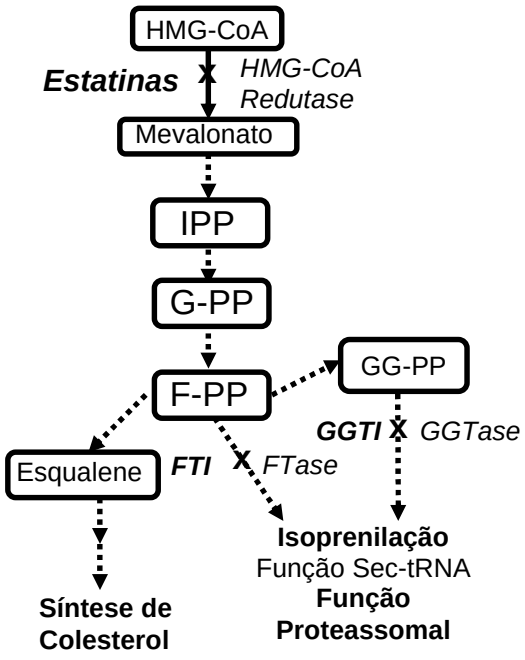

Figura 3. As vias de biosíntese do colesterol e das selenoproteínas. As estatinas inibem a enzima HMG-CoA redutase, que reduz a síntese de colesterol e secundariamente ocorre inibição dos isoprenóides. Isto leva a um prejuízo em várias vias, incluindo a isoprenilação da selenocisteína tRNA, que também é afetada pelos inibidores da isoprenil transferase: FTI e GGTI. GG-PP, geranilgeranil pirofosfato; FTI, inibidor da farnesil transferase e GGTI, inibidor da geranilgeranil transferase. Modificado de (17).

As três desiodases são proteínas de membrana com peso molecular de 29-33 KDa e que apresentam alta homologia (~50% de identidade) (18-21). As três desiodases contêm a dobra do tipo tioredoxina (do inglês: *thioredoxin-fold*, TRX), composta por grupos do tipo βαβ e ββα (19). Esse domínio TRX é interrompido pelo sítio de ligação do substrato da enzima lisossomal α-L-iduronidase (IDUA) (19), fazendo com que o core básico das desiodases seja definido pelos motivos β1-α1-β2 do *TRX-fold* e pelo elemento IDUA (22).

As três desiodases apresentam-se na forma de homodímero. Estudos em modelos celulares com expressão transitória das desiodases e utilizando-se de imunoprecipitação seletiva e eletroforese não desnaturante mostraram a existência dos dímeros de D1, D2 e D3 (23). Somente na forma dimérica as desiodases possuem atividade catalítica.

1.1 Desiodase de iodotironina do tipo 1 (D1)

A primeira desiodase a ser reconhecida por ensaios bioquímicos de conversão de T4 a T3 foi a D1 (1). A D1 é uma enzima que apresenta Km para o T4 de 1μM e Km para rT3 de 0.5 μM e uma meia-vida de aproximadamente 8h (1, 2, 18, 19). A D1 é a única dentre estas enzimas com a capacidade de catalisar a desiodação do anel interno e do anel externo das iodotironinas (24, 25). Além disso, a D1 apresenta uma sensibilidade à inibição por propiltiouracil (PTU). A D1 é expressa no fígado, rins, hipófise, tiroide, intestino e placenta (26), sendo que em humanos está ausente no sistema nervoso central (SNC) (27). Os níveis de RNAm para a D1 no fígado de ratos e camundongos são aumentados pelo T3 (28).

As iodotironinas estão sujeitas a conjugação do grupo hidroxil no anel externo com o ácido glucorônico ou com um sulfato, uma reação que inativa e que também muda a afinidade pelas desiodases. Estudos em hepatócitos isolados de ratos indicaram que o T3 é metabolizado em três vias (29): 1) glucoronização (T3 → T3G); 2) desiodação do anel interno (IRD) seguida pela sucessiva sulfatação e desiodação do anel externo (ORD) (T3 → 3,3'-T2 → 3,3'-T2S → I^-); e 3) a sulfatação, rapidamente seguida pela sucessiva IRD e ORD (T3 → T3S → 3,3'T2S → I^-). Então, as iodotironinas glucoronizadas são excretadas na bile e eliminadas através das fezes ou recicladas no ciclo entero-hepático, enquanto que iodotironinas sulfatadas são desiodadas rapidamente. A sulfatação é uma forma de inativar o hormônio tiroideano: T3S não se liga aos receptores de T3 e isto impede sua ação em vários sistemas celulares (30). As sulfotransferases são enzimas citoplasmáticas solúveis que são expressas em vários tecidos, como, por exemplo, fígado e rins (31). Embora a D2 e a D3 não processam o T4 e o T3 sulfatados, como substrato, a desiodação mediada pela D1 é acelerada após a sulfatação destes substratos. A desiodação do anel externo do T4 e do T3 pela D1 aumentam em ~200 vezes e ~40 vezes, respectivamente (32). O papel da D1 no metabolismo e na eliminação das iodotironinas sulfatadas é bem evidenciado em camundongos com deleção da D1, que apresentam uma mudança na excreção de iodotironinas da urina para as fezes (33).

1.2 Desiodase de iodotironina do tipo 2 (D2)

A D2 é uma selenodesiodase do anel externo, que cataliza a ativação do T4 para T3, aumentando a ação local do hormônio tiroideano. A D2 é uma proteína localizada na face citoplasmática do retículo endoplasmático (34), que fornece T3 ao núcleo (35), tendo um Km para T4 e rT3 de 1nM (19). A D2 é encontrada na hipófise, cérebro e tecido adiposo marrom (BAT) de ratos (36-41); em humanos, na tiroide, coração, cérebro, medula espinhal, músculo esquelético e placenta (20, 42-44).

A D2 exibe uma meia-vida de aproximadamente 20-40 min, em função de ser substrato do sistema ubiquitina-proteassomal, i.e. a ubiquitinação inativa a D2, tornando-a alvo da degradação no proteassomo (45-49). A exposição de células ao MG-132, um inibidor do sistema de proteasomes, aumenta a atividade da D2 (47). A maquinaria de ubiquitinação é constituída por enzimas de complexos inespecíficos (E1 e E2) e uma proteína chamada WSB-1 (do inglês: *WD-40-repeat SOCS-box-containing protein 1*) que é o componente do complexo E3 que interage com a D2 através de um *loop* específico que confere instabilidade a D2 (50-52). Estruturalmente, esta proteína contém sete repetições de WD-40 que forma uma estrutura β-hélice, medeiando a interação com proteínas (53, 54). Além disso, o WSB-1 contém um supressor da sinalização de citocinas (SOCS) box na região carboxi terminal, o que faz dessa proteína um componente do complexo E3 que interage com a D2 (53). Da mesma forma, a D2 pode ser desubiquitinada pelas proteínas chamadas protease específica de ubiquitina (do inglêa, *ubiquitin specific protease*, USP 33 e USP20), constituindo um importante passo regulatório da função protéica em diferentes processos fisiológicos (55).

1.3 Desiodase de iodotironina do tipo 3 (D3)

A D3 inativa tanto o T4 (a rT3) quanto o T3 (a T2) através da desiodação do anel interno da molécula, minimizando as ações do hormônio tiroideano (2) em tecidos específicos. Neste sentido, pode-se assumir que a D3 desempenha um importante papel no controle local da ação do hormônio tiroideano. A D3 apresenta um Km para o T3 de 1 nM e para o T4 de 40 nM (82) e tem meia-vida de aproximadamente 12 h (19). A D3 é expressa universalmente durante o período embrionário e após o nascimento está localizada no SNC, pele e placenta (32), sendo que em outros tecidos sua expressão é baixa ou quase indetectável. Entretanto, o

dano/lesão tecidual e processos inflamatórios podem levar a indução da D3 em certos tecidos, que normalmente não expressam D3. A reativação da D3 é parte de um mecanismo sensível ao fator indutor de hipóxia-1α (do inglês, *hypoxia-inducible factor 1α*, HIF-1α), o qual aumenta em resposta a hipóxia, lesão ou isquemia, como, por exemplo, hipóxia cerebral ou miocárdica (56).

A D3 é codificada pelo gene do *Dio*3 (57) e é a única entre as desiodases cujo gene é "imprinted". Este é um processo em que o gene é expresso ou reprimido dependendo de sua origem materna ou paterna. O imprinting genômico é decorrente de um evento epigenético, onde os alelos gênicos podem ser marcados por modificações que controlam a expressão genética como, por exemplo. a metilação do DNA (58). Apesar dos dois alelos gênicos terem a mesma sequência genética, nos genes "imprinted" as modificações epinegéticas fazem com que apenas um dos alelos seja predominantemente expresso: para alguns desses genes, o alelo materno é expresso, enquanto que, para outros, o alelo paterno é expresso (59-61), e este padrão pode ser tecido específico. Por exemplo, nós demonstramos que no coração de camundongos o imprinting do *Dio*3 é paterno e que este imprinting é tecido específico, uma vez que os cérebros destes animais apresentam atividade normal da D3 (62, 63).

O imprinting está envolvido em uma série de processos durante o desenvolvimento, capazes de afetar o crescimento e a diferenciação de alguns tecidos e em processos que modulam as funções neurologógicas e metabólicas pós-natal (64, 65). Estudos em camundongos têm indicado que o domínio *Dlk-1-Dio3* é importante numa séries de funções biológicas, como, por exemplo, crescimento relacionado com defeitos na ossificação endocondral, desenvolvimento do músculo esquelético (66), set point de inserção do TRH (62, 67) e metabolismo energético (68). A sequência gênica delineada entre o gene homólogo delta do tipo 1 (do inglês, *delta-like 1 homolog,* Dlk1) e o gene do *Dio*3 (*Dlk1-Dio*3) (62, 69-71), está posicionada no cromossomo 12 distal de camundongos e cromossomo 14 de humanos (71). Esse domínio contêm três genes codificadores de proteína expressos no alelo paterno e que dividem o mesmo elemento regulatório: o gene Dlk1, o gene retrotransposon do tipo 1 (do inglês, *retrotransposon-like gene*, Rtl1) e o gene *Dio* 3 (Figura 4) (72).

2. Ações dos hormônios tiroideanos

Ao nível celular, o hormônio tiroideano exerce seu efeito fisiológico se ligando a receptores nucleares específicos (TR) α e β, que são amplamente distribuídos pelo corpo (73). Assim sendo, a sinalização do hormônio tiroideano depende dos níveis de saturação dos TRs, que são determinadas pela afinidade dos TRs pelo T3 e da concentração de T3 no núcleo. Além do mais, as concentrações de T3 intracelular são controladas por dois mecanismos locais. O primeiro é a entrada para a célula através de transportadores específicos de T4 e T3 localizados na membrana plasmática (74). O segundo mecanismo é o controle das concentrações de T3 pela D2 e D3. A importância dos transportadores de hormônio tiroideano é bem ilustrada pelo fenótipo severo causado pelas mutações no gene do transportador monocarboxilase 8 (do inglês, *monocarboxylate TH transporter-8*, MCT8), o qual inclui vários níveis de retardo mental e a falta de desenvolvimento da fala, hipotonia muscular e disfunção endócrina (75, 76). A ausência do gene do MCT8 em camundongos (Mct8KO) também prejudica a captação de hormônio tiroideano no cérebro e resulta em alterações nos níveis plasmáticos de hormônio tiroideano, perfil característico em humanos com mutação do MCT8 (77). Um mecanismo compensatório provável para a falta do MCT8 envolve a elevação da atividade da D2. Apesar dos níveis plasmáticos de T3 promoverem um sinal homogêneo para todos os tecidos, a sinalização resultante do hormônio tiroideano não é homogênea. Mudanças na atividade das desiodases podem modificar a ação do T3 em resposta a diferentes moléculas ou vias de sinalização tais como sinais ambientais, i.e. frio (78) ou hipóxia (79).

2.1 Efeitos no desenvolvimento

Como durante o desenvolvimento fetal ocorrem rápida proliferação e diferenciação celular, os níveis adequados de hormônio tiroideano são importantes para coordenar os processos de desenvolvimento em todos os vertebrados. Durante a embriogênese, a disponibilidade do hormônio tiroideano controla o balanço entre proliferação e diferenciação através do controle da expressão gênica. De uma forma geral, o T3 atenua a proliferação e promove diferenciação celular (80, 81).

Durante a embriogênese, a D3 é crítica para a homeostase do hormônio tiroideano, por estar relacionada em impedir a formação de tecidos expostos a inadequados níveis do mesmo. Da mesma forma, a expressão da D2 também é fundamental durante o período do desenvolvimento. No cérebro de ratos, a D2 aumenta rapidamente depois do nascimento, alcançando altos níveis perto do dia 28 e, então, níveis de adultos pelo dia 50 (82).

Durante o seu desenvolvimento, os níveis de D3 são inversamente coordenados com a D2; então, a sinalização do hormônio tiroideano em um dado tecido pode ser controlada de acordo com o estágio de desenvolvimento (83). Por exemplo, em um período de 3 dias durante o qual o tecido adiposo marrom (BAT) é formado (E 16.5-18.5), há uma diminuição simultânea da D3 e um aumento da D2, aumentando a concentração local de T3 e a sinalização do hormônio tiroideano (84).

A relevância fisiológica da D3, durante o desenvolvimento, foi estudada em camundongos com deficiência da D3 (D3KO). Animais D3KO são expostos a altos níveis de T3 durante a vida fetal e neonatal, que são críticos para a maturação do eixo hipotálamo-hipófise-tiróide (HPT). Como resultado, os animais D3KO apresentam um complexo fenótipo que incluem letalidade embrionária, moderado grau de hipotiroidismo, consequência de defeitos na regulação do eixo HPT, além de retardo no crescimento e infertilidade (67).

2.2 Efeitos na termogênesis

Animais homeotérmicos têm a capacidade de controlar sua temperatura corporal independente do meio ambiente, o que representa uma característica de suma importância evolutiva. Nos animais homeotérmicos, o hormônio tiroideano promove a produção de calor, a termogênese (85, 86). Assim sendo, pacientes hipotiroideos são intolerantes ao frio e podem ter hipotermia e o contrário é observado durante a tirotoxicose. A taxa metabólica basal é definida como o gasto energético mínimo necessário para sustentar as funções homeostáticas em repouso e à temperatura ambiente. Nessas condições, a manutenção do pool de ATP, que é o combustível para o gasto energético basal, resulta em produção de substancial calor, que é chamada termogênesis obrigatória. A produção de calor é explicada pela ineficiência termodinâmica intrínseca da transformação de energia. O calor derivado do aumento da taxa metabólica é conhecido como termogênese adaptativa, que ocorre em resposta ao frio, dietas hipercalóricas, atividade física, entre outros (87).

Pode-se definir a zona de termoneutralidade como à temperatura ambiente em que a termogênese obrigatória é suficiente para manter a temperatura corporal de 37ºC sem a participação de nenhum outro mecanismo termorregulador. Assim sendo, a taxa metabólica basal é fortemente influenciada pelo tamanho do animal uma vez que pequenas espécies perdem muito calor para o ambiente devido a sua alta relação superfície-volume. Surpreendentemente, pouco é sabido sobre os mecanismos moleculares e celulares mediando o aumento do gasto energético pelo hormônio tiroideano. A lista de genes envolvidos no controle do metabolismo energético que são responsivos ao T3 é muito curta. Entretanto, admite-se que, no músculo esquelético, esses genes codifiquem proteínas que diminuem a eficiência da síntese de ATP e/ou aumentem a taxa de turnover do ATP.

A termogênese adaptativa pode ser induzida pelo frio ou pela dieta hipercalórica que serão discutidos a seguir.

A) Termogênese adaptativa induzida pelo frio

Animais homeotérmicos, incluindo mamíferos, exibem um controle sobre a taxa de gasto energético e na termogênesis, adaptando-se bem à maioria dos ambientes terrestres que representam um desafio térmico. Para pequenos roedores, tais como ratos e camundongos, à temperatura ambiente (i.e. 18-22ºC) representa um significativo stress térmico, o qual exige a aceleração do gasto energético e da termogênesis para manter a temperatura corporal (88, 89).

Durante a aclimatação ao frio, o hipotálamo inicia a termogênese adaptativa induzida pelo frio por um mecanismo involuntário que é o tremor muscular. Porém, esse tremor muscular ocasiona perda de calor por convecção devido a oscilações corpóreas e é, consequentemente, uma forma menos econômica de gerar calor. Isso é especialmente válido para mamíferos pequenos e seres humanos recém-nascidos, que apresentam alta razão de área de superfície da massa corporal. Por esse motivo, a termogênese que não envolve tremorigênese (ou tremor muscular) é a principal fonte de calor em mamíferos de pequeno porte (85). Entretanto, em grandes mamíferos, como humanos, esse mecanismo é importante devido à grande quantidade de músculo esquelético (SKM).

Em pequenos roedores e seres humanos recém-nascidos, o principal tecido envolvido na termogênesis adaptativa é o tecido adiposo marrom (BAT). A termogênese adaptativa no

BAT se inicia no hipotálamo através da ativação do sistema nervoso simpático (SNS), liberando noradrenalina que estimula os receptores adrenérgicos β (90, 91) com consequente produção de AMPc. O aumento do AMPc acelera rapidamente a lipólise, e o aumento dos ácidos graxos livres iniciam a produção de calor através da proteína desacopladora 1 (UCP-1), uma proteína mitocondrial que promove o retorno de prótons da membrana interna para a matriz mitocondrial sem que haja produção de ATP; desacoplando o combustível oxidativo da fosforilação do ADP (92-94) (Figura 5).

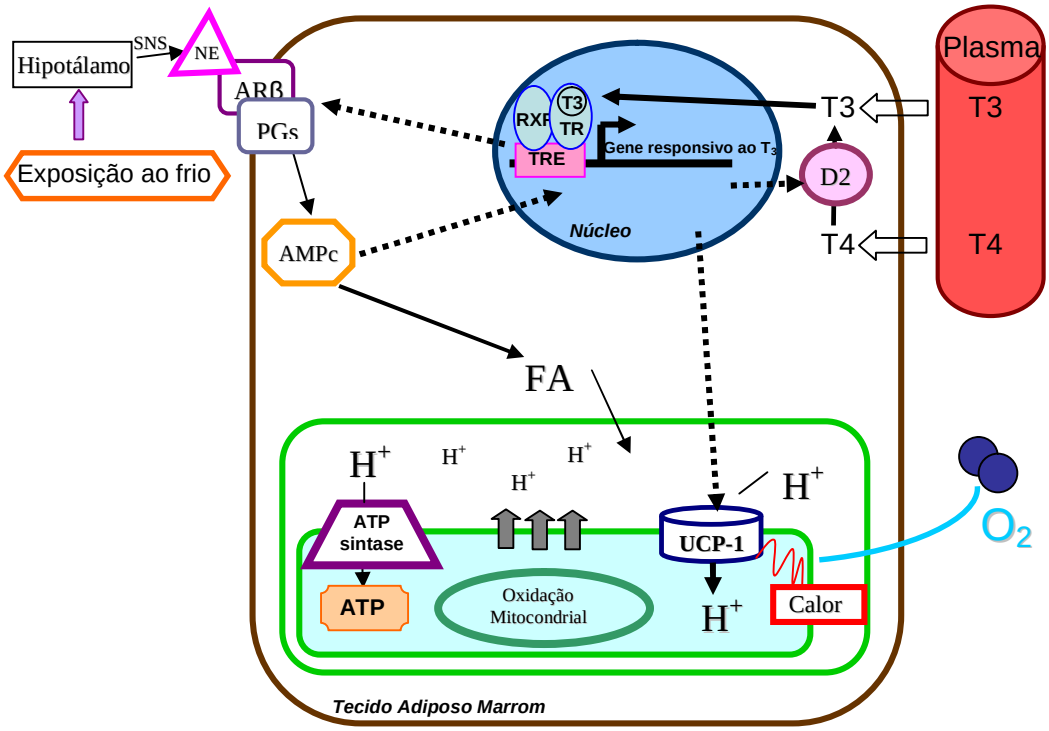

Figura 5. Mecanismo de geração de T3 através da D2 no tecido adiposo marrom. O adipócito marrom é estimulado pela noradrenalina (NE) liberado das terminações simpáticas no BAT. A NE interage com os receptores adrenérgicos β (ARβ) que aumentam os níveis de AMPc. Este ativa a quebra dos triglicérides (lipólise) em ácidos graxos (FA) e a expressão de uma série de genes dependentes de AMPc, chamados UCP-1, D2 e genes envolvidos na via de sinalização adrenérgica. As concentrações de T3 intracelular aumentam como resultado da ativação pela D2. O T3 também aumenta a expressão de genes envolvidos no gasto energético e na termogênese. Modificado de (95).

O adipócito marrom constitui um exemplo único da complexa interação sinergística entre o T3 e o SNS, regulando a expressão de vários genes, incluindo o gene da UCP-1 (96). A estimulação do SNS no BAT aumenta em ~50 vezes a D2 induzida pelo AMPc, mediando a saturação dos TRs pelo T3. A importância da produção de T3 dependente de D2 é demonstrada em camundongos com deleção do gene da D2 (D2KO), que apresentam um

prejuízo na termogênese do BAT e desenvolvem hipotermia durante exposição ao frio (95, 97). Além disso, a análise da expressão gênica indica que a expressão de muitos genes envolvidos no gasto energético, mas não o gene da UCP-1, é alterado no adipócito marrom do D2KO, mostrando que a produção de T3 dependente da D2 é independente da UCP-1 (85). Animais D2KO podem sobreviver ao frio somente devido ao aumento da atividade simpática no BAT (97). Entretanto, o BAT hipotiroideo é menos responsivo à estimulação dos receptores adrenérgicos e falham em aumentar o AMPc normalmente (98-100). Como resultado, mamíferos hipotiroideos, inclusive roedores e seres humanos expostos ao frio, tornam-se profundamente hipotérmicos, devido à falha em ativar a termogênese adaptativa no BAT (78, 101).

Além do mecanismo compensatório entre o T3 e o SNS, também deve-se levar em consideração a existência de mecanismos alternativos para a termogênese adaptativa. A evidência que sustenta que o BAT não é o único local onde ocorre a termogênese facultativa, vem de observações feitas em animais *knockout* para a UCP-1. Esses animais são intolerantes ao frio em temperatura ambiente (94) que é revertida quando estes animais são expostos ao frio. Essa adaptação ao frio é explicada pela tremorigênese crônica que ocorre no músculo (102). Nosso estudo em camundongos hipotiroideos também revelou diferenças fundamentais entre a ativação do programa termogênico do BAT e do SKM e as formas como estas vias são influenciadas pelo T3 e pela temperatura do ambiente (103). O programa termogênico do SKM, mas não do BAT, foi reduzido pelo hipotiroidismo ou pela aclimatização à termoneutralidade. De fato, o programa termogênico do BAT só foi reduzido quando o hipotiroidismo foi associado com a termoneutralidade, indicando que a resposta metabólica ao hipotiroidismo depende da temperatura do ambiente.

B) Termogênese adaptativa induzida pela dieta

Dado o seu papel na termogênesis induzida pelo frio no BAT, poderia assumir-se que o hormônio tiroideano também é crítico para a termogênesis induzida pela dieta. Além disso, uma vez que quantidades substanciais de BAT foram encontradas em humanos adultos, é possível que esse tecido desempenhe um papel metabólico importante, inclusive podendo ser alvos de novas moléculas para o tratamento da obesidade (104).

A atividade simpática do BAT é aumentada pela dieta hipercalórica (105), levando a termogênese induzida pela dieta, mas o papel desempenhado pelo hormônio tiroideano neste processo não é claro. Embora exista um conceito intuitivo de que animais/humanos hipotiroideos tendem a ser obesos, um vasto número de estudos mostram que indivíduos que transitam do hipotiroidismo para o hipertiroidismo, e vice-versa, exibem somente uma pequena mudança da composição corporal (106-108). De fato, nosso grupo havia demonstrado que ratos hipotiroideos à temperatura ambiente e tratados com dieta hipercalórica não acumulam mais gordura que controles eutiroideos (109), questionando o papel do hormônio tiroideano nesse processo.

Uma condição importante em pesquisas sobre o metabolismo é o fato de que camundongos são normalmente aclimatados em condições de estresse térmico crônico, como já foi mencionado. Recentes estudos têm investigado os efeitos metabólicos, eliminando o estresse térmico, colocando o camundongo à termoneutralidade, isto é, 30°C. Esses estudos podem ser relevantes para se entender a obesidade em humanos, desde que o homen moderno vive uma vida à termoneutralidade e além da identificação de BAT metabolicamente ativo. Um exemplo dos efeitos causados pela termoneutralidade é o fato de camundongos com deficiência de UCP-1 serem obesos quando tratados com dieta padrão e este efeito obesogênico é aumentado quando animais são tratados com dieta hipercalórica, devido à inabilidade em ativar a termogênese adaptativa induzida pela dieta, mostrando que esta via é dependente da ativação da UCP-1 (88). O mesmo efeito foi observado em animais D2KO que apresentam maior susceptibilidade à obesidade quando tratados com dieta hipercalórica e aclimatados à termoneutralidade, o que nos levou a descobrir o papel desempenhado pela via da D2 no controle e na resposta do metabolismo à dieta hipercalórica (110).

Além disso, quando não ocorre produção de T3 pela D2, como em animais D2KO, há um aumento compensatório da atividade simpática no BAT para compensar o hipotiroidismo em nível tecidual. Este resultado revelou um novo aspecto do sinergismo entre o hormônio tiroideano e o SNS e estudar os efeitos da aclimatação à termoneutralidade, que reduz a atividade do SNS, expõem o importante papel desempenhado pelo hormônio tiroideano na termogênese do BAT e SKM. Aqui demonstramos que na temperatura ambiente, camundongos hipotiroideos estão protegidos da obesidade induzida pela dieta, um

mecanismo que é perdido à termoneutralidade, em que camundongos hipotiroideos tornam-se obesos quando tratados com dieta hipercalórica (103).

2.3 Efeitos cardiovasculares

O T3 tem muitos efeitos no coração e no sistema cardiovascular, tais como: aumento da frequência cardíaca e da força de contração do miocárdio; aumento da fração de ejeção e do débito cardíaco; diminuição da resistência vascular periférica e do tempo de contração isovolumétrico (111-113). O T3 diminui a resistência vascular periférica pela dilatação da arteríolas de resistência da circulação periférica (114). A vasodilatação é devido a um efeito direto do T3 nas células do músculo liso vascular promovendo o relaxamento (115). O hormônio tiroideano aumenta o volume sanguíneo, devido à diminuição da resistência vascular sistêmica, a eficiência do volume de enchimento arterial cai, resultando no aumento da liberação de renina e ativação do eixo angiotensina-aldosterona (116). Isto, por sua vez, estimula a reabsorção de sódio nos rins, levando a um aumento do volume plasmático.

Dado que o coração é um alvo muito sensível ao hormônio tiroideano, é de grande valia se entender o envolvimento deste hormônio na performance cardíaca. O T3 controla a expressão de genes que codificam proteínas regulatórias e estruturais. As duas cadeias pesadas de miosina (α-MHC e β-MHC) são proteínas miofibrilares diferentemente reguladas pelo T3. Em animais, o T3 ativa a α-MHC e reprime a β-MHC (117, 118). Em humanos, o T3 inativa a β-MHC, causando insuficiência cardíaca (119, 120). Outros genes responsivos ao T3 no coração são: ATPase ativada pelo cálcio (Ca^{2+}-ATPase) e fosfolamban (PLB) (121, 122). A liberação de cálcio e sua captação pelo retículo endoplasmático são os determinantes da função contrátil sistólica e do relaxamento diastólico. O transporte ativo de cálcio para o lúmem do retículo sarcoplasmático pela Ca^{2+}-ATPase é regulada pelo PLB.

Além disso, o *status* da tiróide altera a atividade adrenérgica, aumentando a frequência cardíaca e o débito cardíaco. Tentativas anteriores de promover o aumento da sinalização dos hormônios tiroideanos no coração usando-se transgênicos que superexpressão a D2 no miocárdio, resultou no aumento da sinalização adrenérgica e da expressão de genes dependentes de T3 (123, 124).

No miocárdio de ratos, por exemplo, a hipertrofia do ventrículo direito induzida pela hipertensão arterial pulmonar, resulta na indução em ~5 vezes na atividade local da D3, que

diminui a expressão gênica da Ca^{2+}-ATPase do tipo 2 do retículo endoplasmático (SERCA-2) e da α-MHC e aumenta os níveis de RNAm da β-MHC, um padrão tipicamente visto em corações hipotiroideos (125). De fato, a indução da D3 em modelos animais está relacionada com a acumulação do fator indutor de hipóxia-1α no miocárdio, criando uma redução anatomicamente específica local do conteúdo e ação de T3 (79). O infarto do miocárdio em ratos (126) e camundongos (127) também leva à reativação da D3. Neste último modelo, medidas *in vivo* da atividade transcricional dependente de T3 em cardiomiócitos usando-se ensaio *reporter* de luciferase, revelou uma diminuição pós-infarto do miocárdio, que foi associado com uma diminuição de 50% das concentrações de T3 no ventrículo esquerdo.

Entretanto, a questão levantada por estes estudos é se a reativação da D3 é necessária para o remodelamento do miocárdio. Para entender o papel da D3 neste processo, estudamos camundongos com deficiência da D3 exclusivamente no miocárdio (HtzD3KO) (63). Nossos dados mostram que a ausência da D3 causa cardiomiopatia restritiva, devido ao aumento cardíaco-específico da sinalização do hormônio tiroideano, incluindo a fibrose do miocárdio, prejuízo na força de contração do miocárdio e disfunção diastólica. Após o tratamento com isoproterenol, animais HtzD3KO apresentaram piora da disfunção diastólica e cardiomiopatia restritiva, resultando em insuficiência cardíaca congestiva e ao aumento da mortalidade. Nossos achados revelam o crucial papel da D3 na função cardíaca e no remodelamento, que poderiam ter implicações patofisiológicas para a cardiomiopatia restritiva em humanos.

II. Objetivos

1. **Primeiro Artigo: Statins and downstream inhibitor of the isoprenilation patway increase type 2 iodothyronine deiodinase activity.**
   Investigar o efeito das estatinas e inibidores da isoprenilação na sinalização do hormônio tiroideano via seus efeitos na via de síntese da D2.

2. **Segundo Artigo: Responsiveness to thyroid hormone and to ambient temperature underlies differences between brown adipose tissue and skeletal muscle thermogenesis in a mouse model of diet-induced obesity.**
   Definir o papel da temperatura ambiente no efeito metabólico do hormônio tiroideano na dissipação de calorias provenientes da dieta.

3. **Terceiro Artigo: Absence of myocardial thyroid hormone inactivating deiodinase results in restrictive cardiomyopathy in mice.**
   Avaliar o papel desempenhado pela inativação cardíaca da D3 na função e no remodelamento cardíaco.

CAPÍTULO 2

Primeiro Artigo

Statins and Downstream Inhibitors of the Isoprenylation Pahway Increase Type 2 Iodothyronine Deiodinase Activity

Miller, B.T.[*]; Ueta, C.B.[*]; Lau V.; Jacomino, K.G.; Wasserman, L.M.; Kim, B.W.

[*]Estes autores tiveram igual contribuição para este trabalho.

Endocrinology 153:4039-4048, 2012

Statins and Downstream Inhibitors of the Isoprenylation Pathway Increase Type 2 Iodothyronine Deiodinase Activity

B. T. Miller,* C. B. Ueta,* V. Lau, K. G. Jacomino, L. M. Wasserman, and Brian W. Kim

Division of Endocrinology, Diabetes, and Metabolism, University of Miami, Miller School of Medicine, Miami, Florida 33136

The type 2 iodothyronine selenodeiodinase (D2) is a critical determinant of local thyroid signaling, converting T_4 to the active form T_3 at the cytoplasmic face of the endoplasmic reticulum, thus supplying the nucleus with T_3 without immediately affecting circulating thyroid hormone levels. Although inhibitors of the cholesterol synthesis/isoprenylation pathway, such as hydroxy-methyl-glutaryl-coenzyme A reductase inhibitors (statins) have been to shown to down-regulate selenoproteins via interruption of normal selenocysteine incorporation, little is known about the effect of statins on D2. Here, we report that statins and prenyl transferase inhibitors actually increase D2 activity in cells with endogenous D2 expression. Although we confirmed that lovastatin (LVS) decreases the activity of transiently expressed D2 in HEK-293 cells, the prenyl transferase inhibitors increase activity in this system as well. LVS treatment increases endogenous *Dio2* mRNA in MSTO-211H cells but does not alter transiently expressed *Dio2* mRNA in HEK-293 cells. The prenyl transferase inhibitors do not increase *Dio2* mRNA in either system, indicating that a posttranscriptional mechanism must exist. Cotreatment with LVS or the prenyl transferase inhibitors with the proteasome inhibitor MG-132 did not lead to additive increases in D2 activity, indirectly implicating the ubiquitin-proteasomal system in the mechanism. Finally, C57BL/6J mice treated with LVS or farnesyl transferase inhibitor-277 for 24 h exhibited increased D2 activity in their brown adipose tissue. These data indicate that statins and downstream inhibitors of the isoprenylation pathway may increase thyroid signaling via stimulation of D2 activity. **(*Endocrinology* 153: 4039–4048, 2012)**

An emerging concept in the field of thyroid hormone action is that metabolism can be regulated on a tissue-specific basis by local mechanisms controlling thyroid hormone signaling (1). Clinically, this concept is important because it reminds us that measurement of thyroid hormone levels in the blood, *i.e.* systemic thyroid hormone levels, may not reflect dynamic changes in the intensity of thyroid signaling occurring in specific tissues. The therapeutic implication is that pharmacologic regulation of local thyroid hormone signaling could be a potential strategy for the treatment of obesity and the metabolic syndrome.

The type 2 iodothyronine selenodeiodinase (D2) is a critical determinant of local thyroid hormone signaling, acting to convert T_4 to the active form T_3 at the cytoplasmic face of the endoplasmic reticulum, thus supplying the nucleus with T_3 without immediately altering circulating thyroid hormone levels (2). D2 is one of three iodothyronine deiodinases: the inactivating D3 decreases the intensity of local thyroid hormone signaling, and the bifunctional activating/inactivating D1 plays less of a role in local control (3). In recent years, an important metabolic role for D2 has emerged, most notably from a study dem-

ISSN Print 0013-7227 ISSN Online 1945-7170
Printed in U.S.A.

doi: 10.1210/en.2012-1117 Received January 28, 2012. Accepted May 29, 2012.
First Published Online June 19, 2012

* B.T.M. and C.B.U. contributed equally to this work.

Abbreviations: AOSMC, Aortic smooth muscle cell; BAT, brown adipose tissue; D2, type 2 iodothyronine selenodeiodinase; FBS, fetal bovine serum; FTase, farnesyl transferase; FTI, FTase inhibitor; GGTase, geranylgeranyl transferase; GGTI, GGTase inhibitor; HMG-CoA, hydroxy-methyl-glutaryl-coenzyme A; LVS, lovastatin; MLL, mevalonolactone; PVS, pravastatin; sec-tRNA, selenocysteine tRNA; UCP-1, uncoupling protein-1; VDU-1, von Hippel-Lindau interacting deubiquitinating enzyme-1; VDU-2, von Hippel-Lindau interacting deubiquitinase-2.

onstrating that bile acids increase the energy expenditure of brown adipose tissue (BAT) via activation of the G protein-coupled receptor TGR5; the mechanism requires downstream transcriptional up-regulation of D2 (4). The thiazolidinedione drug pioglitizone has also been shown to up-regulate D2 in skeletal myocytes (5). Given that D2 is expressed in a number of metabolically important tissues, including BAT and vascular smooth muscle, these discoveries have established D2 as an important target in the effort to achieve pharmacologic tissue-specific control of metabolism (6–12).

D2 is dynamically regulated, with a short half-life on the order of 20–40 min secondary to tight control of activity and stability via the ubiquitin-proteasomal system (13–17). Current models suggest that D2 exists in a pool of active/unubiquitinated and inactive/ubiquitinated forms (18). The ubiquitination of D2 can be accelerated by increasing substrate concentration, *i.e.* increased D2 catalysis is linked to an accelerated rate of D2 ubiquitination; the covalent attachment of ubiquitin inactivates the enzyme and ultimately targets it for proteasomal degradation (15, 19, 20).

A largely unexplored potential mechanism for down-regulating D2 is by interruption of the isoprenylation pathway. The deiodinases are selenoproteins, each having the rare amino acid selenocysteine in their active center (3). Proper selenoprotein synthesis requires a specific selenocysteine tRNA (sec-tRNA), and for normal function, this sec-tRNA must undergo isoprenylation, *i.e.* addition of an isoprene to an adenine nucleoside near the anticodon (21). For proteins, the isoprenylation machinery attaches a farnesyl or geranylgeranyl moiety to a cysteine residue in the carboxy terminus. The pathways for farnesylation and geranylgeranylation are branches of the cholesterol synthesis pathway, with the rate-limiting enzyme being hydroxy-methyl-glutaryl-coenzyme A (HMG-CoA) reductase, which converts HMG-CoA to mevalonolactone (MLL), a precursor for both cholesterol and other isoprenoids (see figure 7 below). Inhibitors of HMG-CoA reductase, such as the "statin" class drugs, can therefore down-regulate the synthesis of selenoproteins, and this mechanism has been proposed as an explanation for some of their clinical effects (22, 23).

At the same time, studies have suggested that inhibition of the isoprenlyation pathway also leads to a decrease in proteasome activity (24–26). Because D2 is degraded in the proteasome, this might be expected to increase D2 activity; D2-expressing cells treated with the proteasome inhibitor MG-132 exhibit a large increase in D2 activity (17). One previous study examined the effect of statins on deiodinases, finding that lovastatin (LVS) interferes with the synthesis of transiently expressed D1 and D2 in Chinese hamster ovary cells (21). Thus, the current model holds that isoprenlyation inhibition decreases deiodinase activity.

In this study, we sought to further characterize the potential for statins to alter thyroid signaling via their effects on the deiodinases. Our preliminary findings were remarkable: both statins and downstream inhibitors of the isoprenylation pathway significantly increased, rather than decreased, the activity of endogenously expressed D2 in cultured MSTO-211H cells. We therefore undertook the investigations described herein to understand how D2 activity could be induced by isoprenlyation pathway inhibitors.

Materials and Methods

Reagents

Unless otherwise specified, all reagents were purchased from Sigma-Aldrich (St. Louis, MO). Outer ring-labeled ^{125}I-T_4 (specific activity 4400 Ci/mmol), ^{125}I-T_3 (specific activity 2200 Ci/mmol), and ^{125}I-rT_3 (specific activity 2200 Ci/mmol) were purchased from PerkinElmer (Boston, MA) and purified on LH-20 columns before use. LVS was converted to its active carboxylate form following published methods (27, 28). Briefly, 25 mg of the lactone form were dissolved in 500 μl of 100% ethanol, alkalinized by adding 250 μl of 0.6 M NaOH, incubated at 50 C for 2 h, neutralized with 0.4 M HCl (pH 7.5), and brought to 10 mM with H_2O.

Cell culture

Unless otherwise noted, cell lines were purchased from the American Type Culture Collection (Manassas, VA) and were cultured in a humidified atmosphere with 5% CO_2 at 37 C. HEK-293 (immortalized human embryonic kidney), HepG2 (human hepatocellular carcinoma), and SK-N-AS (human neuroblastoma) cells were cultured in DMEM (Sigma-Aldrich) supplemented with 10% fetal bovine serum (FBS). MSTO-211H (human mesothelioma) cells were cultured in RPMI 1640 (Sigma-Aldrich) supplemented with 10% FBS. Primary human aortic smooth muscle cells (AOSMC) were purchased from Lonza (Basel, Switzerland). AOSMC were cultured using media and reagents from the manufacturer, supplemented with sodium selenite to 100 nM, and assayed before 15 doublings as per the manufacturer's instructions.

Transfection studies

Transient transfection was performed in HEK-293 cells using Lipofectamine 2000 (Invitrogen, Carlsbad, CA) according to the manufacturer's instructions. Twenty-four hours before transfection, cells were plated in six-well dishes and allowed to reach 75% confluence. The ratio of DNA to Lipofectamine 2000 reagent used was 1:3. After a 12-h incubation, media were replaced by the cell propagation media (DMEM plus 10% FBS), and drug treatments were begun. Transfection efficiency was controlled via β-galactosidase cotransfection and ortho-Nitrophenyl-β-galactoside spectrophometric assay as previously described (18).

For transient expression, constructs for full-length wild-type human *Dio2* coding sequence (with the rat Selenoprotein P selenocysteine insertion sequence) in mammalian D10 expression vector were kind gifts from Antonio C. Bianco (University of Miami) (for details, see reference Ref.17). For *Dio2* promoter studies, a 6.9-kb 5′-flanking region human *Dio2* construct with firefly luciferase reporter was also a gift from the Bianco lab and was performed as described previously (29). Luciferase activity was quantified in 1×10^5 cells using the Dual-Luciferase Reporter Assay System (Promega, Madison, WI) accordingly to the manufacturer instruction and detected by Veritas Microplate Luminometer (Turner BioSystems, Sunnyvale, CA). All experiments were conducted in triplicate.

RNA isolation and mRNA quantitation

Total cellular RNA was isolated using TRIzol reagent (Invitrogen) as per manufacturer's instructions. RNA was then treated with TURBO DNA-free (Ambion, Austin, TX) following the manufacturer's instructions. Reverse transcription of 1 μg of total RNA was performed using the High Capacity cDNA kit (Applied Biosystems/Invitrogen, Carlsbad, CA). Abundance of specific mRNA molecules was analyzed via quantitative SYBR Green-based real-time PCR using the iCycler iQ Real-Time PCR Detection System (Bio-Rad Laboratories, Hercules, CA). Relative quantitation was determined using the standard curve method and the iCycler software and normalized for the expression of cyclophilin A. Relative mRNA quantitation was also confirmed using TaqMan gene expression assays following the manufacturer's instructions in a StepOnePlus real-time PCR system (Applied Biosystems/Invitrogen). Relative quantitation was analyzed via δ cycle threshold method (30).

Deiodinase assays

D1, D2, and D3 assays were performed as previously described (5, 30). D3 assays were performed as previously described using an ACQUITY system Ultra High Performance Liquid Chromatography (Waters Corp., Milford, MA) (31). Endogenous deiodinase activities for vehicle-treated cells ranged from 18 to 22 pmol/min[chmep]mg for D1 in HepG2 cells, 3 to 6 fmol/min[chmep]mg for D2 in MSTO-211H cells, 0.05 to 0.5 fmol/min[chmep]mg for D2 in AOSMC, and 0.3 to 0.6 fmol/min[chmep]mg for D3 in SK-N-AS cells. All deiodinase assays for *in vitro* studies were performed with each data point in duplicate, and with each experimental group having three to six samples. Mouse BAT D2 activity was approximately 0.1 fmol/min[chmep]mg in wild-type mice at room temperature.

Animal studies

Animal studies were approved by the Institutional Animal Care and Use Committee of the University of Miami in compliance with National Institutes of Health standards. Mice were treated with a standard mouse chow diet and water *ad libitum* under a 12-h light, 12-h dark cycle. All experiments were conducted in 8- to 10-wk-old male C57BL/6J mice obtained from The Jackson Laboratory (Bar Harbor, ME). Activated LVS and farnesyl transferase (FTase) inhibitor (FTI)-277 were diluted in PBS and administered via ip injection at a dose of 10 mg/kg body weight, with a second dose given 12 h after the first. At the end of the 24-h treatment period (12 h after the second dose), mice were euthanized by CO_2 asphyxiation. BAT samples were collected and immediately stored in liquid nitrogen. Frozen samples of BAT samples were processed for D2 activity assay or mRNA analysis as previously reported (32). Protease inhibitor cocktail (catalog no. S8820–20TAB; Sigma-Aldrich) was added to the assay buffer before processing. Experimental groups had four mice, and the experiment was performed three times.

Statistical analysis

Data were analyzed by Student's *t* test or one-way ANOVA with Newman-Keuls *post hoc* testing when multiple comparisons were made, using GraphPad PRISM 5 software (GraphPad, La Jolla, CA). Significance was held at $P < 0.05$ (two-tailed).

Results

Regulation of endogenously expressed deiodinase activities by LVS

To characterize the effect of statins on endogenous deiodinase activities, we exposed cells endogenously expressing D1 (HepG2), D2 (MSTO-211H), or D3 (SK-N-AS) to 10 μM LVS for 8 h and then measured the appropriate deiodinase activity (Fig. 1). Remarkably, endogenous D2 activity was significantly increased, whereas endogenous D1 and D3 activities were not significantly altered compared with vehicle. Given the longer half-lives of D1 and D3, we repeated these assays at 16 and 24 h but found no differences compared with vehicle (data not shown). These data demonstrate that LVS has a stimulatory effect on endogenous D2 activity that would not have been predicted based on previous studies in which D2 was transiently expressed.

Characterization of the stimulatory effect of LVS on D2 activity

To further characterize the positive effect of LVS on D2 activity, we performed dose-response and time-course studies in MSTO-211H cells (Fig. 2). Addition of LVS (2.5–10 μM) for 8 h resulted in a marked dose-dependent

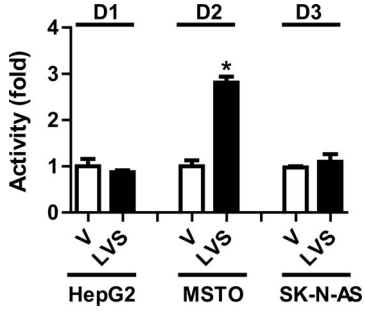

FIG. 1. Effect of LVS treatment on endogenous deiodinase activities. D1 activity in HepG2 cells, D2 activity in MSTO-211H, or D3 activity in SK-N-AS cells was measured after 8 h of incubation with LVS (10 μM) or vehicle (V). *Bars* represent mean fold activity relative to vehicle ± SEM; *, $P < 0.05$ *vs.* vehicle. Typical experiments are shown out of five experiments for D1, 10 experiments for D2, and six experiments for D3.

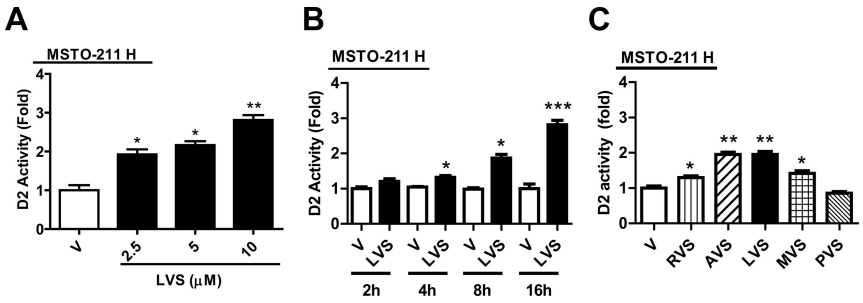

FIG. 2. Characterization of LVS effect on D2 activity in MSTO-211H cells. A, Dose response of D2 activity in cells treated with LVS (μM as indicated, 8 h). B, Time course of D2 activity in cells treated with 10 μM LVS (hours as indicated). C, Effect of various statins (10 μM, 8 h treatment) on D2 activity. Data presented as mean fold activity relative to vehicle ± SEM; *, $P < 0.05$ *vs.* vehicle (V); **, $P < 0.01$ *vs.* vehicle; ***, $P < 0.01$ *vs.* all other groups. RVS, Rosuvastatin; AVS, atorvastatin; MVS, mevastatin; PVS, pravastatin. All experiments performed in triplicate; typical experiments shown.

increase in D2 activity (Fig. 2A). The increase in D2 activity was detectable in 4 h with 10 μM LVS (Fig. 2B). Incubations longer than 16 h were not associated with further increases in activity (data not shown). To determine whether this was a statin class effect, we tested other statins (10 μM for 8 h), including atorvastatin, mevastatin, rosuvastatin, and pravastatin (PVS) (Fig. 2C). With the exception of PVS, the other statins also increased D2 activity, indicating that this is a class effect.

The isoprenylation pathway and D2

Given that statins inhibit HMG-CoA reductase, we hypothesized that the isoprenlyation pathway is relevant with regards to the stimulatory effect on D2. To test this hypothesis, we exposed MSTO-211H cells to LVS with or without the downstream product of HMG-CoA reductase, MLL (100 μM), for 8 h (Fig. 3A). Cotreatment with LVS and the downstream product of the enzyme (MLL) led to a loss of the stimulatory effect on D2 activity, indicating that the upstream blockade of HMG-Co reductase leads to downstream effects important for D2 regulation.

Next, we tested whether direct inhibitors of the major downstream branch-point enzymes FTase and geranylgeranyl transferase (GGTase) would also increase D2 activity (Fig. 7). Dose-dependent increases in D2 activity were found for inhibitors of FTase, FTI-277 and FPT-II, with maximal increases at 10 μM (Fig. 3B). The GGTase inhibitor (GGTI)-298 did not significantly increase D2 activity in MSTO-211H cells, but GGTI-2147 did significantly increase D2 activity at 20 μM. Given that FTI-277 and GGTI-2147 had strong positive effects, subsequent MSTO-211H studies used only these prenyl transferase inhibitors. These data confirm that downstream inhibition of the isoprenlyation pathway is sufficient to induce D2 in MSTO-211H cells and establish that blockade of either pathway is sufficient.

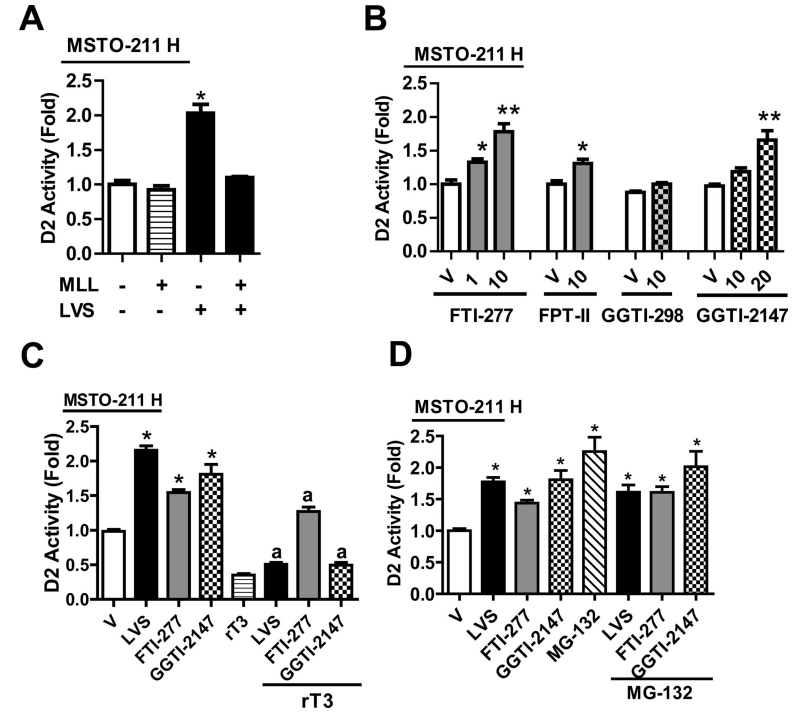

FIG. 3. Cholesterol-synthesis/isoprenylation pathway inhibition and D2 activity in MSTO-211H cells. A, D2 activity in cells treated with 10 μM LVS, 100 μM MLL, or a combination of both drugs for 8 h. B, Dose response of D2 activity in cells treated for 8 h with FTI-277, FPT-II, GGTI-298, or GGTI-2147 (dose in μM). C, D2 activity after 8 h of treatment with pathway inhibitors (10 μM) with or without rT_3 (1 μM) as indicated. D, D2 activity after 8 h of treatment with pathway inhibitors (10 μM) alone and in combination with 1 μM MG-132 as indicated. A–D, Data presented as mean fold activity relative to vehicle (V) ± SEM; *, $P < 0.05$ *vs.* vehicle; **, $P < 0.05$ *vs.* vehicle and lower doses of same drug; [a], $P < 0.05$ *vs.* rT_3 alone and drug alone. All experiments performed in triplicate; typical experiment shown.

Ubiquitin-proteasomal regulation of D2 *vs.* isoprenlyation inhibitors

Next, we investigated whether the inhibitors disrupt the ubiquitination and/or proteasomal degradation of endogenously expressed D2. We first examined ubiquitination by treating MSTO-211H cells with the inhibitors in the presence or absence of 1 μM rT_3; this dose of rT_3 has been previously shown to strongly promote substrate-accelerated ubiquitination and thus inactivation of D2 (33). As expected, rT_3 was associated with strong suppression of

D2 activity (Fig. 3C). When rT_3 was combined with LVS or GGTI-2147, the net D2 activity was intermediate between the levels seen with each drug alone and also lower than vehicle (being about ~25% higher than with rT_3 alone). When rT_3 was combined with FTI-277, D2 activity was also intermediate compared with either drug alone, although in this case, the net activity was still slightly higher than vehicle. These equivocal results do not rule out partial inhibition of substrate-accelerated ubiquitination by the isoprenlyation inhibitors. We measured mRNA expression of the deubiquitinases von Hippel-Lindau interacting deubiquitinating enzyme-1 (VDU-1) and von Hippel-Lindau interacting deubiquitinase-2 (VDU-2) after treatment with the inhibitors, finding no significant change in MSTO-211H-treated cells relative to vehicle (LVS, 0.9 ± 0.3 VDU-1 and 1.19 ± 0.3 VDU-2; FTI-277, 1.48 ± 0.5 VDU-1 and 1.56 ± 0.4 VDU-2; and GGTI-2147, 0.53 ± 0.5 and 0.57 ± 0.5; all not significant).

To test whether the inhibitors increase D2 activity via inhibition of the proteasome, MSTO-211H cells were incubated with these drugs in the presence of the proteasome inhibitor MG-132. Exposure to MG-132 alone increased D2 activity as expected (Fig. 3D). Combined treatment with the inhibitor drugs and MG-132 resulted in no further increase in endogenous D2 activity (Fig. 3D). The absence of either an additive or synergistic effect provides indirect support for the hypothesis that both statins and the downstream isoprenylation inhibitors increase D2 activity by interfering with proteasomal degradation.

Effect of isoprenylation inhibitors on transiently expressed D2 in HEK-293 cells

The only previous study of statins and deiodinases reported that LVS decreases the activity of transiently expressed D2, but no previous data exists regarding the downstream inhibitors of isoprenylation and D2 (21). Thus, we characterized the effects of LVS, FTI-277, GGTI-298, and GGTI-2147 in HEK-293 cells transiently expressing human D2. Consistent with the previous study, LVS treatment lead to a decrease in transiently expressed D2 activity (Fig. 4A); this stands in contrast to the results with cells endogenously expressing D2. FTI-277 (10 μM), GGTI-298 (10 μM), and GGTI-2147 (at 20 μM) treatment all increased transiently expressed D2 activity, indicating that downstream inhibition of the pathway still has the same positive effect even for transiently expressed D2.

HEK-293 cells were also used to test whether the inhibitors could activate the *Dio2* (D2 gene) promoter: when cells transiently expressing a human *Dio2*-promoter/luciferase reporter construct were treated with the inhibitors, no promoter activation was seen (Fig. 4B). To ensure that the stimulatory effect of the inhibitors in HEK-293 cells was not related to a direct effect on the D2/luciferase vector, HEK-293 cells transiently expressing a luciferase reporter in the same vector as used for the D2 studies were treated with the inhibitors, finding no increase in luciferase activity (Supplemental Fig. 1A, published on The Endocrine Society's Journals Online web site at http://endo.endojournals.org). Furthermore, there was no overt effect of the inhibitors on the β-galactosidase transfection control (Supplemental Fig. 1B). These data suggest that the dominant mechanism by which the downstream prenyl transferase inhibitors increase D2 is posttranscriptional.

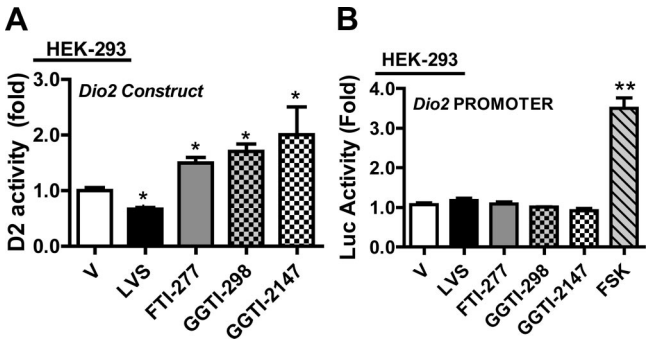

FIG. 4. Effect of isoprenylation inhibition on transiently expressed D2 in HEK-293 cells. A, D2 activity in HEK-293 cells transiently expressing D2 after 8 h of treatment with drugs as indicated (10 μM). B, Luciferase activity in HEK-293 cells transiently expressing a human *Dio2*-promoter/luciferase reporter construct after 8 h of treatment with the drugs as indicated (10 μM) or forskolin (FSK) positive assay control. A and B, Data presented as mean fold activity normalized for transfection efficiency via β-galactosidase activity ± SEM; *, $P < 0.05$ *vs.* vehicle (V); **, $P < 0.01$ *vs.* vehicle. All experiments performed in triplicate; typical experiments are shown.

Endogenous D2 in human primary AOSMC

To determine whether the effects of the isoprenylation inhibitors were limited to immortalized cells, we investigated their effects on endogenous D2 in human primary AOSMC (Fig. 5). Treatment with LVS (10 μM) for 8 h significantly induced D2 activity, although the magnitude of increase was smaller than that seen in MSTO-211H (Fig. 5A). Treatment with GGTI-298 increased D2 activity (GGTI-2147 did not, data not shown). FTI-277 strongly increased D2 activity in AOSMC. The time course of stimulation was more rapid in AOSMC, with significant differences being observable within 2 h (Fig. 5B). When AOSMC were treated with inhibitors combined with rT_3, the net D2 effects were intermediate to those seen with rT_3 or the drugs alone (Fig. 5C). When the inhibitors were combined with MG-132, net D2 activity was not higher than MG-132. *In toto*, these data indicate that the stimulatory effect of the isoprenylation inhibitors on D2 is relevant for primary cells and is not limited to immortalized cells.

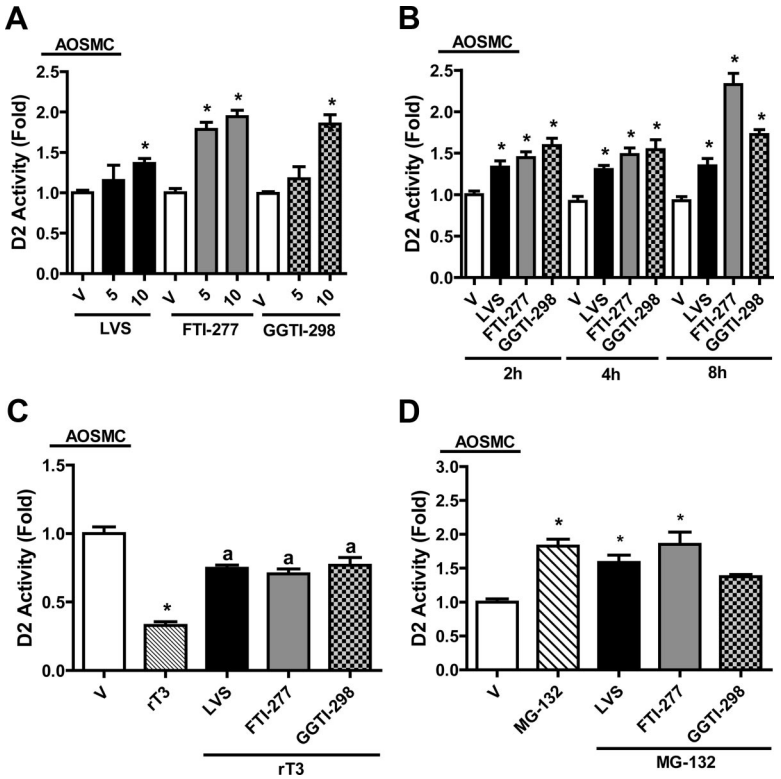

FIG. 5. Effect of isoprenylation inhibitors on endogenous D2 activity in human primary AOSMC. A, Dose response of D2 activity in AOSMC treated with LVS, FTI-277, and GGTI-298 (μM as indicated, 8 h of treatment). Data for LVS are pooled from six independent cell preparations, for FTI-277 and GGTI-298 from five different cell preparations. B, Time course of D2 activity in cells treated with isoprenlyation inhibitors as indicated (10 μM) typical experiment of three shown. C, Effect of cotreatment with isoprenlyation inhibitors and rT3 (1 μM). D, Effect of cotreatment with MG-132. A–D, *Bars* represent mean fold activity ± SEM; *, $P < 0.0.5$ *vs.* vehicle; [a], $P < 0.05$ *vs.* T_3 and vehicle. C and D, Typical of three experiments is shown.

Effects of the inhibitors on *Dio2* mRNA

Next, we analyzed the expression of *Dio2* gene in cells treated with LVS and the prenyl transferase inhibitors that increased D2 activity. In MSTO-211H cells, we found that LVS significantly increased *Dio2* mRNA at 8 h by 2-fold relative to vehicle (2.0 ± 0.26, $P < 0.02$). However, neither FTI-277 (1.16 ± 0.11, ns) nor GGTI-2147 (1.81 ± 0.6, ns) significantly changed *Dio2* mRNA. In HEK-293 cells, mRNA of the transfected human *Dio2* was not significantly changed by any of the inhibitors (LVS, 0.66 ± 0.3; FTI-277, 1.19 ± 0.1; GGTI-298, 1.26 ± 0.3; and GGTI-2147, 1.03 ± 0.15; all ns). In AOSMC, we did not find a significant increase in *Dio2* mRNA with any of the drugs (LVS, 0.9 ± 0.09; FTI-277, 1.1 ± 0.09; and GGTI-298, 0.76 ± 0.09; all ns). These data indicate that although LVS may increase D2 transcriptionally to some extent in MSTO-211H, the predominant mechanism(s) must be posttranscriptional.

Isoprenylation of D2 and/or its associated proteins

We enquired whether D2 itself could be isoprenylated. However, the human *Dio2* amino acid sequence lacks the classical carboxy-terminal "C-A-A-X" (cysteine-aliphatic-aliphatic-any amino acid) isoprenylation domain (34). Similarly, we analyzed the human amino acid sequences of known D2 interacting proteins for the CAAX motif but found no matches (Table 1).

LVS and D2 activity in murine BAT

To determine whether the effects seen *in vitro* could be extended to the *in vivo* setting, we treated 8- to 10-wk-old C57BL/6J mice with LVS for 24 h (10 mg/kg body weight, two ip doses given 12 h apart), and then measured D2 activity in BAT. LVS administration was associated with an approximately 2.75-fold increase in BAT D2 activity (Fig. 6). *Dio2* mRNA was increased by approximately 1.4-fold (1.42 ± 0.09, $P < 0.02$). The T_3-sensitive gene uncoupling protein-1 (*UCP-1*) mRNA increased by approximately 1.9-fold (~1.86 ± 0.3, $P < 0.05$). When the experiment was repeated with FTI-277 (10 mg/kg body weight, two ip doses given 12 h apart), again D2 activity was increased (~1.4-fold), albeit to a lesser extent than seen with LVS. For FTI-277, *Dio2* mRNA was not increased (1.01 ± 0.3-fold) nor was UCP-1 (0.95 ± 0.3-fold). These data establish that the effects of LVS and FTI-277 on D2 are not limited to the *in vitro* setting but can also be recapitulated in living animals.

TABLE 1. Carboxy-terminal amino acid sequences for D1, D2, and proteins associated with D2

Protein	NP no.	C terminus (15 amino acids)
Dio1	NP000783.2	Y N P E E V R A V L E K L H S
Dio2	NP000784.2	E K N F S K R U K K T R L A G
WSB-1	NP056441.6	E L P L P S K L L E F L S Y R
VDU-1	NP055832.3	I L Q A E E K L E V E T R S L
VDU-2	NP001008563	N L H G E Q K L E A E T R A V
TEB-4	NP005876.2	G K Q G S S P P P P Q S S Q E
UBE2J2	NP919296.1	F A Y T V K Y V L R S L A Q E
UBE2G2	NP003334.2	F Y K I A K Q I V Q K S L G L
Elongin B	NP009039.1	K P Q D S G S S A N E Q A V Q
Elongin C	NP005639.1	E I A L E L L M A A N F L D C
CUL5	NP003469.2	I R R D E S D I N T F I Y M A
RBX1	NP055063.1	C P L D N R E W E F Q K Y G H

U denotes selenocysteine. Dio 1, Type 1 Deiodinase; Dio 2, type 2 deiodinase; WSB-1, WD repeat and SOCS box containing-1; TEB-4, membrane-associated ring finger (C3HC4) 6; UBE2J2, ubiquitin conjugating enzyme E2, J2 homolog; UBE2G2, ubiquitin conjugating enzyme E2G2; CUL5, cullin 5, RBX1, ring-box 1.

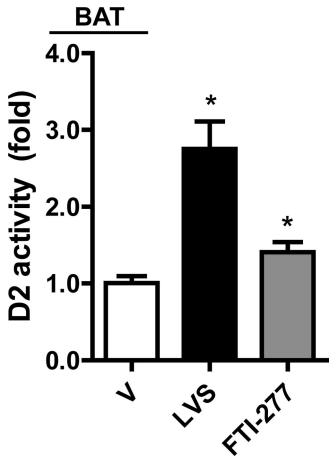

FIG. 6. Effect of LVS or FTI-277 injection on murine BAT D2 activity. D2 activity in BAT of 8- to 10-wk-old C57BL/6J mice treated with LVS (10 mg/kg body weight, two doses over 24 h), or FTI-277 (10 mg/kg body weight, two doses over 24 h). Data presented as mean fold activity relative to vehicle (V) ± SEM; *, $P < 0.05$ *vs.* vehicle-treated mice, n = 4 mice per group. Typical experiment out of three for each drug is shown.

Discussion

The major findings of this study are that endogenous D2 activity in cultured immortalized or primary cells is significantly increased by inhibitors of the isoprenylation pathway. We also performed a "proof of concept" experiment showing an increase in BAT D2 activity and mRNA in mice treated with LVS or FTI-277, extending the potential significance of the data to the *in vivo* realm. This stimulation of D2 activity by statins and prenyl transferase inhibitors is unexpected, considering the previous finding of Warner *et al.* (21) that LVS decreases the activity of transiently expressed D2, as well as the known dependence of selenoprotein synthesis on isoprenylation of the sec-tRNA (22, 23).

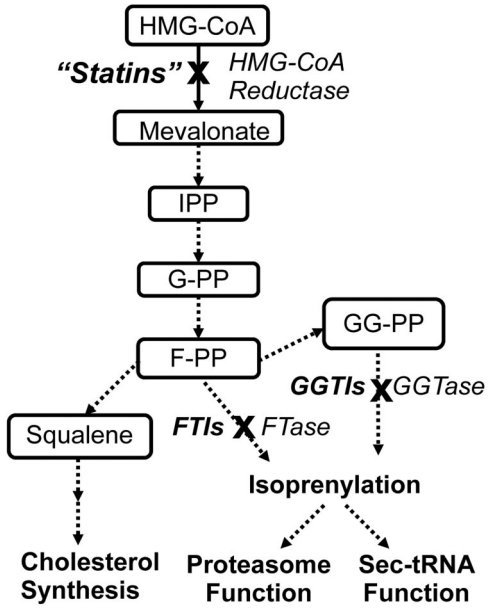

FIG. 7. The cholesterol synthesis and isoprenylation pathway. IPP, Isopentyl pyrophosphate; G-PP, geranyl pyrophosphate; F-PP, farnesyl pyrophosphate; GG-PP, geranylgeranyl pyrophosphate.

Significant regulatory complexity appears to exist in the relationship between isoprenylation pathway inhibitors and D2. Of note, various statins did not increase D2 in direct proportion to their potency with regards to inhibition of HMG-CoA reductase or low-density lipoprotein reduction (Fig. 2C); for example, rosuvastatin is the most potent HMG-CoA reductase inhibitor but only weakly increased D2. One could speculate that as the inhibition of cholesterol synthesis increases beyond a certain threshold, it might negatively impact D2 activity. On the other hand, molecule-specific factors, such as hydrophobicity, may play role, because PVS (the most hydrophobic statin tested) (35) had no stimulatory effect.

The finding that the FTase and GGTase inhibitors, when used at concentrations at which they exhibit high enzyme specificity, can individually increase D2 activity indicates that both the farnesylation and geranylation downstream branches of the pathway are mechanistically relevant. Although there is often redundancy between the prenyl transferases in terms of their protein targeting, it would seem that in this setting both pathways must be operating normally, else D2 activity increases. We ruled out *in silico* that human D2 or its known associated proteins contain the classical targeting sequence for isoprenylation (Table 1), so barring nonclassical isoprenlyation, there must be an isoprenylated protein, nucleoside, or other molecule (or molecules) important for D2 activity. The list of known suspects includes more than 100 proteins that are thought to be isoprenylated, having a vast array of functions spanning the gamut from proliferation to oxidative stress (36, 37). Our review of the known isoprenylated targets suggests many potential mechanisms but no obviously favored mechanisms to explain the increase in D2 activity. Thus, future studies utilizing a systematic approach to identify connections between D2 and known isoprenylated factors will be required.

Even without knowing the identity of the exact isoprenylated factor affecting D2 activity, mechanistic details have emerged from the current data. The observation that the inhibitor drugs cannot increase D2 activity beyond levels seen with MG-132 in the cotreatment studies in either MSTO-211 or AOSMC indirectly supports the hypothesis that inhibition of isoprenlyation interrupts normal ubiquitin-proteasomal degradation of D2 (Figs. 3D and 5D). It should be noted that mechanism may not be specific to D2; indeed, any drug or process that inhibits the proteasome might increase D2 activity by augmenting the pool of ubiquitinated D2.

Dissecting out where in the ubiquitination-proteasomal degradation pathway the inhibitors may be working will require further studies. Keeping in mind that ubiquitination (which deactivates D2) and proteasomal degradation are linked but separate processes, the interpretation of the intermediate D2 activities seen when inhibitors were combined with rT_3 (Figs. 3C and 5C) is complex: if the statins/prenyl transferase inhibitors induce D2 activity via total inhibition of substrate-accelerated ubiquitination, one would predict that the negative effect of rT_3 would be lost, but this was not seen. Thus, the results of the experiment were equivocal: the intermediate D2 activities are consistent either with partial inhibition of substrate-accelerated ubiquitination, or with the summation of a positive ubiquitination-independent effect of the inhibitors and the negative ubiquitination-mediated effect of rT_3. An additional possibility that remains to be explored is whether isoprenylation inhibitors could somehow increase the expression or activity of deubiquitinases that reactivate ubiquitinated D2. However, if this were the case, one would expect that cotreatment with the inhibitors and MG-132 would increase D2 activity higher than with MG-132 alone (38), but this was not seen, nor was VDU-1 or VDU-2 mRNA increased. *In toto*, the current data support a mechanism by which an unidentified isoprenylated factor or factors act to decrease the overall ubiquitin-mediated proteolysis of D2, but whether the critical issue is ubiquitination, translocation of ubiquitinated D2 to the proteasome, deubiquitination, or proteasomal degradation of ubiquitinated D2 itself remains to be determined.

Why LVS does not increase transiently expressed D2 is intriguing (Fig. 4A). One issue may be that the transcriptional increase seen in MSTO-211H cells was not present in HEK-293 (Fig. 4B). This may relate to the nonnative promoter and the 3′un-translated region used in the construct. Although we could not detect a significant LVS-mediated increase in *Dio2* mRNA in AOSMC myocytes, the magnitude of D2 induction was also lower in these cells, leaving open the possibility that a small increase in *Dio2* mRNA was present. Another possibility is that HEK-293 may be more sensitive to intracellular cholesterol depletion; note that the prenyl transferase inhibitors would be expected to affect cholesterol synthesis less than the statins, and this might explain some of the differences seen between LVS and the downstream inhibitors in all the cell types. LVS may therefore invoke multiple mechanisms increasing D2 activity, overlapping with the proteasomal-mechanism that predominates for the downstream inhibitors.

Cell type-specific differences among the prenyl transferases are notable in our studies, *e.g.* GGTI-298 and 2147 work differently in MSTO-211H *vs.* AOSMC. However, these differences are not unexpected given previous studies showing that different cell types have unique patterns of response to these drugs (39, 40). The fact that different FTase and GGTase inhibitors increase endogenously expressed D2 activity lends confidence that the mechanism is universal. A multitude of hypothetical explanations have be proposed to explain these cell line-specific differences, *e.g.* different pharmacologic kinetics of the drugs in the cell lines, or different expression patterns of critical isoprenylation targets. As more is learned about these drugs in other studies, unexpected clues as to D2 biology may also arise.

It is tempting to speculate as to whether patients taking statins exhibit any subtle changes in thyroid hormone signaling in their D2-expressing statin-exposed tissues. It should be remembered that such changes would not definitively be reflected by changes in plasma thyroid hormone levels or TSH, because D2 is capable of inducing tissue-specific changes. However, the low micromolar concentrations of statins (and prenyl transferases) used in these experiments must be considered a significant caveat. Although standard in the experimental literature (41–43), these concentrations are much higher than what is typically achieved in human plasma, except in rare patients receiving chemotherapeutic doses (44, 45). Thus, additional studies will be required before the clinical significance of these findings can be validated. The murine BAT data (Fig. 6) can be considered a first step. One could take the fact that *Dio2* mRNA was induced slightly with LVS but not FTI-277 to be indirect evidence that the same mechanisms apply in mice as in cells. The changes in *UCP-1* mRNA may relate to the extent of D2 stimulation, but it must be noted that the sensitivity of *UCP-1* to changes in D2-generated T_3 would be expected to be low in room-temperature animals (as opposed to in the cold, in which case *UCP-1* mRNA increases by many fold under the primary control of cAMP) (46). The next steps will be to extend the findings in mice, with a full characterization of thyroid hormone status in the plasma and in individual D2-expressing tissues under various statin and prenyl transferase inhibitor-exposure conditions, in particular examining chronic low-dose treatment effects.

In conclusion, the data indicate that the relationship between isoprenylation and D2-mediated regulation of thyroid hormone signaling is considerably more complex than once believed. The predominant mechanism appears to be largely posttranscriptional, likely involves the proteasome, and, for endogenously expressed D2, can outweigh any concomitant negative effect on D2 protein synthesis caused by impairment of sec-tRNA function.

Acknowledgments

We thank Gordana Simovic for assistance with Ultra High Performance Liquid Chromatography, Dr. Tatiana Fonseca for assistance with animal work, and Dr. Barry Hudson for comments regarding the manuscript.

Address all correspondence and requests for reprints to: Brian W. Kim, M.D., University of Miami, Division of Endocrinology, Diabetes, and Metabolism, Batchelor building, Room 610, 1580 North West 10th Avenue, Miami, Florida 33136. E-mail: bkim@med.miami.edu.

This work was supported by an American Thyroid Association research grant (B.W.K.).

Disclosure Summary: The authors have nothing to disclose.

References

1. **Bianco AC, Ribich S, Kim BW** 2007 An inside job. Endocrinology 148:3077–3079
2. **Gereben B, Zavacki AM, Ribich S, Kim BW, Huang SA, Simonides WS, Zeöld A, Bianco AC** 2008 Cellular and molecular basis of deiodinase-regulated thyroid hormone signaling. Endocr Rev 29:898–938
3. **Bianco AC, Salvatore D, Gereben B, Berry MJ, Larsen PR** 2002 Biochemistry, cellular and molecular biology and physiological roles of the iodothyronine selenodeiodinases. Endocr Rev 23:38–89
4. **Watanabe M, Houten SM, Mataki C, Christoffolete MA, Kim BW, Sato H, Messaddeq N, Harney JW, Ezaki O, Kodama T, Schoonjans K, Bianco AC, Auwerx J** 2006 Bile acids induce energy expenditure by promoting intracellular thyroid hormone activation. Nature 439:484–489
5. **Grozovsky R, Ribich S, Rosene ML, Mulcahey MA, Huang SA, Patti ME, Bianco AC, Kim BW** 2009 Type 2 deiodinase expression is induced by peroxisomal proliferator-activated receptor-γ agonists in skeletal myocytes. Endocrinology 150:1976–1983
6. **Marsili A, Ramadan W, Harney JW, Mulcahey M, Castroneves LA, Goemann IM, Wajner SM, Huang SA, Zavacki AM, Maia AL, Dentice M, Salvatore D, Silva JE, Larsen PR** 2010 Type 2 iodothyronine deiodinase levels are higher in slow-twitch than fast-twitch mouse skeletal muscle and are increased in hypothyroidism. Endocrinology 151:5952–5960
7. **Tu HM, Kim SW, Salvatore D, Bartha T, Legradi G, Larsen PR, Lechan RM** 1997 Regional distribution of type 2 thyroxine deiodinase messenger ribonucleic acid in rat hypothalamus and pituitary and its regulation by thyroid hormone. Endocrinology 138:3359–3368
8. **Visser TJ, Kaplan MM, Leonard JL, Larsen PR** 1983 Evidence for two pathways of iodothyronine 5′-deiodination in rat pituitary that differ in kinetics, propylthiouracil sensitivity, and response to hypothyroidism. J Clin Invest 71:992–1002
9. **Koenig RJ, Leonard JL, Senator D, Rappaport N, Watson AY, Larsen PR** 1984 Regulation of thyroxine 5′-deiodinase activity by 3,5,3′-triiodothyronine in cultured rat anterior pituitary cells. Endocrinology 115:324–329
10. **Silva JE, Larsen PR** 1983 Adrenergic activation of triiodothyronine production in brown adipose tissue. Nature 305:712–713
11. **Mizuma H, Murakami M, Mori M** 2001 Thyroid hormone activation in human vascular smooth muscle cells: expression of type II iodothyronine deiodinase. Circ Res 88:313–318
12. **Maeda A, Toyoda N, Yasuzawa-Amano S, Iwasaka T, Nishikawa M** 2003 Type 2 deiodinase expression is stimulated by growth factors in human vascular smooth muscle cells. Mol Cell Endocrinol 200:111–117
13. **Botero D, Gereben B, Goncalves C, De Jesus LA, Harney JW, Bianco AC** 2002 Ubc6p and ubc7p are required for normal and substrate-induced endoplasmic reticulum-associated degradation of the human selenoprotein type 2 iodothyronine monodeiodinase. Mol Endocrinol 16:1999–2007
14. **Kim BW, Zavacki AM, Curcio-Morelli C, Dentice M, Harney JW, Larsen PR, Bianco AC** 2003 ER-associated degradation of the human type 2 iodothyronine deiodinase (D2) is mediated via an association between mammalian UBC7 and the carboxyl region of D2. Mol Endocrinol 17:2603–2612
15. **Steinsapir J, Harney J, Larsen PR** 1998 Type 2 iodothyronine deiodinase in rat pituitary tumor cells is inactivated in proteasomes. J Clin Invest 102:1895–1899
16. **Steinsapir J, Bianco AC, Buettner C, Harney J, Larsen PR** 2000 Substrate-induced down-regulation of human type 2 deiodinase (hD2) is mediated through proteasomal degradation and requires interaction with the enzyme's active center. Endocrinology 141:1127–1135
17. **Gereben B, Goncalves C, Harney JW, Larsen PR, Bianco AC** 2000 Selective proteolysis of human type 2 deiodinase: a novel ubiquitin-proteasomal mediated mechanism for regulation of hormone activation. Mol Endocrinol 14:1697–1708
18. **Zavacki AM, Arrojo E Drigo R, Freitas BC, Chung M, Harney JW, Egri P, Wittmann G, Fekete C, Gereben B, Bianco AC** 2009 The E3 ubiquitin ligase TEB4 mediates degradation of type 2 iodothyronine deiodinase. Mol Cell Biol 29:5339–5347
19. **St Germain DL** 1988 The effects and interactions of substrates, inhibitors, and the cellular thiol-disulfide balance on the regulation of type II iodothyronine 5′-deiodinase. Endocrinology 122:1860–1868
20. **Leonard JL, Siegrist-Kaiser CA, Zuckerman CJ** 1990 Regulation of type II iodothyronine 5′-deiodinase by thyroid hormone. Inhibition of actin polymerization blocks enzyme inactivation in cAMP- stimulated glial cells. J Biol Chem 265:940–946
21. **Warner GJ, Berry MJ, Moustafa ME, Carlson BA, Hatfield DL, Faust JR** 2000 Inhibition of selenoprotein synthesis by selenocysteine tRNA[Ser]Sec lacking isopentenyladenosine. J Biol Chem 275:28110–28119
22. **Kromer A, Moosmann B** 2009 Statin-induced liver injury involves cross-talk between cholesterol and selenoprotein biosynthetic pathways. Mol Pharmacol 75:1421–1429
23. **Moosmann B, Behl C** 2004 Selenoproteins, cholesterol-lowering drugs, and the consequences: revisiting of the mevalonate pathway. Trends Cardiovasc Med 14:273–281
24. **Rao S, Porter DC, Chen X, Herliczek T, Lowe M, Keyomarsi K** 1999 Lovastatin-mediated G1 arrest is through inhibition of the proteasome, independent of hydroxymethyl glutaryl-CoA reductase. Proc Natl Acad Sci USA 96:7797–7802
25. **Efuet ET, Keyomarsi K** 2006 Farnesyl and geranylgeranyl transferase inhibitors induce G1 arrest by targeting the proteasome. Cancer Res 66:1040–1051
26. **Ludwig A, Friedel B, Metzkow S, Meiners S, Stangl V, Baumann G, Stangl K** 2005 Effect of statins on the proteasomal activity in mammalian endothelial and vascular smooth muscle cells. Biochem Pharmacol 70:520–526
27. **Morimoto K, Janssen WJ, Fessler MB, McPhillips KA, Borges VM, Bowler RP, Xiao YQ, Kench JA, Henson PM, Vandivier RW** 2006 Lovastatin enhances clearance of apoptotic cells (efferocytosis) with implications for chronic obstructive pulmonary disease. J Immunol 176:7657–7665
28. **Kita T, Brown MS, Goldstein JL** 1980 Feedback regulation of 3-hydroxy-3-methylglutaryl coenzyme A reductase in livers of mice treated with mevinolin, a competitive inhibitor of the reductase. J Clin Invest 66:1094–1100
29. **Fekete C, Gereben B, Doleschall M, Harney JW, Dora JM, Bianco**

AC, Sarkar S, Liposits Z, Rand W, Emerson C, Kacskovics I, Larsen PR, Lechan RM 2004 Lipopolysaccharide induces type 2 iodothyronine deiodinase in the mediobasal hypothalamus: implications for the nonthyroidal illness syndrome. Endocrinology 145:1649–1655

30. **Medina MC, Molina J, Gadea Y, Fachado A, Murillo M, Simovic G, Pileggi A, Hernández A, Edlund H, Bianco AC** 2011 The thyroid hormone-inactivating type III deiodinase is expressed in mouse and human β-cells and its targeted inactivation impairs insulin secretion. Endocrinology 152:3717–3727
31. **Rosene ML, Wittmann G, Arrojo e Drigo R, Singru PS, Lechan RM, Bianco AC** 2010 Inhibition of the type 2 iodothyronine deiodinase underlies the elevated plasma TSH associated with amiodarone treatment. Endocrinology 151:5961–5970
32. **Kang HW, Ribich S, Kim BW, Hagen SJ, Bianco AC, Cohen DE** 2009 Mice lacking Pctp/StarD2 exhibit increased adaptive thermogenesis and enlarged mitochondria in brown adipose tissue. J Lipid Res 50:2212–2221
33. **Curcio C, Baqui MM, Salvatore D, Rihn BH, Mohr S, Harney JW, Larsen PR, Bianco AC** 2001 The human type 2 iodothyronine deiodinase is a selenoprotein highly expressed in a mesothelioma cell line. J Biol Chem 276:30183–30187
34. **Kitten GT, Nigg EA** 1991 The CaaX motif is required for isoprenylation, carboxyl methylation, and nuclear membrane association of lamin B2. J Cell Biol 113:13–23
35. **Gazzerro P, Proto MC, Gangemi G, Malfitano AM, Ciaglia E, Pisanti S, Santoro A, Laezza C, Bifulco M** 2012 Pharmacological actions of statins: a critical appraisal in the management of cancer. Pharmacol Rev 64:102–146
36. **Reid TS, Terry KL, Casey PJ, Beese LS** 2004 Crystallographic analysis of CaaX prenyltransferases complexed with substrates defines rules of protein substrate selectivity. J Mol Biol 343:417–433
37. **Takemoto M, Liao JK** 2001 Pleiotropic effects of 3-hydroxy-3-methylglutaryl coenzyme a reductase inhibitors. Arterioscler Thromb Vasc Biol 21:1712–1719
38. **Curcio-Morelli C, Zavacki AM, Christofollete M, Gereben B, de Freitas BC, Harney JW, Li Z, Wu G, Bianco AC** 2003 Deubiquitination of type 2 iodothyronine deiodinase by pVHL-interacting deubiquitinating enzymes regulates thyroid hormone activation. J Clin Invest 112:189–196
39. **Lerner EC, Zhang TT, Knowles DB, Qian Y, Hamilton AD, Sebti SM** 1997 Inhibition of the prenylation of K-Ras, but not H- or N-Ras, is highly resistant to CAAX peptidomimetics and requires both a farnesyltransferase and a geranylgeranyltransferase I inhibitor in human tumor cell lines. Oncogene 15:1283–1288
40. **Morgan MA, Wegner J, Aydilek E, Ganser A, Reuter CW** 2003 Synergistic cytotoxic effects in myeloid leukemia cells upon cotreatment with farnesyltransferase and geranylgeranyl transferase-I inhibitors. Leukemia 17:1508–1520
41. **Bauer S, Wanninger J, Schmidhofer S, Weigert J, Neumeier M, Dorn C, Hellerbrand C, Zimara N, Schäffler A, Aslanidis C, Buechler C** 2011 Sterol regulatory element-binding protein 2 (SREBP2) activation after excess triglyceride storage induces chemerin in hypertrophic adipocytes. Endocrinology 152:26–35
42. **Tsuchiya M, Hosaka M, Moriguchi T, Zhang S, Suda M, Yokota-Hashimoto H, Shinozuka K, Takeuchi T** 2010 Cholesterol biosynthesis pathway intermediates and inhibitors regulate glucose-stimulated insulin secretion and secretory granule formation in pancreatic β-cells. Endocrinology 151:4705–4716
43. **Kwak B, Mulhaupt F, Myit S, Mach F** 2000 Statins as a newly recognized type of immunomodulator. Nat Med 6:1399–1402
44. **Azie NE, Brater DC, Becker PA, Jones DR, Hall SD** 1998 The interaction of diltiazem with lovastatin and pravastatin. Clin Pharmacol Ther 64:369–377
45. **van de Donk NW, Kamphuis MM, Lokhorst HM, Bloem AC** 2002 The cholesterol lowering drug lovastatin induces cell death in myeloma plasma cells. Leukemia 16:1362–1371
46. **de Jesus LA, Carvalho SD, Ribeiro MO, Schneider M, Kim SW, Harney JW, Larsen PR, Bianco AC** 2001 The type 2 iodothyronine deiodinase is essential for adaptive thermogenesis in brown adipose tissue. J Clin Invest 108:1379–1385 Abbreviations: HMG-CoA hydroxymethylglutaryl coenzyme A, IPP isopentyl pyrophosphate, G-PP geranyl pyrophosphate, F-PP farnesyl pyrophosphate, GG-PP geranylgeranyl pyrophosphate, FTAse farnesyl transferase, FTIs farnesyl transferase inhibitors, GGTase geranylgeranyl transferase, GGTIs geranylgeranyl transferase inhibitors, Sec-tRNA selenocysteine tRNA.

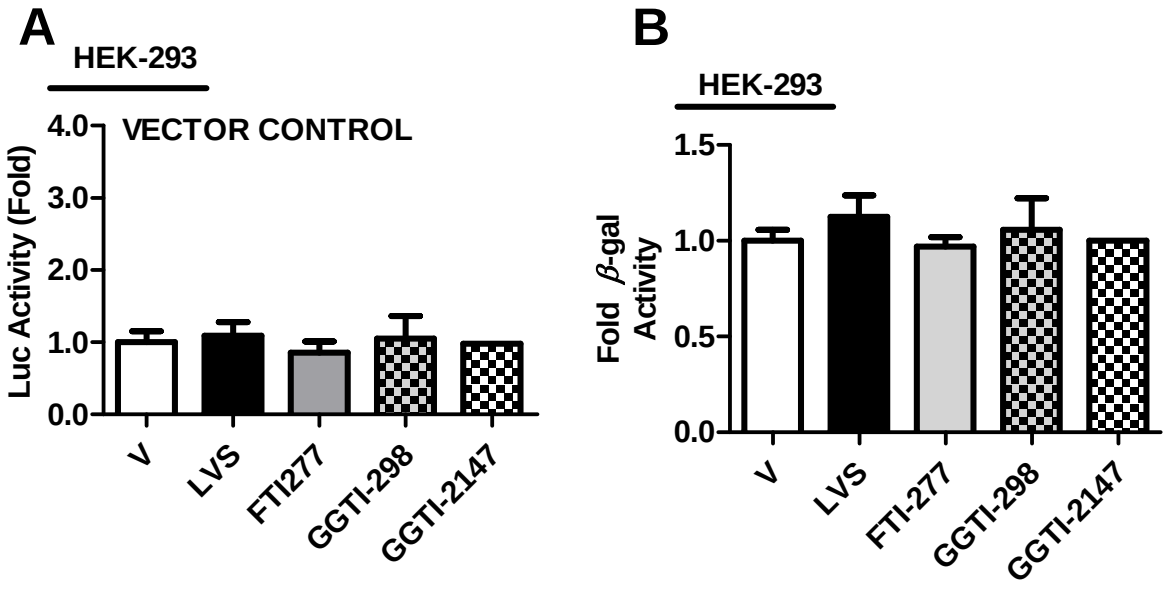

Supplemental Figure 1

CAPÍTULO 3

Segundo Artigo

Responsiveness to thyroid hormone and to ambient temperature underlies differences between brown adipose tissue and skeletal muscle thermogenesis in a mouse model of diet-induced obesity

Cintia B. Ueta, Emerson L. Olivares and Antonio C. Bianco

Endocrinology 152:3571-3581, 2011

Responsiveness to Thyroid Hormone and to Ambient Temperature Underlies Differences Between Brown Adipose Tissue and Skeletal Muscle Thermogenesis in a Mouse Model of Diet-Induced Obesity

Cintia B. Ueta, Emerson L. Olivares, and Antonio C. Bianco

Division of Endocrinology, Diabetes and Metabolism, University of Miami, Miller School of Medicine, Miami, Florida 33136

Thyroid hormone accelerates energy expenditure (EE) and is critical for cold-induced thermogenesis. To define the metabolic role played by thyroid hormone in the dissipation of calories from diet, hypothyroid mice were studied for 60 d in a comprehensive lab animal monitoring system. Hypothyroidism decreased caloric intake and body fat while down-regulating genes in the skeletal muscle but not brown adipose tissue thermogenic programs, without affecting daily EE. Only at thermoneutrality (30 C) did hypothyroid mice exhibit slower rate of EE, indicating a metabolic response to hypothyroidism that depends on ambient temperature. A byproduct of this mechanism is that at room temperature (22 C), hypothyroid mice are protected against diet-induced obesity, *i.e.* only at thermoneutrality did hypothyroid mice become obese when placed on a high-fat diet (HFD). This is in contrast to euthyroid controls, which on a HFD gained more body weight and fat at any temperature while activating the brown adipose tissue and accelerating daily EE but not the skeletal muscle thermogenic program. In the liver of euthyroid controls, HFD caused an approximately 5-fold increase in triglyceride content and expression of key metabolic genes, whereas acclimatization to 30 C cut triglyceride content by half and normalized gene expression. However, in hypothyroid mice, HFD-induced changes in liver persisted at 30 C, resulting in marked liver steatosis. Acclimatization to thermoneutrality dramatically improves glucose homeostasis, but this was not affected by hypothyroidism. In conclusion, hypothyroid mice are metabolically sensitive to environmental temperature, constituting a mechanism that defines resistance to diet-induced obesity and hepatic lipid metabolism. **(*Endocrinology* 152: 3571–3581, 2011)**

For over 110 yr now, it has been recognized that thyroid hormone plays a metabolic role accelerating the rate of basal energy expenditure (EE) in most mammalian tissues as assessed by indirect calorimetry (1, 2). By accelerating EE, thyroid hormone increases thermogenesis as a result of the intrinsic thermodynamic inefficiency of energy transformation. Thus, it is generally accepted as a dogma that hypothyroid rodents and humans exhibit a slower rate of EE and eventually develop hypothermia, a life-threatening complication of severe hypothyroidism.

Homeothermic animals, including mammals, exhibit tight control over the rate of EE and thermogenesis, adapting well to most earthly environments that pose a thermal challenge. In response to cold exposure, there is homeostatic heat production known as adaptive thermogenesis (3). Thyroid hormone is well known for its critical role in this process, and hypothyroid mammals succumb rapidly after being moved to cold environment (4, 5). In small rodents and human newborns, the chief tissue involved in adaptive thermogenesis is the brown adipose tissue (BAT),

ISSN Print 0013-7227 ISSN Online 1945-7170
Printed in U.S.A.

doi: 10.1210/en.2011-1066 Received April 2, 2011. Accepted June 22, 2011.
First Published Online July 19, 2011

Abbreviations: ACC, Acetyl-CoA carboxylase; ApoB, apolipoprotein B; ARβ3, β-adrenergic receptor 3; ATP5g1, ATP synthase, H^+ transporting, mitochondrial F0 complex, subunit c-1; BAT, brown adipose tissue; BW, body weight; CoA, coenzyme A; COX-IV, cytochrome C oxidase; CPT-1β, carnitine-palmitoyl transferase-1β; Dio, deiodinase; D2KO, knockout of the type II deiodinase; EE, energy expenditure; ERR-α, estrogen-related receptor α; FATP, fatty acid transport protein; FGF-21, fibroblast growth factor 21; FOXO-1, forkhead box 01; Glut-4, glucose transport 4; HFD, high-fat diet; HMGCS-2, 3-hydroxy-3 methylglutaryl-CoA synthase 2; IPGTT, intraperitoneal glucose tolerance test; LCAD, long-chain acyl-CoA-dehydrogenase; MCAD, medium-chain acyl-CoA-dehydrogenase; mTFA, mitochondrial transcription factor A; NRF-1, nuclear respiratory factor-1; PDK-4, pyruvate dehydrogenase kinase 4; PGC-1, peroxisome proliferator-activated receptor γ coactivator 1; PPAR, peroxidase proliferator-activated receptor; UCP, uncoupling protein; RQ, respiratory exchange ratio; SDHA, succinate dehydrogenase; SKM, skeletal muscle; SNS, sympathetic nervous system; SOD, superoxide dismutase; Spot-14, thyroid hormone-inducible hepatic protein; WAT, white adipose tissue.

a recognized target of thyroid hormone (6). Also, in the adult human, there are significant amounts of BAT that rapidly respond to environmental temperature (7). The sympathetic nervous system (SNS) controls BAT, where a synergism between the adrenergic and the thyroid hormone signaling pathways leads to rapid activation of heat production: both cAMP and T_3 up-regulate the expression of the uncoupling protein (*UCP-1*) gene (8), the key BAT protein that explains how mitochondria in this tissue rapidly accelerate and sustain high rates of respiration without the corresponding ATP synthesis.

Adaptive thermogenesis can also be triggered by excessive caloric intake, in what is known as diet-induced thermogenesis. In this case, a substantial fraction of diet-induced thermogenesis is activated by the SNS and takes place in the BAT (9, 10). Thus, given its role in cold-induced BAT thermogenesis, one would assume that thyroid hormone is also critical for diet-induced thermogenesis. However, despite the intuitive association between hypothyroidism and obesity, it is less than clear that thyroid hormone plays a role in this process. The analysis of several studies indicates that there are only minor changes in body composition of individuals transitioning from hypo- to hyperthyroidism and *vice versa* (11–13). In fact, we have previously shown that, compared with euthyroid rats, hypothyroid rats ingest as much calories and gain as much body fat when placed on a hypercaloric diet (14), questioning a role for thyroid hormone in diet-induced EE.

Recently, we have reported that disruption of thyroid hormone activation via knockout of the type II deiodinase (D2KO) increases susceptibility to high-fat diet (HFD), glucose intolerance, and liver steatosis only when animals are acclimatized to thermoneutrality (15), the environment temperature (30 C) at which the heat derived from the basal metabolic rate is sufficient to maintain normal core temperature. In these animals, disruption of the D2 mechanism is offset by an increase in BAT sympathetic activity, which led us to uncover the critical role played by the D2 pathway in metabolic control and response to HFD.

We now report that at room temperature, hypothyroid animals have a relatively mild metabolic phenotype. In fact, oxygen consumption (VO_2), respiratory exchange ratio (RQ), and EE are preserved in chronically hypothyroid mice, and only at thermoneutrality does total daily EE drop in hypothyroid mice. As a consequence, at room temperature, hypothyroid mice are protected against diet-induced obesity, a mechanism that is also lost at thermoneutrality. Furthermore, only at 30 C did hypothyroid mice develop glucose intolerance and severe liver steatosis, supporting our observations that the effect of thyroid hormone on hepatic lipid metabolism is strongly influenced by the environmental temperature.

Materials and Methods

Animals

All experimental procedures were approved by the local Institutional Animal Care and Use Committee. All drugs and reagents were purchased form Sigma Chemical Co. (St. Louis, MO), except when indicated otherwise. Male, 3-month-old C57BL/J6 mice purchased from The Jackson Laboratory (Bar Harbor, ME) were used throughout. Mice were kept at thermoneutrality (30 C; Columbus Instruments, Columbus, OH) or room temperature (22 C), with a 12-h light, 12-h dark cycle starting at 0600 h and housed in standard plastic cages as described (15). Hypothyroidism was induced by treatment with methimazole (0.1%) and sodium perchlorate (1%) in the drinking water. Euthyroid control animals remained on tap water *ad libitum*. Two weeks later, animals were started on HFD (4.5 Kcal/g, 15.3% protein, 42.7% carbohydrate, and 42% fat, TD 95121; Harlan Teklad, Indianapolis, IN) or remained on chow diet (3.3 Kcal/g, 28.8% protein, 58.8% carbohydrate, and 12.7% fat, 5010 LabDiet laboratory autoclavable rodent diet; PMI Nutrition, Richmond, IN) for 8 wk. Body weight (BW) and food intake were measured daily.

Body composition

Animals were fasted overnight, and total skeleton area, lean body mass, and fat mass were determined by dual energy x-ray absorptiometry (Lunar Pixi, Janesville, WI). For the procedure, mice were anesthetized with ketamine/xylazine (200 and 7–20 mg/kg) before imaging as described (15).

Indirect calorimetry

Mice were individually housed and acclimatized to the calorimeter cages for 2 d followed by 2 d of data collection of gas exchanges as described (15). Indirect calorimetry was performed in a comprehensive lab animal monitoring system (Columbus Instruments), a computer-controlled open circuit calorimetry system. Metabolic profiles were generated based on real-time data obtained in successive 26-min cycles. Studies were performed at 22 and 30 C. The sensors were calibrated against a standard gas mixture containing defined quantities of O_2 and CO_2 (Airgas, Tampa, FL). VO_2 was expressed as milliliters per minute per kilogram lean body mass. The RQ was calculated as the ratio between CO_2 production (liters) and O_2 consumption (liters). EE was calculated using the following formula: $(3.815 + 1.232 \times VCO_2/VO_2) \times VO_2$.

Intraperitoneal glucose tolerance test (IPGTT)

Mice were fasted the night before and glucose (1 g/kg BW) was administrated by ip injection as described (15). Blood samples were collected from the tail at various times after the glucose load, as indicated, and glycemia was immediately determined on a glucose analyzer (Bayer, Tarrytown, NY).

Intraperitoneal insulin tolerance test

Food was removed 4 h before the experiment. Blood samples were collected from the tail at various times after insulin (0.75

U/kg BW) was administered by ip injection, as indicated, and glycemia was immediately determined on the glucose analyzer as described (15).

Euthanasia and postmortem analyses

At the end of the experimental period, mice were euthanized by asphyxiation in a CO_2 chamber. The epididymal white adipose tissue (WAT) and retroperitoneal WAT were removed, weighted, and results expressed as a function of tibial length. The latter was manually measured after the right tibia of each mouse was dissected. The Liver, BAT, and gastrocnemius [skeletal muscle (SKM)] were rapidly removed and frozen in the liquid nitrogen. Blood was collected and plasma levels of TSH, T_4, and T_3 determined using a MILLIPLEX rat thyroid hormone panel kit as described by the manufacturer (Millipore Corp., Billerica, MA) and read on a BioPlex (Bio-Rad, Hercules, CA). Immediately after being killed, liver fragments were obtained and fixed in 4% paraformaldehyde in 0.1 ml PBS for 24 h at 4 C, frozen sectioned, and stained with Oil Red O. Frozen liver fragments (~200 mg) were homogenized and lipids extracted using chloroform:methanol (2:1) and 0.05% sulfuric acid as described (15). An aliquot of the organic phase was collected and mixed with chloroform containing 1% Triton, dried under nitrogen stream, and resuspended in water. Triglycerides were determined using a commercially available kit (Sigma-Aldrich, St. Louis, MO).

Gene expression analysis

Total RNA was extracted from SKM, BAT, and liver using Trizol (Life Technologies, Inc., Carlsbad, CA), according to the manufacturer's instructions. The extracted RNA was quantified with a NanoDrop spectrophotometer, and 1.0 μg of total RNA was reverse transcribed into cDNA by using High Capacity cDNA reverse Transcription kit (Applied Biosystems, Foster City, CA). Genes of interest were measured by RT-PCR (Bio-Rad iCycler iQ Real-Time PCR Detection System) using the iQ SYBR Green Supermix (Bio-Rad) with the following conditions: 15 min at 94 C (hot start), 30–50 sec at 94 C, 30–50 sec at 55–60 C, and 45–60 sec at 72 C for 40 cycles. A final extension at 72 C for 5 min was performed as well as the melting curve protocol to verify the specificity of the amplicon generation. Standard curves consisted of four to five points of serially diluted mixed experimental and control group cDNA. Cyclophin A was used as a housekeeping internal control gene. The coefficient of correlation was more than 0.98 for all curves, and the amplication efficiency ranged between 80 and 110%. Results are expressed as ratios of test mRNA/cyclophin A mRNA. The mRNA levels of the following genes were measured: mitochondrial transcription factor A (*mTFA*); medium-chain acyl-coenzyme A (*CoA*)-dehydrogenase (*MCAD*); long-chain (*LCAD*); estrogen-related receptor α (ERR-α); nuclear respiratory factor-1 (*NRF-1*); ATP synthase, H^+ transporting, mitochondrial F0 complex, subunit c-1 (ATP5g1); carnitine-palmitoyl transferase-1β (CPT-1β); acetyl-CoA carboxylase (ACC); cytochrome C oxidase (COX-IV); peroxisome proliferator-activated receptor γ coactivator 1-α and β (PGC-1α and PGC-1β); superoxide dismutase 1 and 2 (SOD1 and SOD2); pyruvate dehydrogenase kinase 4 (PDK4); peroxidase proliferator-activated receptor α, γ, and δ (*PPAR*-α, *PPAR*-γ, and *PPAR*-δ); forkhead box 01 (FOXO-1); succinate dehydrogenase (SDHA); fatty acid transport protein (FATP)-2; 3-hydroxy-3 methylglutaryl-CoA synthase 2 (HMGCS-2); thyroid hormone-inducible hepatic protein (Spot-14); UCP-1 and UCP-3; β-adrenergic receptor 3 (ARβ3); deiodinase 1 and 2 (Dio1 and Dio2); glucose transport 4 (Glut-4); apolipoprotein B (ApoB); and fibroblast growth factor 21 (FGF-21).

Statistical analysis

All data were analyzed using PRISM software (GraphPad Software, Inc., San Diego, CA) and expressed as mean ± SD. One-way ANOVA was used to compare more than two groups, followed by the student-Newman-Keuls test to detect differences between two groups. The Student's *t* test was used to compare differences between two groups.

Results

What is the metabolic profile of long-term hypothyroidism in mice?

To define the metabolic profile caused by long-term hypothyroidism, adult mice housed at room temperature were made hypothyroid with the use of antithyroid drugs for 2 wk and followed for the next 8 wk. Hypothyroidism was confirmed by an approximately 14-fold elevation in serum TSH, an approximately 85% drop in serum T_4, and approximately 75% drop in serum T_3, along with an approximately 60% reduction in liver Dio1 activity, a very sensitive tissue marker of thyroid hormone action (16). Hypothyroidism did not affect tibial length or total skeleton area (data not shown) given that mice were about 3 months old (adults) at the beginning of the experiment.

Euthyroid 22 C* vs. *hypothyroid 22 C on a chow diet. Hypothyroidism caused a drop in caloric intake (Fig. 1A), and at the end of the experimental period, hypothyroid animals had gained about 50% less BW (Fig. 1B). The epididymal and retroperitoneal fat pads (Fig. 1, C and D), as well as the total body fat (Fig. 1E), also increased much less than in euthyroid controls. Indirect calorimetry, as assessed during admission for 48 h at the comprehensive lab animal monitoring system, revealed the expected VO_2 circadian pattern, with values substantially higher at night, but no effect of hypothyroidism was observed (Fig. 2A and Supplemental Fig. 1A, published on The Endocrine Society's Journals Online web site at http://endo.endojournals.org). The RQ (Fig. 2B and Supplemental Fig. 1B) and the total daily EE (Fig. 2C and Supplemental Fig. 1C) were also not affected by hypothyroidism. In the gastrocnemius, hypothyroidism caused a generalized decrease in gene expression, including *ERR*α, *NRF-1*, *PPAR*δ, *PPAR*α, *CPT-1*β, *COX-IV*, *ATP5g1*, *PDK-4*, *MCAD*, and *LCAD* (Table 1), whereas expression of *PGC-1*β was increased by hypothyroidism (Table 1). Notably, an increase in *PGC-1*α was the only alteration in BAT gene expression caused by hypothyroidism (Table 1).

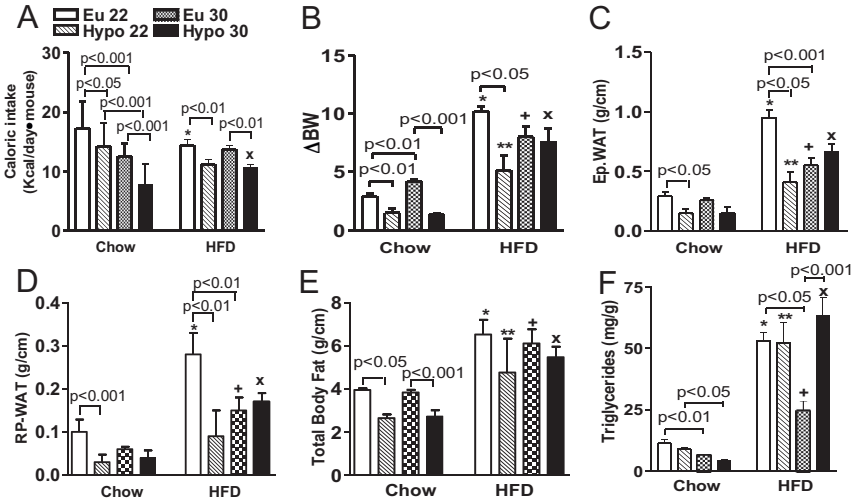

FIG. 1. Effect of ambient temperature and thyroid status on different metabolic parameters of mice kept on a chow diet or on a HFD. Adult euthyroid controls and hypothyroid mice were followed for 8 wk while at 22 C or 30 C. A, Caloric intake was calculated based on daily food consumption. B, BW was measured daily, and variances (ΔBW) are shown. C, The weight of the epididymal fat depot (Ep.WAT) is expressed as a function of the tibial length as assessed during necropsy. D, Retroperitoneal fat depot (RP.WAT) is shown as in C. E, Total body fat as measured by dual energy x-ray absorptiometry. F, Liver triglycerides content. *, $P < 0.001$ *vs.* euthyroid chow 22 C; **, $P < 0.01$ *vs.* hypo chow 22 C; +, $P < 0.01$ *vs.* euthyroid chow 30 C; x, $P < 0.01$ *vs.* Hypo chow 30 C. Entries are mean ± SD of three animals per group; the level of statistical significance is shown accordingly. Eu, Euthyroid; Hypo, hypothyroid.

Glucose and lipid homeostasis. After overnight fasting, blood glucose remained unaffected in hypothyroid animals, but the response to an IPGTT exhibited higher blood glucose at the 30-min time point (Fig. 3A). Tolerance to insulin after a 4-h fasting was not affected by hypothyroidism (Fig. 3H). Although liver triglyceride content was not significantly affected by hypothyroidism (Figs. 1F and 4, A and B), there was an increase in *PPARα* and *FGF-21* mRNA and a decrease in *spot-14* and *ApoB* mRNA (Table 2).

Does acclimatization to thermoneutrality affect the metabolic profile of hypothyroid mice?

To test the hypothesis that the mild metabolic phenotype in the hypothyroid mouse is due to the environmental temperature, we repeated the experiments described above in euthyroid controls and hypothyroid mice that were acclimatized to the thermoneutral temperature of 30 C.

Euthyroid 22 C* vs. *euthyroid 30 C on a chow diet. We looked at the effects of acclimatization to 30 C in euthyroid control animals. Despite a decrease in caloric intake (Fig. 1A), animals gained slightly more BW (Fig. 1B), but no changes were observed in the size of the epididymal (Fig. 1C) and retroperitoneal (Fig. 1D) fat pads or in the total body fat (Fig. 1E). In euthyroid controls, acclimatization to 30 C decreased VO_2 (Fig. 2A and Supplemental Fig. 1A) without affecting RQ (Fig. 2B and Supplemental Fig. 1B). Furthermore, the daily EE was significantly reduced after acclimation to 30 C (Fig. 2C and Supplemental Fig. 1C). This coincided with a reduction in the gastrocnemius expression of *ERRα*, *PPARδ*, *PPARα*, *CPT-1β*, *COX-IV*, *ATP5g1*, *UCP-3*, *PDK-4*, *MCAD*, and *LCAD* while increasing the expression of *SOD-1* and *SOD-2* (Table 1). BAT changes were minimal, restricted to a reduction in ATP5g1 gene expression and an increase in COX-IV and SOD-1 (Table 1).

Hypothyroid 22 C* vs. *hypothyroid 30 C on a chow diet. Inducing hypothyroidism while at thermoneutrality led to a further reduction in caloric intake, still below what was observed in euthyroid controls (Fig. 1A), but no effects were seen in BW gain (Fig. 1B), in the epididymal (Fig. 1C) and retroperitoneal (Fig. 1D) fat pads or in the total body fat (Fig. 1E). Hypothyroid mice also exhibited a reduction in VO_2 (Fig. 2A and Supplemental Fig. 1A) without affecting RQ (Fig. 2B and Supplemental Fig. 1B). Most importantly, there was a reduction in daily EE to values below those found in euthyroid controls (Fig. 2C and Supplemental Fig. 1C). This coincided with a reduction in gastrocnemius *PGC-1β*, *COX-IV*, *UCP-3*, and *Glut-4* mRNA levels (Table 1), with *PGC-1β* mRNA still remaining above that seen in euthyroid controls (Table 1). Similar to euthyroid animals, acclimatization to 30 C increased *SOD-1* mRNA levels in the gastrocnemius of hypothyroid mice (Table 1). Furthermore, the BAT thermogenic program was also down-regulated, with a decrease in *PGC-1α*, *PGC-1β*, *FOXO-1*, *ATP5g1*, *UCP-1*, and *Dio2* mRNA levels at the same time that *NRF-1*, *COX-IV*, *SOD-1*, and *SOD-2* mRNA levels were increased (Table 1).

Glucose and lipid homeostasis. In both euthyroid controls and hypothyroid mice, acclimatization to thermoneutrality lowered overnight fasting glucose levels and improved the overall response to an IPGTT (Fig. 3, B and C). At the same time, acclimatization to 30 C decreased tolerance to insulin in both groups of animals as assessed by the drop in blood glucose (Fig. 3, I and J). Liver triglyceride content in both groups was decreased by 50% during acclimatization to thermoneutrality and was not affected by

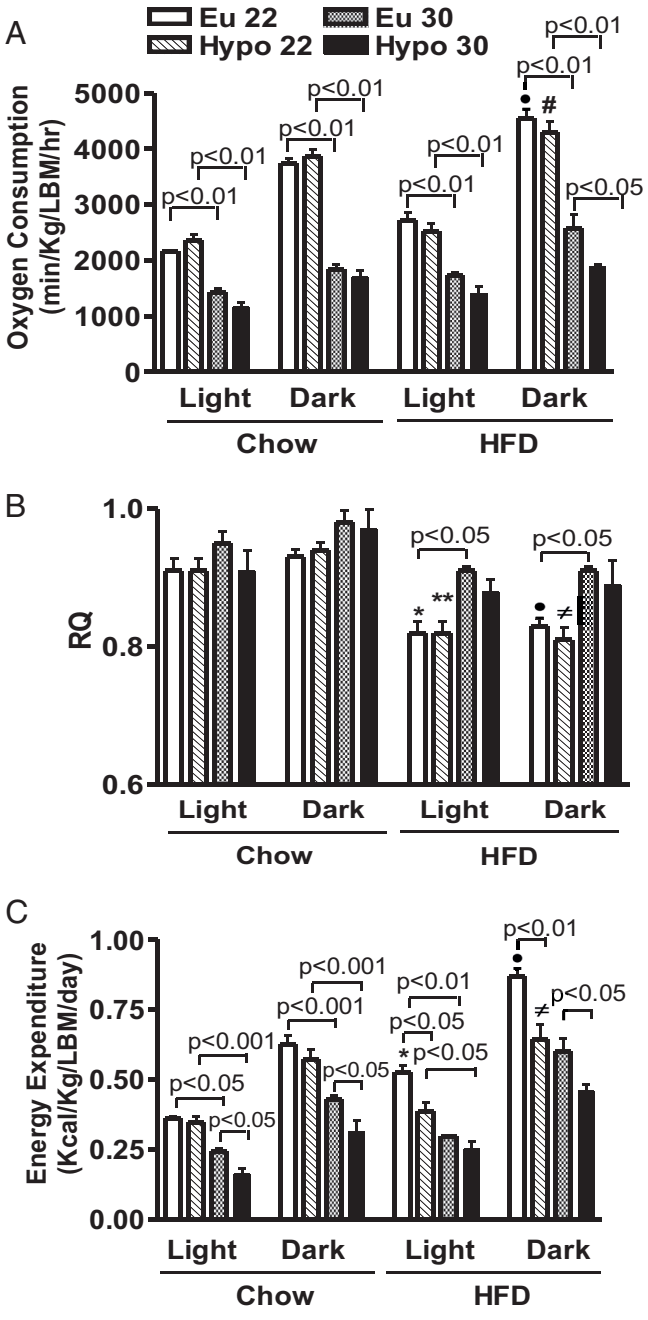

FIG. 2. Metabolic profile of ambient temperature of mice kept on a chow diet or on a HFD. A, VO_2 as assessed during a 48-h period at the end of the experiment. B, Same as in A, except that shown is RQ. C, Same as in A, except that shown is EE. *, $P < 0.001$ *vs.* euthyroid-chow 22 C light; **, $P < 0.01$ *vs.* Hypo-chow 22 C light; ●, $P < 0.01$ *vs.* euthyroid-chow 30 C dark; #, $P < 0.01$ *vs.* Hypo-chow 30 C dark. Entries are mean ± SD of three animals per group; the level of statistical significance is shown accordingly. Eu, Euthyroid; Hypo, hypothyroid.

hypothyroidism (Figs. 1F and 4, A–D). In euthyroid controls, this reduction in triglyceride content coincided with a marked decrease in *PGC-1β* and *ApoB* mRNA levels (Table 1), whereas in hypothyroid animals, the reduction in gene expression was seen with *PGC-1β*, *PPARα*, *CPT-1β*, *FATP-2*, *ApoB*, and *FGF-21* (Table 2).

Is hypothyroidism an aggravating factor in a mouse model of diet-induced obesity?

To test the hypothesis that hypothyroidism worsens the metabolic phenotype when mice are placed on a hypercaloric diet, euthyroid controls and hypothyroid mice were studied in the setting of HFD. Although HFD contains proportionally less carbohydrates and proteins, it is likely that most of the resulting phenotype is due to its 3.3-fold higher fat content.

***Euthyroid-chow 22 C* vs. *euthyroid-HFD 22 C*.** In euthyroid control animals, caloric intake was mildly reduced by HFD (Fig. 1A). However, these animals gained approximately 3.5 times more BW (Fig. 1B) and exhibited much heavier epididymal (Fig. 1C) and retroperitoneal (Fig. 1D) fat pads when compared with animals kept on a chow diet. On HFD, total body fat increased by approximately 50% (Fig. 1E). Nocturnal VO_2 increased (Fig. 2A and Supplemental Fig. 1, A and D), RQ decreased (Fig. 2B and Supplemental Fig. 1, B and E), and the total daily EE was accelerated (Fig. 2C and Supplemental Fig. 1, C and F) in euthyroid control animals placed on a HFD. In these animals, there was an increase in gastrocnemius expression of *SOD-2*, whereas *ERRα* and *COX-IV* mRNA levels were decreased (Table 1). In the BAT, HFD resulted in increased expression of *ERRα*, *NRF-1*, *UCP-1*, *ARβ3*, and *Dio2* (Table 1).

***Hypothyroid-chow 22 C* vs. *hypothyroid-HFD 22 C*.** Hypothyroid animals on a HFD also ingested less calories (Fig. 1A) and gained less BW (Fig. 1B), adiposity (Fig. 1C), and total body fat (Fig. 1E) when compared with euthyroid controls. These animals failed to significantly increase VO_2, but they did lower the RQ (Fig. 2, A and B, and Supplemental Fig. 1, A and B and D and E). Most importantly, they failed to accelerate total daily EE (Fig. 2C and Supplemental Fig. 1, C and F). HFD decreased gastrocnemius *PGC-1β* and *SOD-2* mRNA levels (Table 1), whereas in the BAT, there was a decrease in *NRF-1* and *ATP5g1* mRNA levels (Table 1).

***Glucose and lipid homeostasis*.** HFD caused glucose intolerance in euthyroid controls, whereas it did not significantly affect tolerance to insulin (Fig. 3, D and K). Notably, HFD did not affect IPGTT in hypothyroid animals but increased tolerance to insulin at the 15-min time point (Fig. 3, E and L). Triglyceride content increased by approximately 5-fold in the liver of euthyroid controls placed on HFD (Figs. 1F and 4, A and E), with an increase in expression of *PPARα*, *PPARγ*, *ACC*, *CPT-1β*, *HMGCS-2*, *ApoB*, and *FGF-21* (Table 2). Notably, hypothyroid animals on HFD exhibited a very similar 5-fold elevation in liver triglycerides (Figs. 1F and 4, B and F)

TABLE 1. Effect of ambient temperature and thyroid status on gene expression patterns in mice kept on a chow or HFD in the gastrocnemius (SKM) and BAT

	Chow diet				HFD			
	22 C		30 C		22 C		30 C	
Parameter	Euthyroid	Hypo	Euthyroid	Hypo	Euthyroid	Hypo	Euthyroid	Hypo
SKM								
PGC-1α	1.0 ± 0.4	1.3 ± 0.4	0.9 ± 0.3	0.8 ± 0.2	1.1 ± 0.1	1.0 ± 0.3	1.6 ± 0.6	0.7 ± 0.3
PGC-1β	1.0 ± 0.3	2.6 ± 0.4[a,c]	1.3 ± 0.1	1.7 ± 0.1[b]	1.2 ± 0.1	1.5 ± 0.1	1.0 ± 0.2[a]	1.3 ± 0.3[b]
ERRα	2.4 ± 0.4	0.3 ± 0.1[a]	0.3 ± 0.1[a]	0.3 ± 0.1	1.5 ± 0.3	0.2 ± 0.1[a,d]	0.4 ± 0.1[a,d]	0.4 ± 0.1
NRF-1	1.3 ± 0.4	0.4 ± 0.2[a]	0.8 ± 0.1	0.6 ± 0.3	1.2 ± 0.1	0.6 ± 0.1[d]	0.4 ± 0.2[a,d]	1.0 ± 0.2[e,f]
PPARδ	1.5 ± 0.5	0.5 ± 0.1[a]	0.2 ± 0.1[a]	0.3 ± 0.2	1.0 ± 0.2	0.4 ± 0.1[d]	0.6 ± 0.1[a,c,d]	0.3 ± 0.1[f]
PPARα	1.5 ± 0.3	0.3 ± 0.1[a]	0.2 ± 0.1[a]	0.3 ± 0.1	1.3 ± 0.4	0.3 ± 0.1[d]	0.5 ± 0.1[a,d]	0.5 ± 0.2
mTFA	0.8 ± 0.1	0.9 ± 0.2	0.8 ± 0.2	1.0 ± 0.4	0.7 ± 0.1	0.6 ± 0.1	0.9 ± 0.1[d]	0.7 ± 0.1[f]
FOXO-1	1.2 ± 0.5	1.0 ± 0.3	0.7 ± 0.1	0.8 ± 0.1	1.0 ± 0.1	1.0 ± 0.5	1.9 ± 0.3[c,d]	0.7 ± 0.2[f]
CPT-1β	1.2 ± 0.3	0.6 ± 0.1[a]	0.2 ± 0.1[a]	0.4 ± 0.1	0.9 ± 0.4	0.4 ± 0.1	0.5 ± 0.2[a]	0.6 ± 0.1
COX-IV	0.7 ± 0.1	0.2 ± 0.1[a]	0.1 ± 0.1[a,c]	0.1 ± 0.1[b]	0.1 ± 0.1	0.1 ± 0.1[a]	0.1 ± 0.1[a,c]	0.1 ± 0.1[e]
ATP5g1	3.3 ± 0.8	0.6 ± 0.1[a]	0.4 ± 0.2[a]	0.6 ± 0.2	2.1 ± 0.6	0.5 ± 0.1[d]	0.6 ± 0.1[a,d]	0.6 ± 0.2
UCP-3	1.1 ± 0.4	1.1 ± 0.4	0.5 ± 0.1[a]	0.5 ± 0.1[b]	1.3 ± 0.6	0.6 ± 0.2[d]	1.4 ± 0.3[c]	0.3 ± 0.1[f]
SOD-1	0.2 ± 0.1	0.1 ± 0.1	0.6 ± 0.1[a]	0.8 ± 0.3[b,g]	0.3 ± 0.1	0.2 ± 0.1	0.2 ± 0.1[c]	0.2 ± 0.1
SOD-2	0.4 ± 0.1	0.4 ± 0.1	0.7 ± 0.1[a]	0.4 ± 0.2	1.0 ± 0.2	0.1 ± 0.1[a,d]	0.2 ± 0.1[c,d]	0.3 ± 0.1[b]
SDHA	1.6 ± 0.5	1.5 ± 0.5	2.0 ± 0.7	1.6 ± 0.3	1.5 ± 0.2	1.7 ± 0.4	1.5 ± 0.3	1.3 ± 0.5
PDK-4	1.5 ± 0.5	0.5 ± 0.1[a]	0.2 ± 0.1[a]	0.3 ± 0.2	1.0 ± 0.2	0.4 ± 0.1[d]	0.6 ± 0.1[a,c,d]	0.3 ± 0.1[f]
MCAD	1.7 ± 0.5	0.4 ± 0.1[a]	0.3 ± 0.2[a]	0.6 ± 0.1	1.0 ± 0.2	0.5 ± 0.1[d]	0.5 ± 0.1[a,d]	0.6 ± 0.1
LCAD	1.4 ± 0.5	0.3 ± 0.1[a]	0.2 ± 0.1[a]	0.3 ± 0.1	1.3 ± 0.4	0.3 ± 0.1[d]	0.5 ± 0.1[a,d]	0.5 ± 0.2
Glut-4	1.0 ± 0.1	1.2 ± 0.3	0.8 ± 0.1[c]	0.6 ± 0.1[b]	0.8 ± 0.2	1.2 ± 0.6	0.6 ± 0.1[c]	0.4 ± 0.1
BAT								
PGC-1α	0.5 ± 0.3	1.0 ± 0.1[a]	0.4 ± 0.2	0.4 ± 0.1[b,g]	1.2 ± 0.3	0.6 ± 0.1	0.6 ± 0.2	1.0 ± 0.2
PGC-1β	1.2 ± 0.4	1.3 ± 0.3	0.7 ± 0.3	0.7 ± 0.1[b]	1.6 ± 0.6	1.1 ± 0.3	0.8 ± 0.3	0.5 ± 0.2
ERRα	0.8 ± 0.2	0.7 ± 0.3	0.8 ± 0.2	0.8 ± 0.3	1.6 ± 0.6	0.6 ± 0.3[a,d]	0.5 ± 0.2[d]	1.0 ± 0.4
NRF-1	0.6 ± 0.2	0.8 ± 0.3	0.5 ± 0.1[c]	1.3 ± 0.3[b,c,g]	1.3 ± 0.5	0.3 ± 0.1[a,d]	0.8 ± 0.2	0.4 ± 0.2[b]
PPARγ	0.8 ± 0.1	1.2 ± 0.4	0.3 ± 0.2	0.6 ± 0.2	1.4 ± 0.6	0.7 ± 0.1[d]	0.5 ± 0.2[d]	0.2 ± 0.1[e]
mTFA	0.9 ± 0.3	1.6 ± 0.8	0.5 ± 0.2	0.8 ± 0.1	2.0 ± 0.8	0.7 ± 0.2[d]	0.5 ± 0.2[d]	0.7 ± 0.2
FOXO-1	1.2 ± 0.1	1.1 ± 0.1	1.0 ± 0.3	0.6 ± 0.1[b]	1.7 ± 0.4	0.6 ± 0.1[d]	1.0 ± 0.2[d]	1.1 ± 0.1
CPT-1β	0.9 ± 0.2	0.5 ± 0.2	0.8 ± 0.3	0.6 ± 0.2	1.2 ± 0.1	1.0 ± 0.2	0.5 ± 0.1[d]	0.5 ± 0.1[e]
COX-IV	0.7 ± 0.3	0.3 ± 0.2	2.3 ± 0.5[a]	1.3 ± 0.4[b,c]	1.8 ± 0.7	0.3 ± 0.1[d]	1.4 ± 0.9	1.3 ± 0.3[e]
ATP5g1	1.4 ± 0.2	1.2 ± 0.3	0.4 ± 0.2[a]	0.4 ± 0.1[b]	1.5 ± 0.3	0.1 ± 0.1[d]	0.5 ± 0.2[d]	0.5 ± 0.2[b,e]
UCP-1	1.0 ± 0.2	0.7 ± 0.3	0.8 ± 0.1[c]	0.2 ± 0.1[b,c,g]	1.5 ± 0.2	0.8 ± 0.3[a,d]	0.9 ± 0.2[d]	0.8 ± 0.2
SOD-1	0.7 ± 0.3	0.5 ± 0.3	1.3 ± 0.2[a]	1.0 ± 0.1[b]	1.1 ± 0.2	0.6 ± 0.2	1.2 ± 0.4	0.9 ± 0.2
SOD-2	0.7 ± 0.3	0.5 ± 0.3	0.3 ± 0.2[c]	1.8 ± 0.5[b,c]	1.1 ± 0.2	0.6 ± 0.2	1.1 ± 0.6	0.5 ± 0.2
ARβ3	0.7 ± 0.2	0.4 ± 0.1	0.4 ± 0.3	0.3 ± 0.1[g]	1.4 ± 0.5	0.6 ± 0.1[a,d]	0.4 ± 0.3[d]	1.6 ± 0.4[e,f]
Dio2	0.5 ± 0.3	1.0 ± 0.1	0.7 ± 0.2[c]	0.2 ± 0.1[b,c,g]	1.9 ± 0.6	0.9 ± 0.3[a,d]	0.8 ± 0.3[d]	0.8 ± 0.3
PDK-4	1.0 ± 0.4	1.1 ± 0.4	0.5 ± 0.2	1.2 ± 0.7	1.8 ± 0.4	0.5 ± 0.2[d]	0.5 ± 0.2[d]	0.7 ± 0.2
MCAD	0.7 ± 0.3	0.7 ± 0.3	0.4 ± 0.1	0.7 ± 0.2	1.4 ± 0.8	0.6 ± 0.2	0.4 ± 0.2	0.4 ± 0.2
LCAD	0.8 ± 0.4	1.0 ± 0.3	0.5 ± 0.2[c]	1.1 ± 0.2	1.2 ± 0.4	0.8 ± 0.1	0.6 ± 0.2	1.4 ± 0.3[e,f]
Glut-4	0.9 ± 0.3	0.5 ± 0.2	0.8 ± 0.3	0.5 ± 0.1[g]	1.1 ± 0.3	0.6 ± 0.2[d]	0.5 ± 0.1[d]	1.7 ± 0.1[e,f]

Values are the mean ± SD of three animals; all comparisons by ANOVA. Hypo, Hypothyroid.

[a] $P < 0.001$ *vs.* euthyroid 22 C.

[b] $P < 0.01$ *vs.* Hypo 22 C.

[c] $P < 0.001$ *vs.* euthyroid 30 C.

[d] $P < 0.001$ *vs.* euthyroid + HFD 22 C.

[e] $P < 0.001$ *vs.* Hypo + HFD 22 C.

[f] $P < 0.05$ *vs.* euthyroid + HFD 30 C.

[g] $P < 0.001$ *vs.* Hypo 30 C.

with increases in *PPARγ*, *ACC*, and *ApoB* mRNA levels (Table 2).

Does acclimatization to thermoneutrality affect the susceptibility of hypothyroid mice to diet-induced obesity?

To test the hypothesis that acclimatization to 30 C modifies the susceptibility of hypothyroid mice to HFD, euthyroid controls and hypothyroid mice were placed at thermoneutrality while on HFD.

***Euthyroid-chow 30 C* vs. *euthyroid-HFD 30 C*.** We first looked at euthyroid control animals to define whether their metabolic response to HFD is modified at 30 C. Although caloric intake was not affected (Fig. 1A), the gain in BW (Fig. 1B) and the enlargement of the fat pads were doubled by

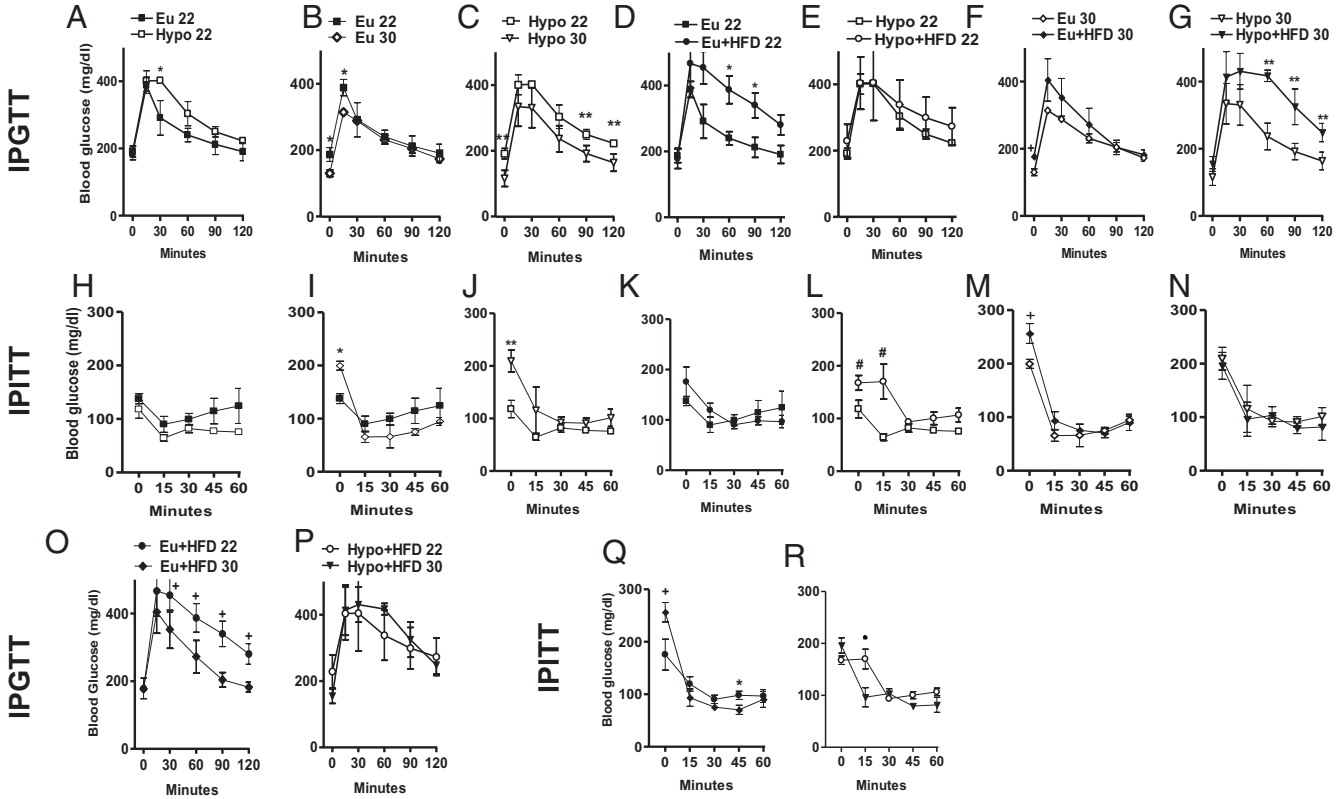

FIG. 3. Effect of ambient temperature and/or type of diet on glucose tolerance, tolerance to insulin. Blood glucose levels before and after ip administration of 1 g/kg glucose (IPGTT; A–G, O and P) or after ip injection of 0.75 U/kg insulin [ip insulin tolerance test (IPITT); H–N, Q and R] at the indicated time points in euthyroid and hypothyroid animals kept on chow or HFD, acclimatized to 22 C or 30 C; *, $P < 0.01$ *vs.* euthyroid 22 C; **, $P < 0.05$ *vs.* Hypo 30 C; +, $P < 0.05$ *vs.* euthyroid +HFD 30 C; #, $P < 0.01$ *vs.* Hypo + HFD 22 C; ●, $P < 0.05$ *vs.* Hypo + HFD 30 C. Entries are mean ± SD of three animals per group. Eu, Euthyroid; Hypo, hypothyroid.

HFD at 30 C (Fig. 1, C and D), resulting in approximately 60% more body fat (Fig. 1E). There was also an increase in the nocturnal VO_2 (Fig. 2A and Supplemental Fig. 1, A and D) and an acceleration of EE (Fig. 2C and Supplemental Fig. 1, C and F), whereas the RQ was decreased without reaching statistical significance (Fig. 2B and Supplemental Fig. 1, B and E). In these animals, there was an increase in gastrocnemius expression of *PPAR-δ*, *FOXO-1*, *UCP-3*, and *PDK-4* and a decrease in *COX-IV*, *SOD-1*, *SOD-2*, and *Glut-4* (Table 1). At the same time, no significant changes in gene expression were detected in the BAT (Table 1).

***Hypothyroid-chow 30 C* vs. *hypothyroid-HFD 30 C*.** Next, we looked at hypothyroid animals to define the role of thyroid hormone on the effects of HFD in the setting of thermoneutrality. In addition to a slight increase in caloric intake (Fig. 1A), at 30 C, hypothyroidism did not prevent the dramatic (~8-fold) increase in BW associated with HFD (Fig. 1B). Similarly, the approximately 3-fold enlargement of the epididymal and retroperitoneal fat pads (Fig. 1, C and D) and 2.2-fold increase in the total body fat was much greater than seen in euthyroid controls (Fig. 1E). Notably, HFD failed to increase VO_2 (Fig. 2A and Supplemental Fig. 1, A and D) or significantly lower RQ (Fig. 2B and Supplemental Fig. 1, B and E), but it did accelerate total daily EE, although to levels significantly lower than euthyroid controls (Fig. 2C and Supplemental Fig. 1, C and F). In these hypothyroid animals, there was a decrease in the gastrocnemius mRNA levels of *SOD-1* (Table 1). At the same time, in the BAT, there was an increase in *PGC-1α*, *UCP-1*, *ARβ3*, *Dio2*, and *Glut-4* mRNA levels (Table 1), whereas *NRF-1* expression was decreased (Table 1).

Glucose and lipid homeostasis. In these animals, there was fasting hyperglycemia with no significant modifications in the overall tolerance to glucose (Fig. 3F). No effects on tolerance to insulin were observed (Fig. 3M). Liver triglyceride content increased by approximately 4-fold in these animals (Figs. 1F and 4, C and G), with a substantial increased in *FGF-21* mRNA levels (Table 1). Hypothyroid mice on a HFD became glucose intolerant at thermoneutrality (Fig. 3G), with no changes in tolerance to insulin (Fig. 3N). Remarkably, in these animals, there was a marked (~13-fold) increase in liver triglyceride content, beyond what was seen in the euthyroid controls (Fig. 1F), resulting in clear liver steatosis (Fig. 4, D and H). In this setting, there was an increase in liver expres-

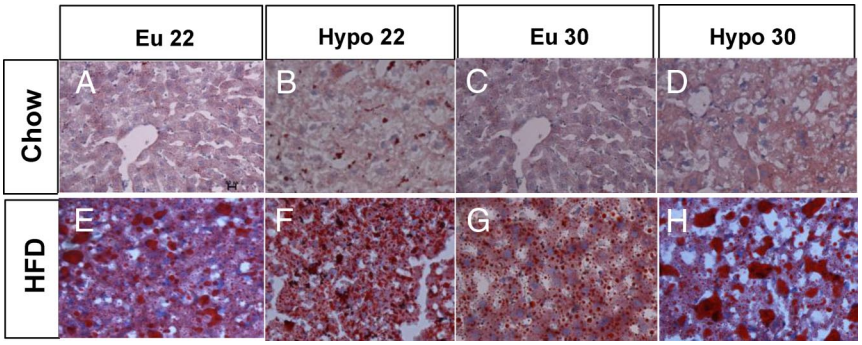

FIG. 4. Effect of acclimation temperature and/or diet on hepatic lipid content. Oil Red O staining of liver sections obtained from euthyroid and hypothyroid fed with chow or HFD for 8 wk, acclimatized at 22 C or 30 C, as indicated (A–H) is shown. A and B, Euthyroid and hypothyroid fed with chow diet, acclimatized 22 C. C and D, Same as in A and B, except acclimatization was at 30 C. E and F, Euthyroid and hypothyroid fed with HFD, acclimatized 22 C. G and H, Same as in E and F, except acclimatization was at 30 C. *Scale bar*, 50 μm. Key is indicated in the images. Eu, Euthyroid; Hypo, hypothyroid.

sion of *ACC*, *SDHA*, *CPT-1β*, *FATP-2*, *HMGCS-2*, *PPARγ*, and *spot-14* (Table 2).

Is acclimatization to thermoneutrality an aggravating factor in a mouse model of diet-induced obesity?

To test the hypothesis that acclimatization to 30 C worsens the metabolic phenotype of hypothyroid mice on HFD, euthyroid controls and hypothyroid mice were placed on a HFD while at thermoneutrality.

Euthyroid-HFD 22 C* vs. *euthyroid-HFD 30 C. Although no differences were observed in caloric intake (Fig. 1A), and in BW gain (Fig. 1B), the enlargement of the fat pads was significantly less at 30 C (Fig. 1, C and D), without affecting total body fat (Fig. 1E). At thermoneutrality, VO_2 decreased (Fig. 2A and Supplemental Fig. 1D), RQ increased (Fig. 2B and Supplemental Fig. 1E), and EE was slowed down (Fig. 2C and Supplemental Fig. 1F). This was accompanied by a decrease in gastrocnemius expression of *ERRα*, *NRF-1*, *PPARδ*, *PPARα*, *ATP5g1*, *SOD-2*, *PDK-4*, *MCAD*, and *LCAD* and increase in *mTFA* and *FOXO-1* mRNA levels (Table 1). In addition, there was a decrease in *ERRα*, *PPARγ*, *mTFA*, *FOXO-1*, *CPT-1β*, *ATP5g1*, *UCP-1*, *ARβ3*, *Dio2*, *PDK-4*, and *Glut-4* (Table 1).

Hypothyroid-HFD 22 C* vs. *hypothyroid-HFD 30 C. Acclimatization to thermoneutrality did not affect caloric intake (Fig. 1A). At the same time, there was a tendency to increase BW gain (Fig. 1B), the enlargement of the fat pads (Fig. 1 C and D) and the total body fat (Fig. 1E), although

TABLE 2. Effect of ambient temperature and thyroid status on gene expression patterns in mice kept on a chow or HFD in the liver

	Chow diet				HFD			
	22 C		30 C		22 C		30 C	
Parameter	Euthyroid	Hypo	Euthyroid	Hypo	Euthyroid	Hypo	Euthyroid	Hypo
Liver								
PGC-1α	0.6 ± 0.1	0.6 ± 0.1	0.4 ± 0.1	0.5 ± 0.1	0.4 ± 0.1	0.7 ± 0.1[d]	0.6 ± 0.1	0.7 ± 0.2
PGC-1β	1.3 ± 0.1	0.6 ± 0.1	0.4 ± 0.1[a]	0.5 ± 0.1[b]	1.2 ± 0.2	1.5 ± 0.4	0.2 ± 0.1[d]	0.5 ± 0.3[e]
PPARα	0.6 ± 0.3	1.2 ± 0.2[a]	0.5 ± 0.1	0.5 ± 0.1[b]	1.1 ± 0.1	1.5 ± 0.1[a]	0.4 ± 0.1[a,d]	0.6 ± 0.1[f,e]
ACC	0.5 ± 0.1	0.4 ± 0.1	0.6 ± 0.3	0.4 ± 0.2[g]	1.1 ± 0.2	0.6 ± 0.1[a]	0.9 ± 0.1	1.1 ± 0.3[b]
CPT-1β	0.5 ± 0.1	0.7 ± 0.1	0.5 ± 0.1	0.3 ± 0.1[b,g]	1.1 ± 0.2	0.8 ± 0.2[a]	0.6 ± 0.1[d]	0.8 ± 0.1
FGF-21	0.3 ± 0.1	0.8 ± 0.2[a]	0.4 ± 0.1	0.4 ± 0.1[b]	1.6 ± 0.3	0.6 ± 0.2[a,d]	1.6 ± 0.5[c]	1.6 ± 0.9
HMGCS-2	0.8 ± 0.2	1.2 ± 0.5	0.9 ± 0.2	0.6 ± 0.1[g]	1.2 ± 0.1	1.4 ± 0.1[a,d]	1.0 ± 0.2	1.1 ± 0.2
PPARγ	0.5 ± 0.1	0.4 ± 0.1	0.6 ± 0.2	0.4 ± 0.1[g]	1.5 ± 0.2	1.7 ± 0.1[a,d]	0.5 ± 0.1[d]	1.0 ± 0.2[b,f,e]
Spot-14	0.6 ± 0.1	0.1 ± 0.1[a]	0.5 ± 0.1[c]	0.1 ± 0.1[c,g]	1.0 ± 0.1	1.3 ± 0.2	0.7 ± 0.1[a,d]	1.0 ± 0.2
SDHA	0.7 ± 0.1	0.9 ± 0.3	0.8 ± 0.2	0.7 ± 0.2[g]	0.8 ± 0.	0.1 ± 0.03[d]	0.4 ± 0.05	0.4 ± 0.1
ApoB	1.0 ± 0.1	0.5 ± 0.1[a]	0.5 ± 0.1[a]	0.2 ± 0.1	1.2 ± 0.1	0.7 ± 0.1[a,d]	0.7 ± 0.3[d]	0.5 ± 0.2[b]
FATP-2	1.0 ± 0.3	0.9 ± 0.1	0.7 ± 0.3	0.3 ± 0.1[b,g]	1.0 ± 0.2	0.9 ± 0.1	0.5 ± 0.1[d]	0.4 ± 0.2

Values are the mean ± SD of three animals, by ANOVA. Hypo, Hypothyroid.

[a] $P < 0.001$ *vs.* euthyroid 22 C.

[b] $P < 0.01$ *vs.* Hypo 22 C.

[c] $P < 0.001$ *vs.* euthyroid 30 C.

[d] $P < 0.001$ *vs.* euthyroid + HFD 22 C.

[e] $P < 0.001$ *vs.* Hypo + HFD 22 C.

[f] $P < 0.05$ *vs.* euthyroid + HFD 30 C.

[g] $P < 0.001$ *vs.* Hypo 30 C.

neither reached statistical significance. At the same time, VO_2 (Fig. 2A and Supplemental Fig. 1D), as well as EE (Fig. 2C and Supplemental Fig. 1F), decreased, with a nonsignificant tendency for the RQ to increase (Fig. 2B and Supplemental Fig. 1E). These changes took place as the gastrocnemius gene expression of *NRF-1* increased and *COX-IV* decreased (Table 1). In the BAT, there was a decrease in *PPARγ* and *CPT-1β* mRNA levels and an increase in *COX-4*, *ATP5g1*, *ARβ3*, *LCAD*, and *Glut-4* mRNA levels (Table 1).

Glucose and lipid homeostasis. Feeding on a HFD while at thermoneutrality improved tolerance to glucose in euthyroid controls without affecting the response of hypothyroid animals (Fig. 3 O and P). At the same time, acclimatization to 30 C decreased insulin tolerance in euthyroid control animals as assessed by the marked drop in blood glucose starting at the 15-min time point (Fig. 3Q). In the hypothyroid animals, there was impaired clearance of blood glucose only at the 15-min time point (Fig. 3R). Although there was a marked drop in liver triglyceride content in euthyroid controls, the same did not happen in the hypothyroid animals (Figs. 1F and 4, E–H). The drop in liver triglyceride in euthyroid controls coincided with a decrease in *PGC-1β*, *PPARα*, *PPARγ*, *CPT-1β*, *FATP-2*, *spot-14*, and *ApoB* mRNA levels, whereas in the hypothyroid liver, the decrease in gene expression was limited to *PPARα* and *PPARγ* (Table 2).

Discussion

For small rodents, particularly mice, room temperature (*i.e.* 18–22 C) represents a significant thermal stress that requires acceleration of EE and obligatory thermogenesis to defend body temperature (17, 18). This is illustrated by the marked drop in daily EE after animals were moved to a thermoneutral temperature (Fig. 2C and Supplemental Fig. 1C). Thyroid hormone plays an important role in setting the level of daily EE in humans and rats (1, 2), and thus, it was unexpected to find that hypothyroid mice sustained normal VO_2 and/or daily EE at room temperature (Fig. 2, A and C, and Supplemental Fig. 1, A and C). Hypothyroid mice exhibited a strong metabolic response that prevented daily EE from dropping. It is likely that BAT is the site where such a compensatory response is taking place, given that its thermogenic program remained unaffected in hypothyroid mice (Table 1), whereas the SKM program was largely down-regulated (Table 1). Two pieces of evidence support this. First, our previous observation that norepinephrine turnover in the mouse BAT is doubled during hypothyroidism (19). Second, our current observation that only at thermoneutrality did hypothyroidism reduce daily EE (Fig. 2C and Supplemental Fig. 1C). Such a tighter control of EE in mice reflects the about 10-fold greater surface/mass ratio when compared with rats, what makes this species particularly reactive to cold stress (20). While considering whether these findings have any significance for humans, it is notable that functional BAT has been identified in adult humans, which could play a role in thermoregulation and energy homeostasis (7). In addition, some have suggested that performing experiments in mice at thermoneutrality is a way to "humanize" their thermal homeostasis, given that most of us live a so called "thermoneutral life" due to clothes and housing (17). All this highlights the importance of our present findings for human physiology and pathophysiology.

A remarkable byproduct of this compensatory mechanism is that at 22 C, hypothyroid mice are protected against diet-induced obesity (Fig. 1), *i.e.* only at thermoneutrality did hypothyroid mice become obese when placed on a HFD (Fig. 1). These findings are reminiscent of the D2KO mouse, *i.e.* 1) increased BAT sympathetic activity and 2) protection against diet-induced obesity at 22 C, both of which are dissipated at thermoneutrality (21). D2KO mice have normal serum T_3 levels, and hypothyroidism is localized to D2-expressing tissues, such as BAT, due to impaired capacity of D2-mediated T_4 to T_3 conversion. Another similar mouse model is the TRα1R384C knockin, which has a 10-fold reduced affinity to the ligand T_3. These animals are lean and resistant to diet-induced obesity due to a hypermetabolic BAT (due to sympathetic activation) (22), a phenotype that is dissipated if the animals are reared at 30 C (23).

Understanding such compensatory mechanisms in hypothyroid mice unveiled fundamental differences between activation of BAT and SKM thermogenic programs and the way these pathways are influenced by thyroid hormone and ambient temperature. The SKM (Table 1), but not the BAT (Table 1), thermogenic program was down-regulated by hypothyroidism or acclimatization to 30 C. In fact, the BAT thermogenic program was only down-regulated when hypothyroidism was combined with thermoneutrality (Table 1), markedly decreasing EE (Fig. 2C and Supplemental Fig. 1C). In addition, placing euthyroid controls on a HFD accelerated EE (Fig. 2C and Supplemental Fig. 1F) and activated BAT (Table 1) but not SKM (Table 1) thermogenic programs. This is in agreement with previous studies that SNS activity in SKM is mostly unresponsive to diet or cold exposure (24). On the other hand, HFD failed to accelerate EE in hypothyroid mice (Fig. 2C and Supplemental Fig. 1F), and neither SKM (Table 1) nor BAT (Table 1) thermogenic programs were activated.

Thus, despite the down-regulation in the SKM thermogenic program caused by hypothyroidism or thermoneutrality, strong compensatory mechanisms in the BAT offset the lesser contribution of SKM to daily EE.

Studying mice acclimatized to thermoneutral temperature, which decrease SNS activity, exposed the important role played by thyroid hormone in BAT and SKM thermogenesis, which is to be expected based on previous studies (1, 2). In the BAT, thyroid hormone stimulates *UCP-1* gene expression and other key metabolic pathways (8, 21, 25). At the same time, thyroid hormone accelerates the turnover rate of a series of ionic and substrate cycles in SKM, including the sarcoplasmic endoplasmatic reticulum calcium ATPase and favoring the expression of myosin heavy chain isoforms with higher catalytic (ATPase) activity (26, 27), all of which accelerates ATP turnover and heat production. However, it is not entirely clear how hypothyroid animals were protected against diet-induced obesity without accelerating daily VO_2 or EE (Fig. 2, A and C, and Supplemental Fig. 1, D and F), even though the much lower RQ in hypothyroid mice placed on a HFD indicates increased fat oxidation (Fig. 2B and Supplemental Fig. 1E). Notably, caloric intake was decreased in hypothyroid mice kept on HFD at 22 C, whereas at thermoneutrality, caloric intake was increased, precisely when they exhibited diet-induced obesity (Fig. 1A). Thus, it seems logical that the combination of sustained BAT activation and decreased in caloric intake would provide hypothyroid mice with protection against diet-induced obesity, a mechanism that is lost at thermoneutrality. Furthermore, alternative thermogenic pathways have been proposed in other models of BAT disruption, *i.e.* the $UCP^{-/-}$ (28) and $Thra^{-/-}$ (thyroid hormone receptor a) (29) mice, and could be playing a role in systemic hypothyroidism as well.

The approximately 50% drop in hepatic triglyceride content as a result of acclimatization to 30 C, regardless of the type of food the animals were given (Fig. 1F), was remarkable. In euthyroid controls kept on a chow diet, this drop was associated with a decrease in *PGC-1β* and *ApoB* mRNA levels (Table 2), whereas on a HFD, there was a reduction in the expression of a much broader group of genes involved in lipid metabolism (Table 2), including lipogenesis (PPARγ and spot-14), β-oxidation (PGC-1β, PPARα, and CPT-1β), and fatty acid transport and secretion (FATP-2 and ApoB). The liver responsiveness to acclimatization to 30 C was quite different in hypothyroid animals (Fig. 1F), which by itself reduced gene expression of PGC-1β, spot-14, ApoB, and increased PPARα mRNA (Table 2). In fact, thyroid hormone is known for stimulating hepatic β-oxidation (30), and T_3 positively regulates hepatic FGF-21 gene expression (31). T_3 and its thyroid hormone receptor selective agonist GC-1 exert a strong inhibitory effect on the development liver triglyceride deposits in the high-fat cholinemethionine-deficient diet model of liver steatosis and hepatocyte injury, possibly by promoting export of lipids from the liver via very low-density lipoproteins and oxidation of excess fatty acids (32–34). Despite this, hypothyroidism did not exaggerate HFD-induced liver steatosis at 22 C (Fig. 1F) but prevented the drop in liver triglyceride caused by thermoneutrality, resulting in severe steatosis (Fig. 4H). At 30 C, only in the hypothyroid animals was there an induction of prolipogenic genes such as *ACC*, *spot-14*, and *PPARγ* by HFD (Table 2), the latter reaching levels that topped those in euthyroid control animals (Fig. 1F). Liver steatosis is also observed in other models of thyroid signaling disruption, such as the $Thrb^{PV/PV}$ mouse, which also has increased PPARγ signaling (35) and in D2KO mouse (15).

Systemic hypothyroidism in mice promotes fasting hyperglycemia (36), and hypothyroid mice exhibit slight glucose intolerance (Fig. 3A). Unexpectedly, in both euthyroid controls and hypothyroid mice, acclimatization to 30 C decreased fasting blood glucose and improved tolerance to glucose (Fig. 3, B and C) via a mechanism that involves enhanced responsiveness to insulin (Fig. 3, I and J). This was also partially observed in euthyroid controls and hypothyroid animals kept on a HFD, although the magnitude of the changes was less impressive (Fig. 3, O-R). These findings are remarkable and indicate that a reduction in thermal stress and sympathetic activity has tremendous beneficial effects in glucose homeostasis, the mechanistic nature of which remains to be elucidated.

In conclusion, systemic or localized disruption of thyroid hormone signaling in mice triggers a strong metabolic response. This response takes place mainly in the BAT and sustains basal metabolic rate despite down-regulation of the SKM thermogenic program. A byproduct of this response is protection against diet-induced obesity when animals are placed on a HFD. This phenotype is reversed at thermoneutrality, and hypothyroid mice become obese when placed on a HFD. These findings highlight the relevance of BAT to the overall thermal homeostasis of small rodents whereas minimizing the role played by SKM in this process. Acclimatization to thermoneutrality dramatically improves glucose homeostasis and lowers hepatic triglyceride content, the latter eliminated by hypothyroidism.

Acknowledgments

Address all correspondence and requests for reprints to: Antonio C. Bianco, M.D., Ph.D., University of Miami Miller School of

Medicine, 1400 North West 10th Street, Dominion Towers Suite 816, Miami, Florida 33136. E-mail: abianco@deiodinase.org.

This work was supported by the National Institute of Diabetes and Digestive and Kidney Diseases Research Grant 65055.

Disclosure Summary: The authors have nothing to disclose.

References

1. **Bianco AC, Maia AL, da Silva WS, Christoffolete MA** 2005 Adaptive activation of thyroid hormone and energy expenditure. Biosci Rep 25:191–208
2. **Silva JE** 2006 Thermogenic mechanisms and their hormonal regulation. Physiol Rev 86:435–464
3. **Lowell BB, Spiegelman BM** 2000 Towards a molecular understanding of adaptive thermogenesis. Nature 404:652–660
4. **Ring GC** 1942 The importance of the thyroid in maintaining an adequate production of heat during exposure to cold. Am J Physiol 137:582–588
5. **Sellers EA, You SS** 1950 Role of the thyroid in metabolic responses to a cold environment. Am J Physiol 163:81–91
6. **Bianco AC, Silva JE** 1987 Intracellular conversion of thyroxine to triiodothyronine is required for the optimal thermogenic function of brown adipose tissue. J Clin Invest 79:295–300
7. **Celi FS** 2009 Brown adipose tissue—when it pays to be inefficient. N Engl J Med 360:1553–1556
8. **Bianco AC, Sheng XY, Silva JE** 1988 Triiodothyronine amplifies norepinephrine stimulation of uncoupling protein gene transcription by a mechanism not requiring protein synthesis. J Biol Chem 263:18168–18175
9. **Young JB, Saville E, Rothwell NJ, Stock MJ, Landsberg L** 1982 Effect of diet and cold exposure on norepinephrine turnover in brown adipose tissue of the rat. J Clin Invest 69:1061–1071
10. **Nedergaard J, Golozoubova V, Matthias A, Asadi A, Jacobsson A, Cannon B** 2001 UCP1: the only protein able to mediate adaptive non-shivering thermogenesis and metabolic inefficiency. Biochim Biophysics Acta 1504:82–106
11. **Lönn L, Stenlöf K, Ottosson M, Lindroos AK, Nyström E, Sjöström L** 1998 Body weight and body composition changes after treatment of hyperthyroidism. J Clin Endocrinol Metab 83:4269–4273
12. **Kyle LH, Ball MF, Doolan PD** 1966 Effect of thyroid hormone on body composition in myxedema and obesity. N Engl J Med 275: 12–17
13. **Wolf M, Weigert A, Kreymann G** 1996 Body composition and energy expenditure in thyroidectomized patients during short-term hypothyroidism and thyrotropin-suppressive thyroxine therapy. Eur J Endocrinol 134:168–173
14. **Curcio C, Lopes AM, Ribeiro MO, Francoso Jr OA, Carvalho SD, Lima FB, Bicudo JE, Bianco AC** 1999 Development of compensatory thermogenesis in response to overfeeding in hypothyroid rats. Endocrinology 140:3438–3443
15. **Castillo M, Hall JA, Correa-Medina M, Ueta C, Won Kang H, Cohen DE, Bianco AC** 2011 Disruption of thyroid hormone activation in type 2 deiodinase knockout mice causes obesity with glucose intolerance and liver steatosis only at thermoneutrality. Diabetes 60:1082–1089
16. **Zavacki AM, Ying H, Christoffolete MA, Aerts G, So E, Harney JW, Cheng SY, Larsen PR, Bianco AC** 2005 Type 1 iodothyronine deiodinase is a sensitive marker of peripheral thyroid status in the mouse. Endocrinology 146:1568–1575
17. **Feldmann HM, Golozoubova V, Cannon B, Nedergaard J** 2009 UCP1 ablation induces obesity and abolishes diet-induced thermogenesis in mice exempt from thermal stress by living at thermoneutrality. Cell Metab 9:203–209
18. **Cannon B, Nedergaard J** 2011 Nonshivering thermogenesis and its adequate measurement in metabolic studies. J Exp Biol 214:242–253
19. **Christoffolete MA, Linardi CC, de Jesus L, Ebina KN, Carvalho SD, Ribeiro MO, Rabelo R, Curcio C, Martins L, Kimura ET, Bianco AC** 2004 Mice with targeted disruption of the Dio2 gene have cold-induced overexpression of the uncoupling protein 1 gene but fail to increase brown adipose tissue lipogenesis and adaptive thermogenesis. Diabetes 53:577–584
20. **Kleiber M** 1972 Body size, conductance for animal heat flow and Newton's law of cooling. J Theor Biol 37:139–150
21. **Hall JA, Ribich S, Cristoffolete MA, Simovic G, Correa-Medina M, Patti ME, Bianco AC** 2010 Absence of thyroid hormone activation during development underlies a permanent defect in adaptive thermogenesis. Endocrinology 151:4573–4582
22. **Sjögren M, Alkemade A, Mittag J, Nordström K, Katz A, Rozell B, Westerblad H, Arner A, Vennström B** 2007 Hypermetabolism in mice caused by the central action of an unliganded thyroid hormone receptor α1. EMBO J 26:4535–4545
23. **Vujovic M, Nordström K, Gauthier K, Flamant F, Visser TJ, Vennström B, Mittag J** 2009 Interference of a mutant thyroid hormone receptor α1 with hepatic glucose metabolism. Endocrinology 150:2940–2947
24. **Dulloo AG, Young JB, Landsberg L** 1988 Sympathetic nervous system responses to cold exposure and diet in rat skeletal muscle. Am J Physiol 255:E180–E188
25. **Carvalho SD, Negrao N, Bianco AC** 1993 Hormonal regulation of malic enzyme and glucose-6-phosphate dehydrogenase in brown adipose tissue. The Am J Physiol 264:E874–E881
26. **Simonides WS, van Hardeveld C** 2008 Thyroid hormone as a determinant of metabolic and contractile phenotype of skeletal muscle. Thyroid 18:205–216
27. **Nunes MT, Bianco AC, Migala A, Agostini B, Hasselbach W** 1985 Thyroxine induced transformation in sarcoplasmic reticulum of rabbit soleus and psoas muscles. Z Naturforsch C 40:726–734
28. **Golozoubova V, Hohtola E, Matthias A, Jacobsson A, Cannon B, Nedergaard J** 2001 Only UCP1 can mediate adaptive nonshivering thermogenesis in the cold. FASEB J 15:2048–2050
29. **Pelletier P, Gauthier K, Sideleva O, Samarut J, Silva JE** 2008 Mice lacking the thyroid hormone receptor-α gene spend more energy in thermogenesis, burn more fat, and are less sensitive to high-fat diet-induced obesity. Endocrinology 149:6471–6486
30. **Araki O, Ying H, Zhu XG, Willingham MC, Cheng SY** 2009 Distinct dysregulation of lipid metabolism by unliganded thyroid hormone receptor isoforms. Mol Endocrinol 23:308–315
31. **Adams AC, Astapova I, Fisher FM, Badman MK, Kurgansky KE, Flier JS, Hollenberg AN, Maratos-Flier E** 2010 Thyroid hormone regulates hepatic expression of fibroblast growth factor 21 in a PPARα-dependent manner. J Biol Chem 285:14078–14082
32. **Lombardi B, Pani P, Schlunk FF** 1968 Choline-deficiency fatty liver: impaired release of hepatic triglycerides. J Lipid Res 9:437–446
33. **Perra A, Simbula G, Simbula M, Pibiri M, Kowalik MA, Sulas P, Cocco MT, Ledda-Columbano GM, Columbano A** 2008 Thyroid hormone (T3) and TRβ agonist GC-1 inhibit/reverse nonalcoholic fatty liver in rats. FASEB J 22:2981–2989
34. **Erion MD, Cable EE, Ito BR, Jiang H, Fujitaki JM, Finn PD, Zhang BH, Hou J, Boyer SH, van Poelje PD, Linemeyer DL** 2007 Targeting thyroid hormone receptor-β agonists to the liver reduces cholesterol and triglycerides and improves the therapeutic index. Proc Natl Acad Sci USA 104:15490–15495
35. **Zhu X, Cheng SY** 2010 New insights into regulation of lipid metabolism by thyroid hormone. Curr Opin Endocrinol Diabetes Obes 17:408–413
36. **Taguchi Y, Tasaki Y, Terakado K, Kobayashi K, Machida T, Kobayashi T** 2010 Impaired insulin secretion from the pancreatic islets of hypothyroidal growth-retarded mice. J Endocrinol 206:195–204

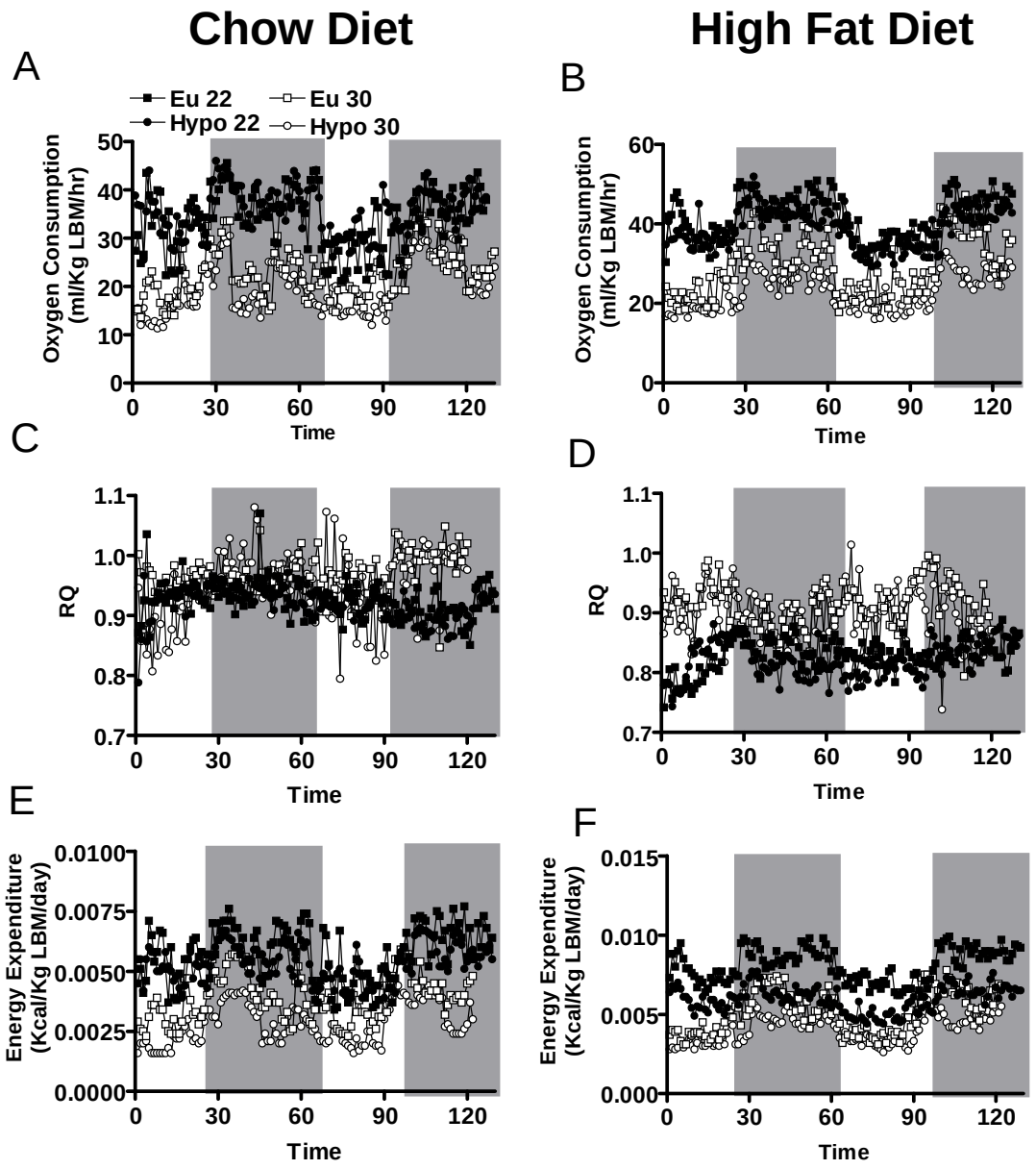

Supplemental Fig. 1

CAPÍTULO 4

Terceiro Artigo

Absence of myocardial thyroid hormone inactivating deiodinase results in restrictive cardiomyopathy in mice

Cintia B. Ueta[*], Behzad N. Oskouei[*], Emerson L. Olivares[*], Jose R. Pinto, Mayrin M. Correa, Gordana Simovic, Warner S. Simonides, Joshua M. Hare, and Antonio C. Bianco

[*]Estes autores tiveram igual contribuição para este trabalho.

Molecular Endocrinology 26: 809-818, 2012

Prêmio: Molecular Endocrinology Student award for an Outstanding Publication in 2012

Absence of Myocardial Thyroid Hormone Inactivating Deiodinase Results in Restrictive Cardiomyopathy in Mice

Cintia B. Ueta,* Behzad N. Oskouei,* Emerson L. Olivares,* Jose R. Pinto, Mayrin M. Correa, Gordana Simovic, Warner S. Simonides, Joshua M. Hare, and Antonio C. Bianco

Division of Endocrinology, Diabetes, and Metabolism (C.B.U., E.L.O., M.M.C., G.S., A.C.B.), Interdisciplinary Stem Cell Institute (B.N.O., J.M.H.), and Department of Molecular and Cellular Pharmacology (J.R.P.), University of Miami Miller School of Medicine, Miami, Florida 33136; and Laboratory for Physiology (W.S.S.), Institute for Cardiovascular Research, VU University Medical Center, 1081 HV Amsterdam, The Netherlands

Cardiac injury induces myocardial expression of the thyroid hormone inactivating type 3 deiodinase (D3), which in turn dampens local thyroid hormone signaling. Here, we show that the D3 gene (*Dio3*) is a tissue-specific imprinted gene in the heart, and thus, heterozygous D3 knockout (HtzD3KO) mice constitute a model of cardiac D3 inactivation in an otherwise systemically euthyroid animal. HtzD3KO newborns have normal hearts but later develop restrictive cardiomyopathy due to cardiac-specific increase in thyroid hormone signaling, including myocardial fibrosis, impaired myocardial contractility, and diastolic dysfunction. In wild-type littermates, treatment with isoproterenol-induced myocardial D3 activity and an increase in the left ventricular volumes, typical of cardiac remodeling and dilatation. Remarkably, isoproterenol-treated HtzD3KO mice experienced a further decrease in left ventricular volumes with worsening of the diastolic dysfunction and the restrictive cardiomyopathy, resulting in congestive heart failure and increased mortality. These findings reveal crucial roles for *Dio3* in heart function and remodeling, which may have pathophysiologic implications for human restrictive cardiomyopathy. **(*Molecular Endocrinology* 26: 809–818, 2012)**

The current model of thyroid hormone action holds that deiodinases mediate intracellular changes in thyroid hormone activation or deactivation that are key to many metabolic effects, regardless of plasma hormone concentrations. These enzymes, such as the type 2 deiodinase (D2), accelerate activation of T_4 to T_3 and increase local thyroid hormone action. In contrast, the type 3 deiodinase (D3) irreversibly inactivates both T_4 and T_3, thereby dampening thyroid hormone action and creating localized hypothyroidism on a cell-specific basis. Importantly, this local control of thyroid hormone action occurs without substantial changes in circulating levels of T_4 and T_3 and thus cannot be predicted by measurements of serum T_4 and/or T_3 levels (1).

There is widespread D3 expression in vertebrates during development, and D3 levels are inversely coordinated with D2, so that thyroid hormone signaling in a given tissue can be controlled according to the developmental stage (2). For example, in the 3-d period during which brown adipose tissue is formed (E16.5–E18.5), there is a simultaneous decrease in D3 and increase in D2, augmenting local T_3 concentration and thyroid hormone signaling (3). After birth, D3 expression subsides in most tissues to background levels, and D3 activity remains largely restricted to brain and skin. However, disease signals in the adult human and other mammals can reactivate D3 expression in a number of tissues (4, 5). In rat

ISSN Print 0888-8809 ISSN Online 1944-9917
Printed in U.S.A.

doi: 10.1210/me.2011-1325 Received November 17, 2011. Accepted February 9, 2012.
First Published Online March 8, 2012

* C.B.U., B.N.O., and E.L.O. contributed equally to this work.

Abbreviations: BW, Body weight; D2, type 2 deiodinase; D3, type 3 deiodinase; EE, energy expenditure; HtzD3KO, heterozygous D3 knockout; ISO, isoproterenol; IVCT, isovolumic ventricular contraction time; LV, left ventricle; MHC, myosin heavy chain; PLN, phospholamban; PV, pressure volume; RQ, respiratory quotient; RV, right ventricular; SERCA-2, sarcoplasmic reticulum Ca2-ATPase type 2; VO_2, oxygen consumption; WT, wild type.

myocardium, for example, right ventricular (RV) hypertrophy caused by pulmonary arterial hypertension results in an approximately 5-fold induction in local D3 activity, which in turn decreases sarcoplasmic reticulum Ca2-ATPase type 2 (SERCA-2)a and α-myosin heavy chain (MHC) gene expression, and increase levels of β-MHC mRNA, a pattern that is typical of the hypothyroid heart (6). In fact, D3 induction in this animal model is linked to RV hypoxia and accumulation of hypoxia inducible factor-1α, creating an anatomically specific reduction in local T_3 content and action (7). Myocardial infarction in rats (8) and mice (9) also leads to a potent chamber-specific induction of D3. In the latter model, *in vivo* measurement of thyroid hormone-dependent transcription activity in cardiomyocytes using a luciferase reporter assay revealed a marked decrease post-myocardial infarction, which was associated with a 50% decrease in left ventricle (LV) T_3 concentration (9).

The paradigm emerging from these studies is that the hypoxic myocardium banks on the D3-mediated decrease in T_3 signaling to ultimately slow down the rate of oxygen consumption (VO_2); it is not clear yet whether local hypothyroidism is necessary for myocardium remodeling. At the same time, the link between hypoxia and D3 induction has also been observed in cultures of hepatocytes and neurons (7, 10), suggesting that these D3-mediated changes in local thyroid hormone action constitute a broad adaptive response. In fact, a number of other disease and tissue injury models exhibit similar D3 reactivation and local down-regulation of thyroid hormone signaling, such as cerebral hypoxia, inflammation or oxidative stress, nerve injury, and liver resection-regeneration, suggesting that D3 induction in the heart is part of the hypoxia inducible factor-1α-orchestrated response generally seen in tissue injury, hypoxia, and/or ischemia (5).

The D3 gene (*Dio3*) is located in the delta-like 1 homolog-*Dio3* domain positioned on distal mouse chromosome 12 and human chromosome 14 (11). The domain contains three paternally imprinting protein-encoding genes that share common regulatory elements, delta-like 1 homolog, retrotransponson-like gene 1, and *Dio3*, *i.e.* only the paternally inherited allele is expressed. This is explained based on the differences between the chromatin structures such as degree of DNA methylation and post-translational modifications to core histone proteins. In mice, *Dio3* imprinting does not happen in all tissues, and even where it happens is not complete, with the paternal allele contributing with approximately 84% of expression in the embryo and 50–60% in the placenta (12). Here, we show that *Dio3* imprinting takes place in the mouse heart but not in the brain, and thus, the heterozygous D3 knockout (HtzD3KO) mice lends itself as a model of cardiac-specific *Dio3* inactivation. Strikingly, the myocardium of 1-d-old HtzD3KO pups is normal but, as a result of the lifelong cardiac increase in thyroid hormone signaling, 4-month-old animals exhibit a unique phenotype of restrictive cardiomyopathy that includes myocardial fibrosis, impaired myocardial contractility, and diastolic dysfunction. A sympathetic overdrive with a 10-d treatment with isoproterenol (ISO) worsened this phenotype, with further reductions in the LV volumes and accentuation of the diastolic dysfunction, which caused congestive heart failure and doubled the mortality rate. In sharp contrast, wild-type (WT) siblings were able to potently reactivate myocardial D3, and cardiac remodeling took place with LV dilatation. Given that D3 reactivation is present in critically ill patients with compromised myocardial perfusion (4), the present findings may have

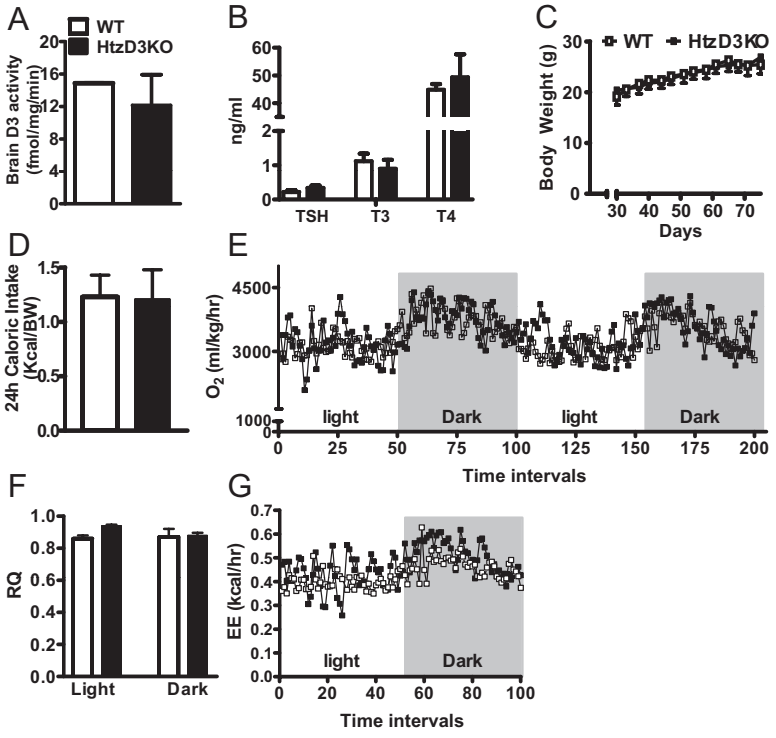

FIG. 1. HtzD3KO mice are systemically euthyroid. Cerebral cortex D3 activity (A), thyrotropin, T_3, and T_4 serum levels (B), body weight (data entries from both groups are superimposed) (C), daily caloric intake (D), VO_2 measure during 48-h period (E), 24-h RQ (F), and EE (total daily EE) (G) in WT and HtzD3KO mice. *Shaded areas* indicate night time. A–G, Data are expressed as mean ± SEM of three to five animals in each group.

pathophysiologic implications for human restrictive cardiomyopathy.

Results

The HtzD3KO mouse is euthyroid

The WT heart exhibits minimal D3 activity (~0.4 fmol T_3/min·mg protein), about 40-fold less than the D3 activity found in the brain (Fig. 1A, see also Fig. 3A below). The HtzD3KO mouse has normal brain D3 activity (Fig. 1A) but lacks cardiac D3 activity (<0.15 fmol T_3/min·mg protein), indicating that the heart is one of the tissues in which *Dio3* is imprinted. Thus, the HtzD3KO mouse constitutes a suitable model of cardiac-specific *Dio3* inactivation in an otherwise systemically euthyroid mouse. Accordingly, HtzD3KO mice exhibit normal serum levels of thyrotropin, T_4 and T_3 (Fig. 1B), and growth rates (Fig. 1C) as compared with the WT siblings. In addition, HtzD3KO mice exhibit normal 24-h caloric intake (Fig. 1D), daily VO_2 (Fig. 1E), respiratory quotient (RQ) (Fig. 1F), and energy expenditure (EE) (Fig. 1G), parameters that are strongly affected by thyroid status and serum thyroid hormone levels.

The HtzD3KO heart exhibits fibrosis, decreased maximal force, and diastolic dysfunction

The neonatal (postnatal day 1) HtzD3KO heart is histologically normal (Fig. 2, A and B) with similar expression pattern of key genes as compared with WT controls (Supplemental Table 1, published on The Endocrine Soceity's Journals Online web site at http://mend.endojournals.org). However, in 4-month-old HtzD3KO mice, the LV exhibits a typical gene expression pattern of increased thyroid hormone signaling (13, 14), *i.e.* an approximately 30% increase in the α-MHC/β-MHC mRNA ratio (Supplemental Table 1). The HtzD3KO LV also exhibits approximately 35% decrease in the SERCA-2/phospholamban (PLN) mRNA ratio as well as an approximately 30% increase in uncoupling protein-2 mRNA (Supplemental Table 1). The expression of other metabolically relevant genes, such as peroxisome proliferator-activated receptor α, glucose transporter-4, glutathione peroxidase-1, was not altered in the HtzD3KO hearts (Supplemental Table 1).

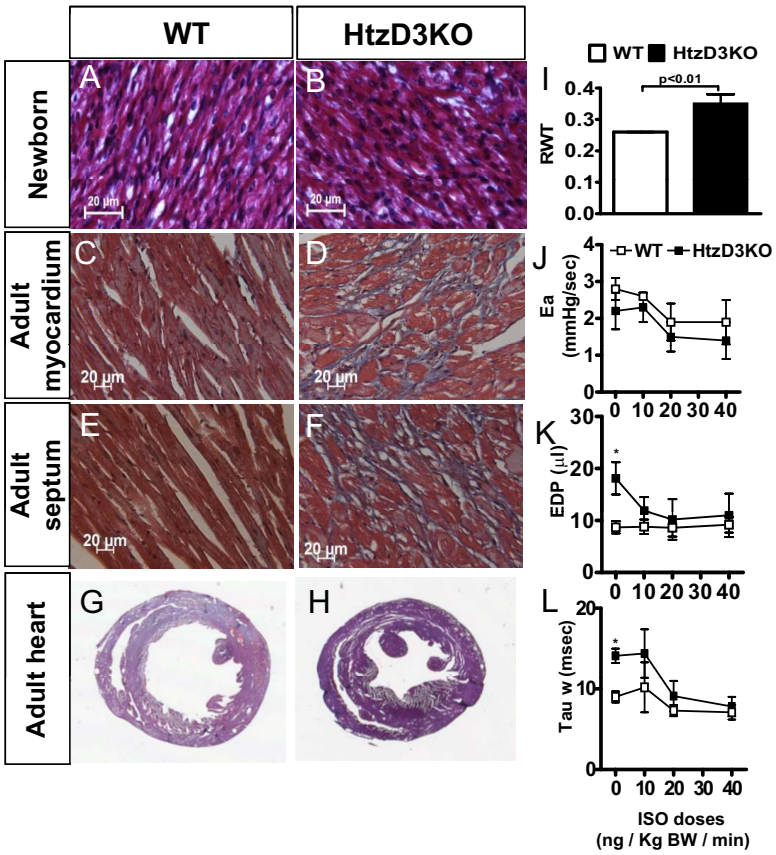

FIG. 2. Effect of life-long D3 inactivation in the heart. Representative sections of newborn LV myocardium (A and B), adult (4 month old) LV myocardium (C and D), adult cardiac septum (E and F), and heart cross-sectional analyses (G and H) of adult WT and HtzD3KO mice obtained after 20 mM KCl was infused for 10 min. *Scale bars*, 20 μm. Relative wall thickness (RWT) is the LV/RV wall ratio (I), arterial elastance (Ea) (J), end-diastolic pressure (EDP) (K), isovolumic relaxation constant (τ) (L) at baseline and during acute ISO infusion at the indicated doses. In A–L, data are expressed as mean ± SEM of three to four animals in each group; *, $P < 0.01$ *vs.* WT siblings.

To study the cardiac impact of life-long localized myocardial increase in thyroid hormone signaling, we first looked at structural parameters. Histologic examination of the HtzD3KO heart revealed that the LV myocardium (Fig. 2, C and D) and cardiac septum (Fig. 2, E and F) had substantial interstitial fibrosis, a feature previously reported in the thyrotoxic heart (15, 16). This coincides with an approximately 12-fold increase in type I collagen mRNA levels observed in the HtzD3KO LV (Supplemental Table 1). HtzD3KO hearts exhibited signs of cardiac hypertrophy (8.8 ± 0.51 *vs.* 7.2 ± 0.27 mg/mm heart weight/tibial length; n = 8; $P = 0.04$) associated with a thicker LV wall (Fig. 2, G–I). The impact of myocardial fibrosis was documented in preparations of HtzD3KO skinned papillary muscles, which exhibited about 30% decrease in calcium-activated maximal force (46 ± 1.2 *vs.* 32 ± 0.88 kN/m^2; n = 14; $P < 0.01$), with a similar stiffness

TABLE 1. Ecochardiographic and Doppler studies of WT and HtzD3KO hearts

Parameter	WT	HtzD3KO
Echocardiographic studies		
Heart rate (bpm)	480.6 ± 13	474.9 ±8.5
LV volume, diastole (μl)	67.8 ±5.6	48.3 ±4.0[a]
LV volume, systole (μl)	27.7 ±3.1	16.2 ±2.7[a]
Fractional shortening (%)	31.1 ±2.1	41.5 ±3.2[a]
Ejection fraction (%)	58.9 ±2.9	70.7 ±3.4[a]
Cardiac output (ml/min)	17.3 ±2.1	14.8 ±1.1[a]
Endocardial stroke volume (μl)	35.9 ±4.0	31.4 ±2.1[a]
Doppler studies		
E/A ratio	1.40±0.2	1.10±0.1[b]
AV peak gradient (mm Hg)	2.70±0.5	1.70±0.2[a]
Ejection time (msec)	47.5 ±2.7	46.5 ±1.2
Isovolumic contraction time (msec)	23.0 ±1.6	25.0 ±1.8
Isovolumic relaxation time (msec)	21.5 ±1.0	22.5 ±2.4
AV peak velocity (mm/sec)	807.0 ± 87	645.0 ±26[b]
MV deceleration time (msec)	20.0 ±5.0	21.0 ±2.0
Aortic acceleration time (msec)	16.0 ±2.9	15.5 ±0.9

Values are the mean ± SEM of 4–20 animals per group.

[a] $P < 0.01$ *vs.* WT, *t* test.

[b] $P < 0.05$ *vs.* WT, *t* rest.

(ranging from ~2 to 18 kN/m^2) during a 10–40% stretch ramp and myofilament calcium sensitivity (pCa_{50} = 5.71 ± 0.01 *vs.* 5.68 ± 0.01).

HtzD3KO LV exhibited impaired diastolic function as assessed by echocardiography (Table 1). Importantly LV volumes were decreased, as was the E/A (early and late/atrial) ratio, an index of diastolic chamber filling. Cardiac expression of brain natriuretic peptide mRNA levels, a sensitive marker of congestive heart failure, was not elevated in HtzD3KO LV (Supplemental Table 1).

Subsequent studies of pressure-volume (PV) relationships at baseline and during acute infusion of increasing doses of ISO indicate that the development of LV hypertrophy and fibrosis is not due to an increase in cardiovascular afterload given that arterial elastance was similar in both groups (Fig. 2J). However, the LV diastolic function assessed by the end-diastolic pressure (Fig. 2K) and by isovolumic relaxation constant (τ) (Fig. 2L) was increased in the HtzD3KO compare with WT at the baseline. Although resting parameters of contractile function and performance were similar between groups, the β-adrenergic contractile reserve was suppressed (Supplemental Fig. 1, published on The Endocrine Society's Journals Online web site at http://mend.endojournals.org), consistent with the findings in isolated muscle strips.

ISO-induced LV D3 expression promotes cardiac-specific hypothyroidism

We next extended our analysis and tested the consequences of absence of cardiac D3 during adrenergic overdrive, a recognized model of endocardial injury and diastolic dysfunction that can lead to heart failure (17). Accordingly, only in WT animals did chronic treatment with ISO stimulated D3 reactivation (~2.5-fold induction) (Fig. 3A) given that induction of *Dio3* is part of the changes in cardiac gene expression associated with ven-

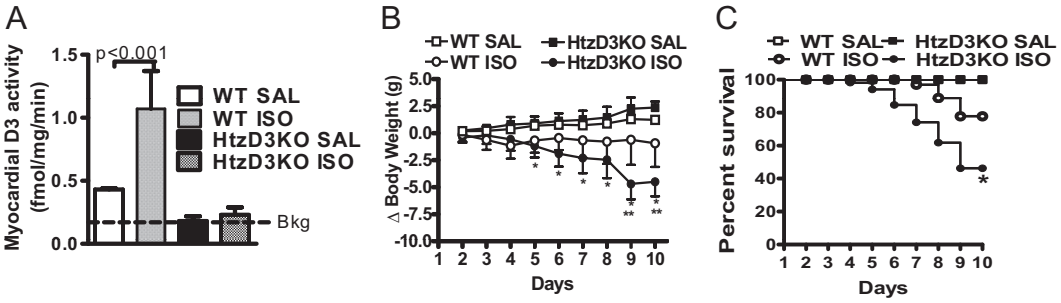

FIG. 3. Effects of treatment with ISO on myocardial D3 activity, body weight, and survival of WT and HtzD3KO mice. A, LV D3 activity after ISO or saline (SAL) injection. Bkg, Background activity. Data are expressed as mean ± SEM of 3–13 animals in each group. B, Animals were weighted daily, and variances (ΔBW) are shown. Data are expressed as mean ± SEM of 5–10 animals in each group; *, $P < 0.01$ *vs.* WT-ISO and **, $P < 0.001$ *vs.* HtzD3KO-SAL. C, Kaplan-Mayer survival plot during ISO treatment. Data are expressed as mean ± SEM of five to eight animals in each group (data entries from WT-SAL and HtzD3KO-SAL are superimposed); $P < 0.01$ *vs.* WT-ISO.

tricular hypertrophy (6, 7). In all animals, RV D3 activity was undetectable (Supplemental Fig. 2).

ISO administration minimally affected body weight in WT siblings ($P > 0.05$) (Fig. 3B), but resulted in an approximately 20% cumulative mortality rate in this group as shown by the Kaplan-Meyer survival curve (Fig. 3C). However, in the HtzD3KO animals, ISO treatment was associated with significant drop in body weight that was evident as early as d 5, reaching approximately 15% at the end of the 10-d treatment period (Fig. 3B). The cumulative mortality rate was doubled in the HtzD3KO animals, reaching about 40% (Fig. 3C). In both groups of animals, death was sudden and associated with signs of pulmonary edema and LV insufficiency.

The potent cardiac induction of D3 in the WT animals triggered by ISO (Fig. 3A) is likely to reduce local thyroid hormone signaling provided by plasma T_3. This is in contrast with the situation in the HtzD3KO heart, to which plasma T_3 has unopposed access given its lack of D3. To test this scenario, we analyzed the isovolumic ventricular contraction time (IVCT), a T_3-sensitive echocardiographic parameter, in both groups of animals before/after treatment with ISO (18). In the WT siblings, which developed the potent cardiac D3 induction (Fig. 3A), treatment with ISO caused an approximately 50% prolongation in the IVCT (Fig. 4A), a finding that is compatible with the D3-mediated reduction in thyroid hormone signaling. However, besides T_3, there are other potential regulators of this parameter, particularly in the context of ISO-induced cardiac hypertrophy. Thus, the T_3 dependency of these changes was established in the HtzD3KO animals, in which there was no induction of D3, and no ISO-induced changes in IVCT were observed (Fig. 4A). At the same time, the isovolumic ventricular relaxation time remained stable in all groups during treatment with ISO (Fig. 4B).

The changes in the myocardial α-MHC/β-MHC ratio correlated only in part with the observed D3-induced modifications in thyroid hormone signaling, given that in the failing heart, there is a natural shift in MHC isoform content from α-MHC to β-MHC and a decrease in the SERCA-2/PLN ratio (13). Thus, in ISO-treated WT siblings, induction of D3 correlated well with a reduction in α-MHC mRNA (1.02 ± 0.02 *vs.* 0.81 ± 0.02, $P < 0.001$; n = 3) and elevation in β-MHC (1.05 ± 0.02 *vs.* 1.23 ± 0.02, $P < 0.003$; n = 3). Furthermore, there was no significant decrease in α-MHC mRNA (1.23 ± 0.02 *vs.* 1.13 ± 0.005, not significant; n = 3) in ISO-treated HtzD3KO animals. Nevertheless, the α-MHC/β-MHC ratio was reduced as in the WT siblings largely due to a marked elevation in β-MHC mRNA (0.98 ± 0.02 *vs.* 0.64 ± 0.64, $P < 0.05$; n = 3). SERCA-2 mRNA levels were not affected by treatment with ISO but SERCA-2/PLN ratio was, dropping about 30% only in the ISO-treated HtzD3KO animals (1.3 ± 0.03 *vs.* 0.96 ± 0.001, $P < 0.0003$; n = 3). Changes in thyroid hormone signaling and gene expression profiles were chamber specific, given that α-MHC/β-MHC and SERCA-2/PLN ratios remained unaffected in the RV of ISO-treated animals (Supplemental Fig. 2).

In WT animals, 10-d treatment with ISO reduced serum T_4 (T_4, 45 ± 2.1 *vs.* 23 ± 1.7 ng/ml; n = 3; $P < 0.001$ by ANOVA) and increase serum T_3 (T_3, 1.06 ± 0.04 *vs.* 1.35 ± 0.02 ng/ml; n = 5; $P < 0.001$), which reflects accelerated D2-mediated conversion of T_4 to T_3, a cAMP-dependent pathway. In the HtzD3KO animals, the interpretation

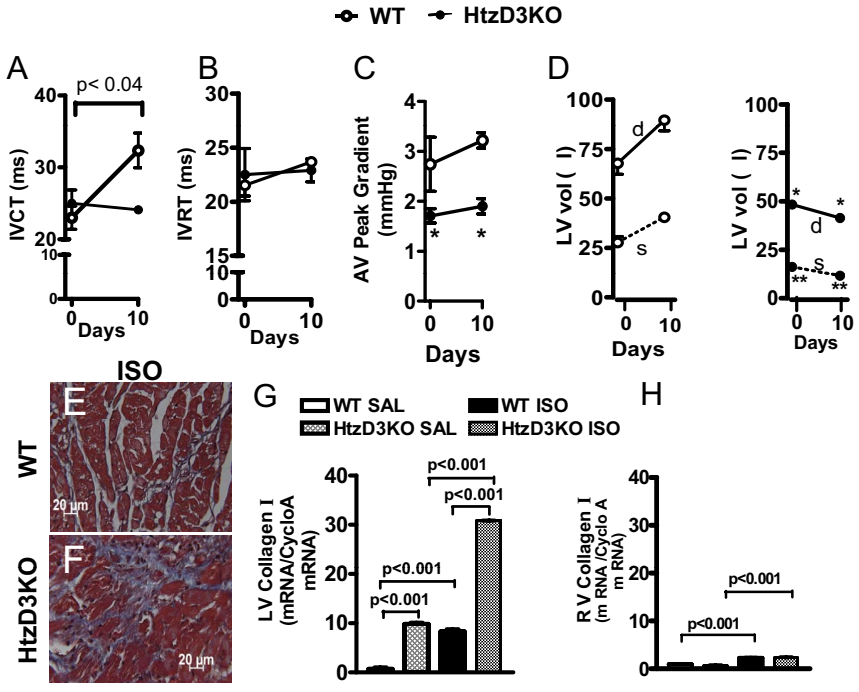

FIG. 4. Cardiac function and the impact of ISO treatment in WT and HtzD3KO mice. IVCT (A), isovolumic ventricular relaxation time (IVRT) (B), and aortic valve (AV) (C) peak gradient as assessed by Doppler at baseline and after 10 d of treatment with ISO; *, $P < 0.01$ *vs.* WT siblings. D, LV volumes (LV vol) detailed as end-diastolic volume (d) and end-systolic volume (s) as assessed by echocardiography at baseline and after 10 d of treatment with ISO; *, $P < 0.01$ *vs.* WT siblings end-diastolic volume and **, $P < 0.0003$ *vs.* WT sibling end-systolic volume. E and F, Representative histological sections of LV myocardium from WT and HtzD3KO mice after ISO treatment. *Scale bars*, 20 μm. Myocardial collagen I mRNA levels in the LV (G) and RV (H). In A—H, data are expressed as mean ± SEM of three to five animals in each group.

of the thyroid function tests is complicated by the weight loss and illness exhibited by these animals (Fig. 3, B and C). In these animals, both serum T_4 (49 ± 8.3 *vs.* 16 ± 2.7 ng/ml; n = 3; $P < 0.001$ by ANOVA) and serum T_3 (0.90 ± 0.04 *vs.* 0.77 ± 0.04 ng/ml; n = 5; $P < 0.05$ by ANOVA) were reduced by treatment with ISO.

The HtzD3KO mouse develops accentuation of restrictive cardiomyopathy during ISO-induced cardiac hypertrophy

To document this further, we used echocardiography and Doppler studies and examined the hearts of the surviving animals at the end of the 10-d ISO treatment, focusing on the LV volumes during the cardiac cycle (Fig. 4). In the WT siblings, the aortic valve peak gradient, which reflects the pressure gradient between the LV and the aorta, was not affected by treatment with ISO in either group, but this parameter was significantly greater in the WT siblings as compared with the HtzD3KO mice (Fig. 4C).

In addition, at baseline, the end-diastolic and end-systolic LV volumes were decreased in the HtzD3KO animals compare with WT siblings, indicating a decrease in LV dimensions (Fig. 4D). In the WT siblings, treatment with ISO increased the end-diastolic and end-systolic LV volumes (Fig. 4D), indicating cardiac remodeling and dilatation. In sharp contrast, in the htzD3KO animals, treatment with ISO decreased both the end-diastolic and the end-systolic ventricular volumes (Fig. 4D), indicating an accentuation of the restrictive cardiomyopathy.

The necropsy of these animals revealed that in both groups treatment with ISO increased heart weight, albeit more pronounced in the HtzD3KO animals (~35 *vs.* ~50% after correction for tibial length) (Supplemental Fig. 3A). At the same time, only in the HtzD3KO animals did ISO treatment result in a heavier lung (Supplemental Fig. 3B) and an approximately 3.5-fold increase in brain natriuretic peptide mRNA levels (Supplemental Fig. 3C), consistent with congestive heart failure. On the other hand, ventricular atrial natriuretic peptide mRNA levels were unaffected (Supplemental Fig. 3D), and liver weight remained similar in all groups, suggesting no or minimal involvement of the RV function (Supplemental Fig. 3E).

There was clear evidence of myocardial fibrosis in the ISO-treated WT siblings (Fig. 4E), whereas the fibrosis observed at baseline in the HtzD3KO animals did seem to intensify further by ISO (Fig. 2, D and F, *vs.* Fig. 4F). These data were largely confirmed by measuring myocardium collagen I mRNA levels by RT-PCR (Fig. 4G). In all groups and times, induction of type I collagen expression was minimal in the RV (Fig. 4H).

Analysis of the skinned cardiac fiber and gene expression profile explain diastolic dysfunction in HtzD3 heart

To understand the nature of the diastolic dysfunction in the ISO-treated HtzD3KO hearts, skinned cardiac fibers were studied *in situ*. Treatment with ISO decreased about 30% the calcium-activated maximal force (Fig. 5A) in the WT fibers, reaching the levels seen in the HtzD3KO. At the same time, both WT and HtzD3KO siblings exhibited a similar increase in basal force as a function of fiber stretch (stiffness), which ranged from about 2 to 50 kN/m^2 (Fig. 5B). The assessment of myofilament calcium sensitivity revealed a leftward shift in the ISO-treated HtzD3KO animals, a typical alteration ob-

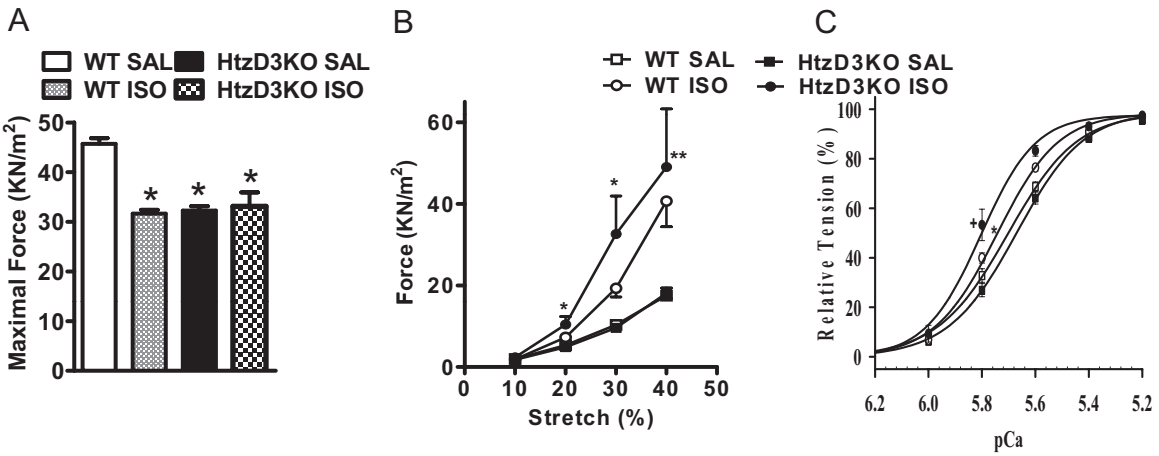

FIG. 5. Functional studies in skinned cardiac fibers of WT and HtzD3KO mice treated with ISO. A, Maximal force (kN/m^2) developed at maximal Ca^{2+} concentrations (pCa 4.0); *, $P < 0.001$ *vs.* WT-saline (SAL). B, Skinned fiber resistance to different stretch levels under resting conditions (pCa 8.0); *, $P < 0.001$ *vs.* HtzD3KO-SAL and **, $P < 0.01$ *vs.* WT-ISO. C, Ca^{2+} dependence of force development; the pCa_{50} (Ca^{2+} concentration needed to reach 50% of the maximum force) and n_{Hill} (index of thin filament cooperativity) values are: 5.7 ± 0.01 and 3.5 ± 0.11, 5.8 ± 0.01 and 3.9 ± 0.14, 5.7 ± 0.01 and 3.6 ± 0.20, and 5.8 ± 0.02 and 4.8 ± 0.52 for WT-SAL, WT-ISO, HtzD3KO-SAL, and HtzD3KO-ISO, respectively. Data are expressed as mean ± SEM of 12–14 data points in each group.

served during hypertrophic cardiomyopathy (Fig. 5C) (19).

Furthermore, the analyses of key myocardium mRNA also indicated a contrasting metabolic profile between WT and HtzD3KO animals after treatment with ISO. Although ISO treatment increased by 3- to 4-fold uncoupling protein-2 and GPX-1 (response to oxidative stress), Glut-4 (glycolysis), and PPARα (α-oxidation) mRNA levels in WT animals, all of these mRNA were decreased by 3- to 4-fold in the HtzD3KO animals, suggesting a maladaptive process (Supplemental Fig. 4).

Discussion

LV hypertrophy is widespread, affecting more than 15% of the United States adult population. It is progressive, and its prevalence increases with age, affecting more than one-third of individuals over the age of 70 (20). Although we do not understand fully the molecular underpinnings of LV hypertrophy, it is remarkable that D3-mediated cardiac-specific hypothyroidism rises as a common denominator and important feature in cardiac remodeling. In addition, other mechanisms to decrease myocardial thyroid hormone signaling that result in a hypothyroid-like mRNA phenotype have been reported during cardiac remodeling, including a decrease in thyroid hormone receptor expression in two rat models of cardiac hypertrophy [voluntary wheel running for 10 wk in adult male Wistar rats or ascending aortic constriction (pressure gradient $\approx$75 mm Hg) for 4 wk] (21). The most striking finding in the present study, however, was the contrasting phenotype caused by the absence of myocardial D3 during adrenergic overdrive (Fig. 4D). Although ISO-treated WT animals develop an enlarged LV, the HtzD3KO animals responded by reducing their LV volumes even further, worsening the restrictive cardiomyopathy and diastolic dysfunction, leading to congestive heart failure (Supplemental Fig. 3, B and C) and increased mortality (Fig. 3C). Thus, HtzD3KO animals have limited ability of cardiac remodeling during adrenergic overdrive likely as a result of the heart's inability to create localized hypothyroidism. Of note, an additional contributing factor to the poor performance exhibited by the HtzD3KO heart is likely to be the baseline cardiac fibrosis already present before ISO treatment was initiated, which is the result of long-term D3 deficiency in the HtzD3KO heart. Collectively, these data constitute strong objective evidence that myocardial D3 reactivation during adrenergic overdrive is adaptive, the absence of which leads to pathological myocardium remodeling.

The presence of myocardium fibrosis (Fig. 2, D and F) with decreased calcium-activated maximal force, LV hypertrophy (Fig. 2, G–I), and diastolic dysfunction (Fig. 2, K and L) underlie a state of restrictive cardiomyopathy in the HtzD3KO mice, revealing an critical role played by D3 in the normal myocardium. The implication of these findings is that the very low level of D3 activity present in the normal heart provides a physiological state of localized hypothyroidism, which the present data indicate is physiologically relevant. Although LV T_3 concentrations were not measured in the present experiments, the relative increase in thyroid hormone signaling is supported by the typical gene expression profile of the HtzD3KO myocardium (Supplemental Table 1) (13), including elevations in the α-MHC/β-MHC and SERCA-2/PLN ratios, despite normal serum T_3. Although of course we cannot discard that the fibrosis *per se* initiated such changes in gene expression, the consistent modification of four different T_3-responsive genes points toward enhanced T_3 signaling. Alternatively, it is conceivable that D3 expression in the "normal" myocardium reflects a small number of cardiomyocytes that are injured or damaged at any given time and are undergoing a remodeling process that requires induction of D3. These areas would thus account for what seems like global low level D3 expression.

Of note, LV afterload was similar between the WT and HtzD3KO animals (Fig. 2J), strongly suggesting that reactive hypertrophy is not operative in the D3KO mice. Thus, it is likely that this relative increase in thyroid hormone signaling underlies the myocardial fibrosis in these animals, given previous reports of myocardial fibrosis in thyrotoxic patients (15, 16). In turn, the fibrosis explains the decreased performance of the HtzD3KO skinned papillary muscle preparations (Fig. 5), leading to the phenotype of restrictive cardiomyopathy. Previous attempts to promote cardiac-specific increase in thyroid hormone signaling by way of transgenic myocardial overexpression of D2 resulted in the expected increase in adrenergic signaling and T_3-dependent gene expression profile such as observed in the present studies, but myocardial fibrosis was not investigated in those studies (22, 23).

The inducible cardiac D3 activity reported in this study (observed in the ISO-treated WT animals) reached about 1 fmol/mg protein/min, a figure that is similar to all other reports of inducible cardiac D3 activity in mice and rats (6, 7, 9). As reported, at these levels of D3 activity, there is reduction of tissue T_3 levels and T_3-dependent transcription of 40–50% (7, 9), indicating that similar mechanisms are taking place in the ISO-treated animals that exhibited D3 induction. Thus, it is not surprising that in our model of ISO-induced cardiac hypertrophy, there was echocardiographic evidence of myocardium hypothy-

roidism such as approximately 60% prolongation of the IVCT (Fig. 4A). Of note, the IVCT is a reliable T_3-sensitive biological parameter that has been widely used in the clinical setting to adjust the replacement dose of levothyroxine T_4 when serum thyrotropin cannot be used, such as in patients with secondary hypothyroidism (24).

In conclusion, the heart's ability to reactivate D3 in response to injury is a critical component of a successful remodeling process. In its absence, there is restrictive cardiomyopathy that is further accentuated in response to an adrenergic overdrive. Although we do not understand the molecular underpinnings of these adaptive mechanisms, it is conceivable that a reduction in thyroid hormone signaling establishes an adaptive transcriptional footprint that is favorable to cardiac remodeling. It is fascinating that D3-mediated hypothyroidism in response to illness is not unique to the heart, being observed in other models of tissue injury and healing, including cerebral ischemia, liver resection, and nerve injury, suggesting that D3 reactivation is part of a much broader adaptive network that is set in motion in response to illness.

Materials and Methods

Mice

All studies were performed according to a protocol approved by the Animal Care and Use Committee of University of Miami in compliance with National Institutes of Health standards. All experiments were conducted in newborns (P1) or 4-month-old 129/Sv/C57 Black/6J male mice. All mice were housed under a 12-h light, 12-h dark cycle at 22 ± 1 C, kept on a chow diet and water *ad libitum*. Mice with targeted disruption of the *Dio3* gene (D3KO) were previously described (25). A colony of animals heterozygous for the D3 inactivating mutation (HtzD3KO) and WT littermates derived from a male HtzD3KO mouse was studied.

Indirect calorimetry

Indirect calorimetry (VO_2, RQ, and EE) was performed in a Comprehensive Lab Animal Monitoring System (Columbus Instruments, Columbus, OH), a computer-controlled open circuit calorimetry system, as described (26).

Treatment with ISO

This was done by sc injections of D-L ISO [100 mg/Kg body weight (BW)/d; Sigma, St. Louis, MO] or 0.9% saline for 10 d.

Transthoracic echocardiography and Doppler studies

Cardiac function was monitored by Vevo 770 imaging system (VisualSonic, Inc., Toronto, Canada) at baseline and at the end of the treatment period. Images were recorded under anesthesia with isoflurane inhalation (1%) at heart rates above 400 bpm and body temperatures of 37 ± 1 C. Heart sonographic structural parameters were determined using the M-mode and two-dimensional images. Doppler echocardiographic images of mitral and aortic valves were recorded and calculated accordingly.

PV loop

Hemodynamic evaluation using a conductance manometry catheter was done while PV loops were recorded. Under general anesthesia (1% isoflurane) mice were intubated, and the internal carotid was canulated so that a PV loop catheter (SPR 839; Millar Instruments, TX) was passed to the LV to allow steady state occlusion parameters to be recorded at baseline and also with three doses of iv ISO infusion (10, 20, and 40 ng/kg BW/min for 5 min).

Euthanasia and serum levels of thyrotropin, T_4, and T_3

At the end of the experimental periods and procedures, mice were euthanized by CO_2 asphyxiation. Blood was collected and serum levels of thyrotropin, T_4, and T_3 measured using a MILLIPLEX rat thyroid hormone panel kit as described by the manufacturer (Millipore Corp., Billerica, MA) and read on a BioPlex (Bio-Rad, Hercules, CA). Heart, lung, and liver were harvested, and organ weights were expressed as a function of the tibial length.

Histological studies

Hearts fixed in 4% paraformaldehyde and placed in a 30% sucrose solution prepared in 0.1 M phosphate buffer. Then samples were snap frozen in liquid nitrogen and stored at −80 C until further processing. Hearts were then sliced transversely (~2 mm) at papillary level, and staining was with hematoxilin and eosin as well as Masson's trichrome.

mRNA analysis

Total heart RNA was extracted using the RNeasy kit (QIAGEN Sciences, Valencia, CA), and 2.5 μg of total RNA were reverse transcribed using High Capacity cDNA Reverse Transcription kit (Applied Biosystem, Foster City, CA). Abundance of mRNA molecules of interest was measured by RT-quantitative PCR (Bio-Rad iCycler iQ Real-Time PCR Detection System). In all assays, amplification efficiency was more than 90% and r^2 more than 0.95. Results are expressed as ratios of mRNA of interest/cyclophilin A mRNA.

D3 assay using ultra performance liquid chromatography

D3 activity was measured in the hearts and brain of all animals. Frozen tissue was processed with a Tissue Tearor (BioSpec Products, Bartlesville, OK) and homogenized in 10 mM dithiothreitol and 0.25 M sucrose. D3 activity was measured as previously described (10) using 150 μg of protein homogenate incubated at 37 C with 0.1 or 100 nM 3,5,[^{125}I]3′-triiodothyronine (PerkinElmer Life and Analytical Sciences, Inc., Waltham, MA) and 30 mM dithiothreitol. Reactions were stopped by addition of methanol and the products of deiodination separated by ultra performance liquid chromatography (ACQUITY; Waters Corp., Milford, MA) and quantified by a flow scintillation analyzer (PerkinElmer, Shelton, CT).

Mouse skinned cardiac fiber preparation and measurement of the Ca^{2+} sensitivity of force development, maximal force, and resistance to stretch

Skinned papillary muscles were prepared from the LV of freshly obtained WT or HtzD3KO mouse hearts following standard protocols of the laboratory (27). Strips of LV papillary muscle were extracted and incubated in a pCa 8.0 solution containing 1% Triton X-100 and 50% glycerol at 4 C for approximately 4–6 h. Fibers were then transferred to the same solution without Triton X-100 and stored at −20 C. Mouse muscle fiber bundles with a diameter varying between 65 and 139 μm, and approximately 1.3 mm of length were attached to tweezer clips connected to a force transducer. To ensure complete membrane removal and complete access to the myofilament, the fibers were treated with pCa 8.0 containing 1% Triton X-100 for 30 min before the beginning of the experiment. To remove the excess Triton X-100 from the fibers, extensive washing was carried out with pCa 8.0, and then the functional parameters were evaluated. To determine the Ca^{2+} sensitivity of force development, the fibers were gradually exposed to solutions of increasing Ca^{2+} concentration from pCa 8.0 to 4.0. Data were analyzed using the following equation: % change in force = $100 \times [Ca^{2+}]^n/([Ca^{2+}]^n + [Ca^{2+}{}_{50}]^n)$, where $[Ca^{2+}{}_{50}]$ is the free $[Ca^{2+}]$ that produces 50% force and n is the Hill coefficient. The maximal force in kN/m^2 developed by the fibers was evaluated by incubating the fiber in pCa 4.0 solution. For the stretch-force relationship measurements, the slack length from the fiber was determined by releasing and stretching until it begins generating tension. We set this point as zero for both the passive force and starting length. After this, the fiber was consecutively stretched 10% of its original length, and the passive force in kN/m^2 was recorded. These experiments were carried out in relaxing solution (pCa 8.0).

Statistical analysis

All data were analyzed using PRISM software (GraphPad Software, Inc., San Diego, CA) and expressed as mean ± SEM. The Student's *t* test was used to compare differences between two groups. One-way ANOVA was used to compare more than two groups, followed by the Student-Newman-Keuls *post hoc* test to detect differences between groups.

Acknowledgments

We thank Jingsheng Liang for the technical assistance with the skinned fiber measurements and Dr. Valery A. Galton, Dr. Arturo Hernandez, and Dr. Donald St. Germain for kindly sharing the D3KO mouse.

Address all correspondence and requests for reprints to: Antonio C. Bianco, M.D., Ph.D., 1400 Northwest 10th Street, Dominion Towers Suite 816, Miami, Florida 33136. E-mail: abianco@deiodinase.org; or Joshua M. Hare, M.D., Biomedical Research Building, 1501 Northwest 10th Avenue, Room 824, P. O. Box 016960 (R125), Miami, Florida 33101. E-mail: jhare@med.miami.edu.

This work was supported by 1K99HL103840-01 and James and Esther King Grant 1KN13-34001 (to J.R.P.); the National Institute of Diabetes and Digestive and Kidney Diseases Research Grant 65055 (to A.C.B.); and HL-HL084275, P20 HL101443, AG025017, HL065455, and HL094849 (to J.M.H.).

Disclosure Summary: The authors have nothing to disclose.

References

1. **Gereben B, Zavacki AM, Ribich S, Kim BW, Huang SA, Simonides WS, Zeöld A, Bianco AC** 2008 Cellular and molecular basis of deiodinase-regulated thyroid hormone signaling. Endocr Rev 29: 898–938
2. **Galton VA** 2005 The roles of the iodothyronine deiodinases in mammalian development. Thyroid 15:823–834
3. **Hall JA, Ribich S, Christoffolete MA, Simovic G, Correa-Medina M, Patti ME, Bianco AC** 2010 Absence of thyroid hormone activation during development underlies a permanent defect in adaptive thermogenesis. Endocrinology 151:4573–4582
4. **Peeters RP, Wouters PJ, Kaptein E, van Toor H, Visser TJ, Van den Berghe G** 2003 Reduced activation and increased inactivation of thyroid hormone in tissues of critically ill patients. J Clin Endocrinol Metab 88:3202–3211
5. **Huang SA, Bianco AC** 2008 Reawakened interest in type III iodothyronine deiodinase in critical illness and injury. Nat Clin Pract Endocrinol Metab 4:148–155
6. **Wassen FW, Schiel AE, Kuiper GG, Kaptein E, Bakker O, Visser TJ, Simonides WS** 2002 Induction of thyroid hormone-degrading deiodinase in cardiac hypertrophy and failure. Endocrinology 143: 2812–2815
7. **Simonides WS, Mulcahey MA, Redout EM, Muller A, Zuidwijk MJ, Visser TJ, Wassen FW, Crescenzi A, da-Silva WS, Harney J, Engel FB, Obregon MJ, Larsen PR, Bianco AC, Huang SA** 2008 Hypoxia-inducible factor induces local thyroid hormone inactivation during hypoxic-ischemic disease in rats. J Clin Invest 118:975–983
8. **Olivares EL, Marassi MP, Fortunato RS, da Silva AC, Costa-e-Sousa RH, Araújo IG, Mattos EC, Masuda MO, Mulcahey MA, Huang SA, Bianco AC, Carvalho DP** 2007 Thyroid function disturbance and type 3 iodothyronine deiodinase induction after myocardial infarction in rats a time course study. Endocrinology 148: 4786–4792
9. **Pol CJ, Muller A, Zuidwijk MJ, van Deel ED, Kaptein E, Saba A, Marchini M, Zucchi R, Visser TJ, Paulus WJ, Duncker DJ, Simonides WS** 2011 Left-ventricular remodeling after myocardial infarction is associated with a cardiomyocyte-specific hypothyroid condition. Endocrinology 152:669–679
10. **Freitas BC, Gereben B, Castillo M, Kalló I, Zeöld A, Egri P, Liposits Z, Zavacki AM, Maciel RM, Jo S, Singru P, Sanchez E, Lechan RM, Bianco AC** 2010 Paracrine signaling by glial cell-derived triiodothyronine activates neuronal gene expression in the rodent brain and human cells. J Clin Invest 120:2206–2217
11. **da Rocha ST, Edwards CA, Ito M, Ogata T, Ferguson-Smith AC** 2008 Genomic imprinting at the mammalian Dlk1-Dio3 domain. Trends Genet 24:306–316
12. **Hagan JP, O'Neill BL, Stewart CL, Kozlov SV, Croce CM** 2009 At least ten genes define the imprinted Dlk1-Dio3 cluster on mouse chromosome 12qF1. PLoS One 4:e4352
13. **Simonides WS, van Hardeveld C** 2008 Thyroid hormone as a determinant of metabolic and contractile phenotype of skeletal muscle. Thyroid 18:205–216
14. **Klein I, Ojamaa K** 2001 Thyroid hormone and the cardiovascular system. N Engl J Med 344:501–509

15. **Sandler G, Wilson GM** 1959 The production of cardiac hypertrophy by thyroxine in the rat. Q J Exp Physiol Cogn Med Sci 44:282–289
16. **Sandler G, Wilson GM** 1959 The nature and prognosis of heart disease in thyrotoxicosis. A review of 150 patients treated with 131 I. Q J Med 28:347–369
17. **Brooks WW, Conrad CH** 2009 Isoproterenol-induced myocardial injury and diastolic dysfunction in mice: structural and functional correlates. Comp Med 59:339–343
18. **Martins MR, Doin FC, Komatsu WR, Barros-Neto TL, Moises VA, Abucham J** 2007 Growth hormone replacement improves thyroxine biological effects: implications for management of central hypothyroidism. J Clin Endocrinol Metab 92:4144–4153
19. **Willott RH, Gomes AV, Chang AN, Parvatiyar MS, Pinto JR, Potter JD** 2010 Mutations in Troponin that cause HCM, DCM AND RCM: what can we learn about thin filament function? J Mol Cell Cardiol 48:882–892
20. **Drazner MH** 2011 The progression of hypertensive heart disease. Circulation 123:327–334
21. **Kinugawa K, Yonekura K, Ribeiro RC, Eto Y, Aoyagi T, Baxter JD, Camacho SA, Bristow MR, Long CS, Simpson PC** 2001 Regulation of thyroid hormone receptor isoforms in physiological and pathological cardiac hypertrophy. Circ Res 89:591–598
22. **Trivieri MG, Oudit GY, Sah R, Kerfant BG, Sun H, Gramolini AO, Pan Y, Wickenden AD, Croteau W, Morreale de Escobar G, Pekhletski R, St Germain D, Maclennan DH, Backx PH** 2006 Cardiac-specific elevations in thyroid hormone enhance contractility and prevent pressure overload-induced cardiac dysfunction. Proc Natl Acad Sci USA 103:6043–6048
23. **Carvalho-Bianco SD, Kim BW, Zhang JX, Harney JW, Ribeiro RS, Gereben B, Bianco AC, Mende U, Larsen PR** 2004 Chronic cardiac-specific thyrotoxicosis increases myocardial β-adrenergic responsiveness. Mol Endocrinol 18:1840–1849
24. **Oliveira JH, Persani L, Beck-Peccoz P, Abucham J** 2001 Investigating the paradox of hypothyroidism and increased serum thyrotropin (TSH) levels in Sheehan's syndrome: characterization of TSH carbohydrate content and bioactivity. J Clin Endocrinol Metab 86:1694–1699
25. **Hernandez A, Martinez ME, Fiering S, Galton VA, St Germain D** 2006 Type 3 deiodinase is critical for the maturation and function of the thyroid axis. J Clin Invest 116:476–484
26. **Castillo M, Hall JA, Correa-Medina M, Ueta C, Kang HW, Cohen DE, Bianco AC** 2011 Disruption of thyroid hormone activation in type 2 deiodinase knockout mice causes obesity with glucose intolerance and liver steatosis only at thermoneutrality. Diabetes 60:1082–1089
27. **Baudenbacher F, Schober T, Pinto JR, Sidorov VY, Hilliard F, Solaro RJ, Potter JD, Knollmann BC** 2008 Myofilament Ca2+ sensitization causes susceptibility to cardiac arrhythmia in mice. J Clin Invest 118:3893–3903

Fig. Supplemental 1. *PV loop at baseline and after ISO infusion (10, 20 and 40 ng/Kg BW/min) in control and HtzD3KO mice.* Dose-response curves for (A) EF, Ejection fraction, (B) SW, stroke work, (C) PRSW, preload recruitable stroke work, (D) ESV, end-systolic and (E) EDV, end-diastolic volume, (F) ESP, end-systolic pressure, (G) ESPVR, end-systolic and (H) EDPVR, end-diastolic pressure volume relationship, (I) dP/dtmax, maximum derivative of change in systolic pressure in time. (J) SV, stroke volume, (K) CO, cardiac output, (L) Emax, maximum chamber elasticity; in *A-L* data are expressed as mean ±SEM of 3-4 animals in each group; *$p<0.01$ vs. WT siblings; **$p<0.01$ vs. HtzD3KO baseline and $^{+}p<0.01$ vs. WT baseline.

Fig. Supplemental 2. *Effect of treatment with isoproterenol on right ventricular (RV) myocardial D3 activity.* RV D3 activity after treatment with ISO or saline (SAL); bkg is background activity. Data are expressed as mean±SEM of 5-10 animals in each group.

Fig. Supplemental 3. *Effect of a 10 d-period ISO-induced cardiac hypertrophy on cardiovascular paramenters.* (A) Heart weight, (B) lung weight, (C) myocardial mRNA levels of brain natriuretic peptide and (D) atrial natriuretic peptide, (E) liver weight; tissue weights were normalized by tibial length. Data are expressed as mean ±SEM of 8 animals in each group.

Fig. Supplemental 4. *mRNA analyses of key myocardium genes by RT-qPCR.* Results are expressed as ratios of test mRNA/cyclophilin mRNA. (A) UCP-2, uncoupling protein 2, (B) Glut-4, glucose transporter 4, (C) PPARα, peroxisome proliferator-activated receptor α, (D) GPX1, glutathione peroxidase 1. Data are expressed as mean±SEM of 8 animals in each group.

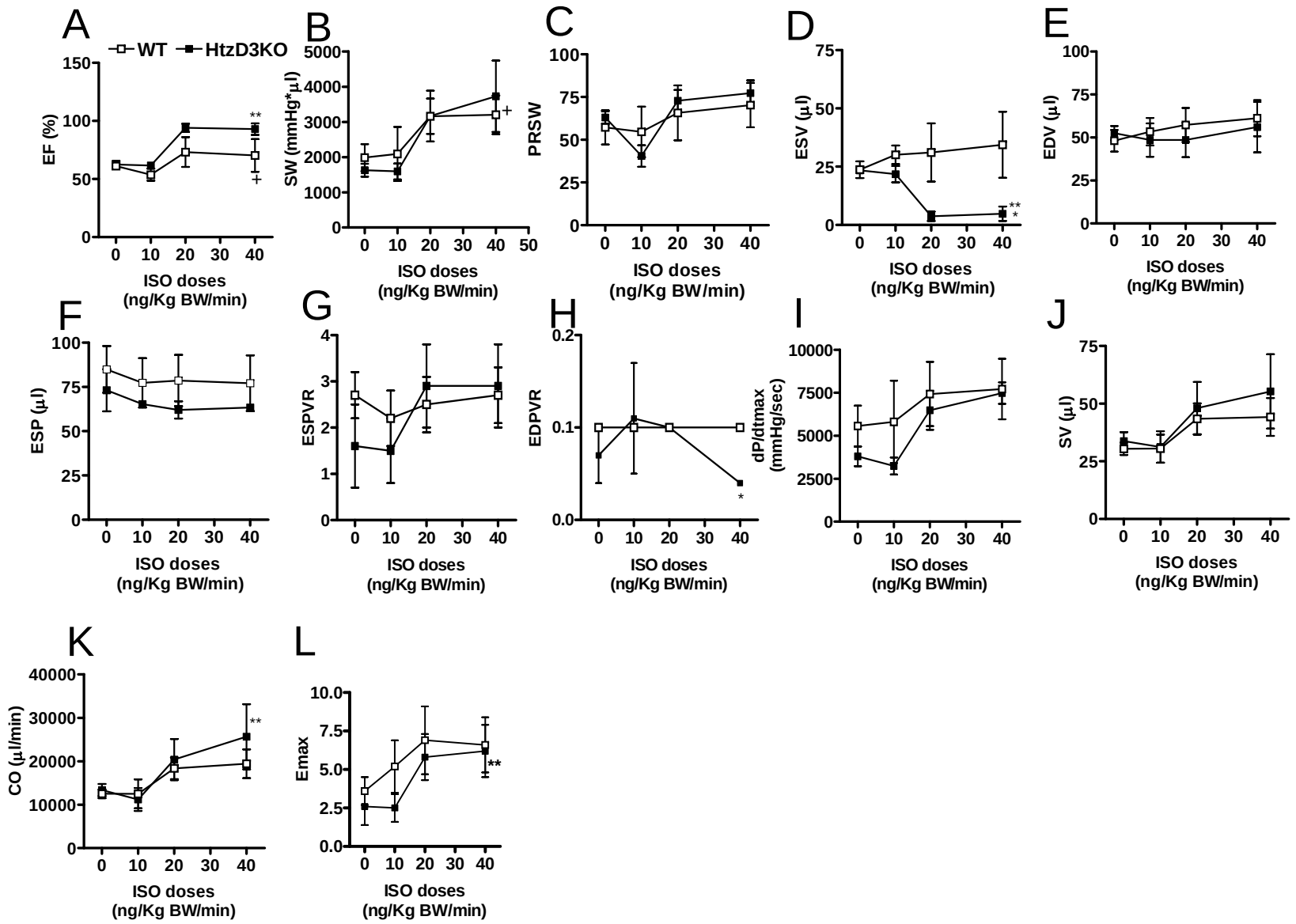

Supplemental Figure 1

Supplemental Figure 2

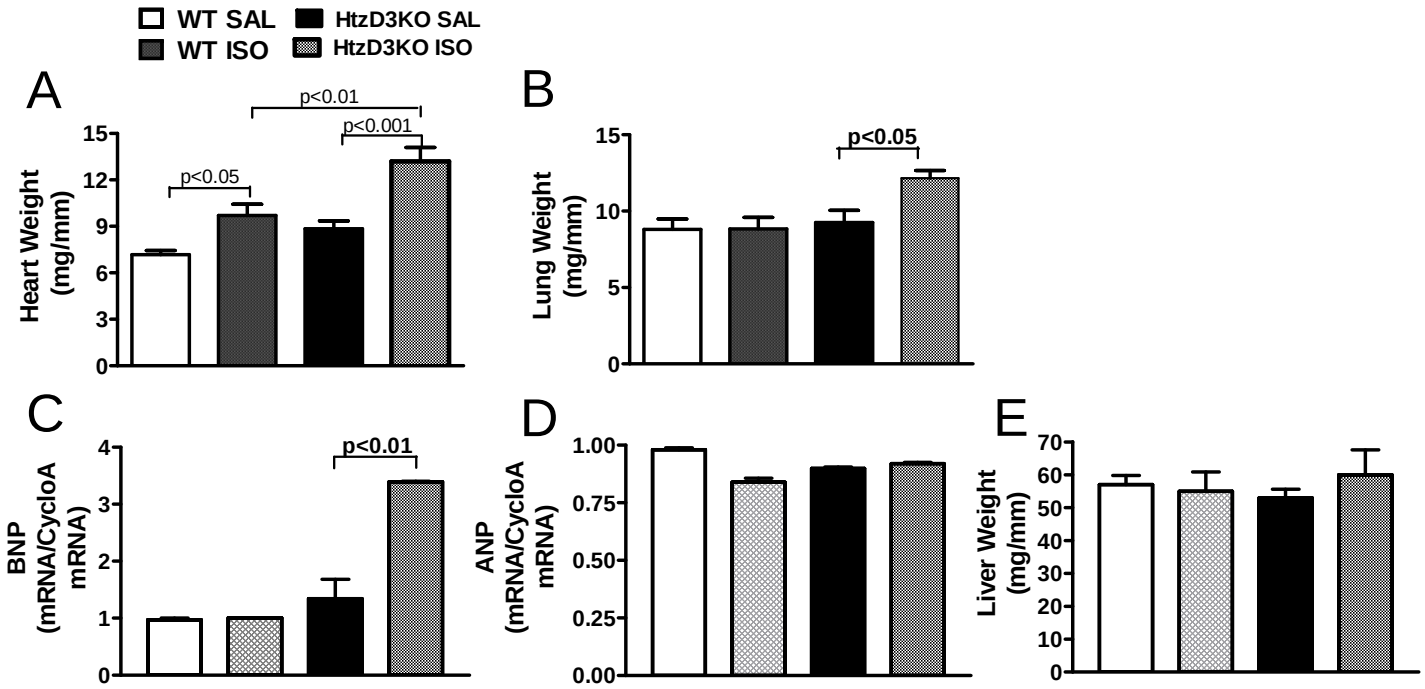

Supplemental Figure 3

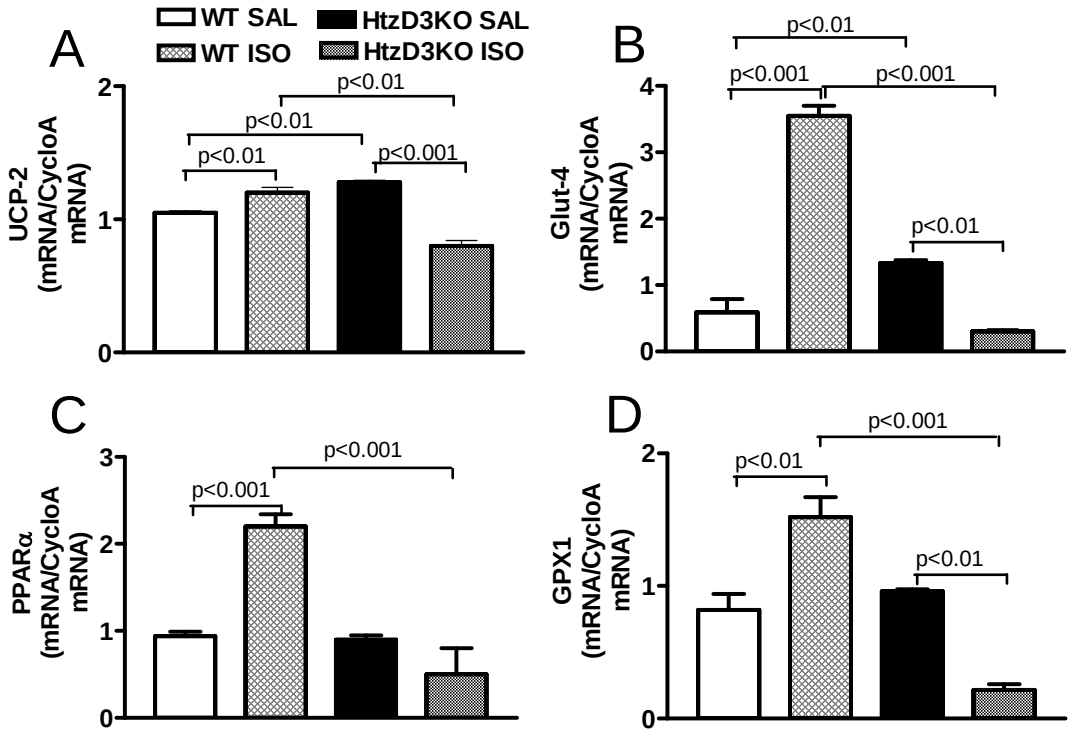

Supplemental Figure 4

Supplemental Table 1. LV mRNA levels of specific genes in adult (4- month old) and newborn (P1) HtzD3KO mice.

Parameter	WT	HtzD3KO
LV mRNA (neonatal - P1)		
SERCA-2	0.76±0.30	0.66±0.06
α-MHC	1.11±0.16	1.10±0.02
β-MHC	0.70±0.06	0.71±0.14
α-MHC/β-MHC ratio	1.57±0.10	1.60±0.29
PLN	1.10±0.10	0.79±0.01*
SERCA-2/PLN ratio	0.69±0.05	0.84±0.09
UCP-2	0.70±0.21	0.49±0.07
GLUT-4	1.04±0.22	0.75±0.11
BNP	0.62±0.25	0.61±0.26
LV mRNA (adult)		
SERCA-2	0.98±0.01	1.04±0.05
α-MHC	1.02±0.02	1.23±0.03*
β-MHC	1.05±0.02	0.90±0.01
α-MHC/β-MHC ratio	0.98±0.02	1.30±0.20*
PLN	1.00±0.01	0.80±0.04 *
SERCA-2/PLN ratio	0.97±0.01	1.30±0.03*
UCP-2	1.00±0.01	1.30±0.01*
GLUT-4	1.04±0.22	0.75±0.11
PPARα	0.94±0.05	0.90±0.05
GPX-1	0.82±0.17	0.96±0.03
BNP	0.97±0.03	1.30±0.34
LV Collagen 1	0.70±0.3	8.33±0.45 *

Values are the mean ± SEM of n=3; *p<0.001 vs. WT.

Capítulo 5

I. Conclusões

1) As estatinas e os inibidores da isoprenil transferase aumentam a atividade da D2 em modelos celulares que expressão endógena D2 e em camundongos. Tratamento com levastatina (LVS) aumenta os níveis de mRNA da D2 em células de mesentelioma (MSTO-211H), mas não alteram sua expressão em células que transitoriamente expressão D2 (HEK-293). Os inibidores da isoprenil transferase não aumentam os níveis de mRNA da D2 em nenhum destes sistemas, indicando que mecanismos pós-transcricionais podem existir. Esse efeito pode explicar alguns dos efeitos benéficos das estatinas que são independentes da redução dos níveis circulantes de colesterol.

2) O impacto do hipotiroidismo sistêmico no camundongo desencadeia uma forte resposta metabólica no BAT que sustenta a taxa metabólica basal apesar da redução do programa termogênico no músculo esquelético. Um subproduto dessa resposta metabólica adaptativa é a proteção contra a obesidade induzida pela dieta, que é revertida pela aclimatação à termoneutralidade. Esses achados realçam a relevância do BAT para a homeostase térmica em pequenos roedores, minimizando o papel desempenhado pelo músculo esquelético neste processo.

3) A habilidade do coração em reativar a D3 em resposta à lesão/dano tecidual é um componente crítico do processo de remodelamento. Na ausência da D3, há cardiomiopatia restritiva que é acentuada em resposta à superestimulação adrenérgica. É possível que a redução da sinalização do hormônio tiroideano pela D3 estabeleça um ambiente transcricional favorável à expressão de genes envolvidos no remodelamento cardíaco. Esse fenomeno não é exclusivo do coração, sendo observado em outros modelos de lesão tecidual, incluindo isquemia cerebral, sugerindo que a reativação da D3 é parte de uma ampla rede adaptativa em resposta à doença.

II. **Anexo**

Produção Científica durante o doutorado

1. Tatiana L. Fonseca, Mayrin Correa-Medina, Maira Campos, Gabor Wittmann, Joao Werneck-de-Castro, Rafael A. Drigo, Magda Mora-Garzon, Cintia B. Ueta, Alejandro Caicedo, Balazs Gereben, Ronald Lechan, Antonio C. Bianco. Coordination of hypothalamic and pituitary T3 production regulates TSH expression. JCI 123:1492-500, 2013.

2. Raffaella Poggioli, Cintia B. Ueta, Rafael Arrojo e Drigo, Melany Castillo, Tatiana L. Fonseca, Antonio C. Bianco. Dexamethasone reduces energy expenditure and increases susceptibility to diet-induced obesity in mice. Obesity, 2013.

3. Bradford T. Miller[*], Cintia B. Ueta[*], Vincent Lau, Kristina G. Jacomino, Lino M. Wasserman and Brian W. Kim. Statins and downstream inhibitors of the isoprenylation pathway increase Type 2 iodothyronine deidinase activity. Endocrinology 153(8):4039-4048, 2012. [*]This authors contributed equally to this work.

4. Cintia B. Ueta[*], Behzad N.Oskouei[*], Emerson L. Olivares[*], Jose R. Pinto, Mayrin M. Correa, Gordana Simovic, Warner S. Simonides, Joshua M. Hare and Antonio C. Bianco. Absence of myocardial thyroid hormone inactivating deiodinase results restrictive cardiomyopathy in mice. Molecular Endocrinology 26:809-818, 2012. [*]This authors contributed equally to this work.

5. Qiang Wang, Konstatin Lvay, Tatyana Chaturiya, Galina Dvoriantchikova, Karen L. Anderson, Suzy D.C. Bianco, Cintia B. Ueta, Damaris Molano, Antonello Pileggi, Eugenia V. Gurevich, Oksana Gavrillova and Vladlen Z. Slepak. Target deletion of one or two copies of the G protein β subunit Gβ5 gene has distinct effects on body weight and behavior in mice. FASEB Journal. 25:3949-3957, 2011.

6. Cintia B. Ueta, Emerson L. Olivares and Antonio C. Bianco. Responsiveness to thyroid hormone and to ambient temperature underlies differences between brown adipose tissue and skeletal muscle thermogenesis in a mouse model of diet-induced obesity. Endocrinology 152:3571-3581, 2011.

7. Melany Castillo, Jessica A. Hall, Mayrin Correa-Medina, Cintia Ueta, Hyu W. Kang, David E. Cohen and Antonio C. Bianco. Disruption of thyroid homrone activation in type 2 deiodinase Knockout mice causes obesity with glucose intolerance and liver steatosis only at thermoneutrality. Diabetes 60:1082-1089, 2011.

III. **Referências Bibliográficas**

1. **Bianco, A.C., Ribich, S., and Kim, B.W. 2007. An inside job. *Endocrinology* 148:3077-3079.**
2. **Bianco, A.C., Salvatore, D., Gereben, B., Berry, M.J., and Larsen, P.R. 2002. Biochemistry, cellular and molecular biology and physiological roles of the iodothyronine selenodeiodinases. *Endocrine Reviews* 23:38-89.**
3. **Bianco, A.C., and Kim, B.W. 2006. Deiodinases: implications of the local control of thyroid hormone action. *J Clin Invest* 116:2571-2579.**
4. **Gereben, B., Zavacki, A.M., Ribich, S., Kim, B.W., Huang, S.A., Simonides, W.S., Zeold, A., and Bianco, A.C. 2008. Cellular and molecular basis of deiodinase-regulated thyroid hormone signaling. *Endocr Rev* 29:898-938.**
5. **Ito, K., Uno, M., and Nakamura, Y. 2000. A tripeptide 'anticodon' deciphers stop codons in messenger RNA. *Nature* 403:680-684.**
6. **Copeland, P.R., Fletcher, J.E., Carlson, B.A., Hatfield, D.L., and Driscoll, D.M. 2000. A novel RNA binding protein, SBP2, is required for the translation of mammalian selenoprotein mRNAs. *Embo J* 19:306-314.**
7. **Bartz, J.K., Kline, L.K., and Soll, D. 1970. N6-(Delta 2-isopentenyl)adenosine: biosynthesis in vitro in transfer RNA by an enzyme purified from Escherichia coli. *Biochem Biophys Res Commun* 40:1481-1487.**
8. **Warner, G.J., Rusconi, C.P., White, I.E., and Faust, J.R. 1998. Identification and sequencing of two isopentenyladenosine-modified transfer RNAs from Chinese hamster ovary cells. *Nucleic Acids Res* 26:5533-5535.**
9. **Moustafa, M.E., Carlson, B.A., El-Saadani, M.A., Kryukov, G.V., Sun, Q.A., Harney, J.W., Hill, K.E., Combs, G.F., Feigenbaum, L., Mansur, D.B., et al. 2001. Selective inhibition of selenocysteine tRNA maturation and selenoprotein synthesis in transgenic mice expressing isopentenyladenosine-deficient selenocysteine tRNA. *Mol Cell Biol* 21:3840-3852.**
10. **Warner, G.J., Berry, M.J., Moustafa, M.E., Carlson, B.A., Hatfield, D.L., and Faust, J.R. 2000. Inhibition of selenoprotein synthesis by selenocysteine tRNA[Ser]Sec lacking isopentenyladenosine. *J Biol Chem* 275:28110-28119.**
11. **Glomset, J.A., Gelb, M.H., and Farnsworth, C.C. 1990. Prenyl proteins in eukaryotic cells: a new type of membrane anchor. *Trends Biochem Sci* 15:139-142.**
12. **Dihanich, M.E., Najarian, D., Clark, R., Gillman, E.C., Martin, N.C., and Hopper, A.K. 1987. Isolation and characterization of MOD5, a gene required for isopentenylation of cytoplasmic and mitochondrial tRNAs of Saccharomyces cerevisiae. *Mol Cell Biol* 7:177-184.**
13. **Benko, A.L., Vaduva, G., Martin, N.C., and Hopper, A.K. 2000. Competition between a sterol biosynthetic enzyme and tRNA modification in addition to changes in the protein synthesis machinery causes altered nonsense suppression. *Proc Natl Acad Sci U S A* 97:61-66.**
14. **Faust, J.R., Brown, M.S., and Goldstein, J.L. 1980. Synthesis of delta 2-isopentenyl tRNA from mevalonate in cultured human fibroblasts. *J Biol Chem* 255:6546-6548.**

15. **Kromer, A., and Moosmann, B. 2009. Statin-induced liver injury involves cross-talk between cholesterol and selenoprotein biosynthetic pathways. *Mol Pharmacol* 75:1421-1429.**
16. **Moosmann, B., and Behl, C. 2004. Selenoproteins, cholesterol-lowering drugs, and the consequences: revisiting of the mevalonate pathway. *Trends Cardiovasc Med* 14:273-281.**
17. **Miller, B.T., Ueta, C.B., Lau, V., Jacomino, K.G., Wasserman, L.M., and Kim, B.W. 2012. Statins and downstream inhibitors of the isoprenylation pathway increase type 2 iodothyronine deiodinase activity. *Endocrinology* 153:4039-4048.**
18. **Croteau, W., Whittemore, S.L., Schneider, M.J., and St Germain, D.L. 1995. Cloning and expression of a cDNA for a mammalian type III iodothyronine deiodinase. *Journal of Biological Chemistry* 270:16569-16575.**
19. **Bianco, A.C. 2004. Triplets! Unexpected structural similarity among the three enzymes that catalyze initiation and termination of thyroid hormone effects. *Arq Bras Endocrinol Metabol* 48:16-24.**
20. **Buettner, C., Harney, J.W., and Larsen, P.R. 2000. The role of selenocysteine 133 in catalysis by the human type 2 iodothyronine deiodinase. *Endocrinology* 141:4606-4612.**
21. **Berry, M.J., Kieffer, J.D., Harney, J.W., and Larsen, P.R. 1991. Selenocysteine confers the biochemical properties of the type I iodothyronine deiodinase. *Journal of Biological Chemistry* 266:14155-14158.**
22. **Friesema, E.C., Kuiper, G.G., Jansen, J., Visser, T.J., and Kester, M.H. 2006. Thyroid hormone transport by the human monocarboxylate transporter 8 and its rate-limiting role in intracellular metabolism. *Mol Endocrinol* 20:2761-2772.**
23. **Curcio-Morelli, C., Gereben, B., Zavacki, A.M., Kim, B.W., Huang, S., Harney, J.W., Larsen, P.R., and Bianco, A.C. 2003. In vivo dimerization of types 1, 2, and 3 iodothyronine selenodeiodinases. *Endocrinology* 144:937-946.**
24. **Oppenheimer, J.H., Schwartz, H.L., and Surks, M.I. 1972. Propylthiouracil inhibits the conversion of L-thyroxine to L-triiodothyronine: An explanation of the antithyroxine effect of propylthiouracil and evidence supporting the concept that triiodothyronine is the active thyroid hormone. *Journal of Clinical Investigation* 51:2493-2497.**
25. **Fekkes, D., Hennemann, G., and Visser, T.J. 1982. Evidence for a single enzyme in rat liver catalyzing the deiodination of the tyrosyl and the phenolic ring of iodothyronines. *Biochemistry Journal* 201:673-676.**
26. **Campos-Barros, A., Hoell, T., Musa, A., Sampaolo, S., Stoltenburg, G., Pinna, G., Eravci, M., Meinhold, H., and Baumgartner, A. 1996. Phenolic and tyrosyl ring iodothyronine deiodination and thyroid hormone concentrations in the human central nervous system. *The Journal of Clinical Endocrinology and Metabolism* 81:2179-2185.**
27. **Nishikawa, M., Toyoda, N., Yonemoto, T., Ogawa, Y., Tabata, S., Sakaguchi, N., Tokoro, T., Gondou, A., Yoshimura, M., Yoshikawa, N., et al. 1998. Quantitative measurements for type 1 deiodinase messenger ribonucleic acid in human peripheral blood mononuclear cells: mechanism of the preferential increase of T3 in hyperthyroid Graves' disease. *Biochem Biophys Res Commun* 250:642-646.**

28. **Maia, A.L., Kieffer, J.D., Harney, J.W., and Larsen, P.R. 1995. Effect of 3,5,3'-Triiodothyronine (T3) administration on dio1 gene expression and T3 metabolism in normal and type 1 deiodinase-deficient mice.** ***Endocrinology*** **136:4842-4849.**

29. **Eelkman Rooda, S.J., Kaptein, E., and Visser, T.J. 1989. Serum triiodothyronine sulfate in man measured by radioimmunoassay.** ***J Clin Endocrinol Metab*** **69:552-556.**

30. **Spaulding, S.W., Smith, T.J., Hinkle, P.M., Davis, F.B., Kung, M.P., and Roth, J.A. 1992. Studies on the biological activity of triiodothyronine sulfate.** ***J Clin Endocrinol Metab*** **74:1062-1067.**

31. **Visser, T.J., Kaptein, E., Glatt, H., Bartsch, I., Hagen, M., and Coughtrie, M.W. 1998. Characterization of thyroid hormone sulfotransferases.** ***Chem Biol Interact*** **109:279-291.**

32. **Visser, T.J. 1994. Role of sulfation in thyroid hormone metabolism.** ***Chem Biol Interact*** **92:293-303.**

33. **Schneider, M.J., Fiering, S.N., Thai, B., Wu, S.Y., St Germain, E., Parlow, A.F., St Germain, D.L., and Galton, V.A. 2006. Targeted disruption of the type 1 selenodeiodinase gene (Dio1) results in marked changes in thyroid hormone economy in mice.** ***Endocrinology*** **147:580-589.**

34. **Baqui, M.M., Gereben, B., Harney, J.W., Larsen, P.R., and Bianco, A.C. 2000. Distinct subcellular localization of transiently expressed types 1 and 2 iodothyronine deiodinases as determined by immunofluorescence confocal microscopy.** ***Endocrinology*** **141:4309-4312.**

35. **Larsen, P.R., Silva, J.E., and Kaplan, M.M. 1981. Relationships between circulating and intracellular thyroid hormones: physiological and clinical implications.** ***Endocrine Reviews*** **2:87-102.**

36. **Visser, T.J., Leonard, J.L., Kaplan, M.M., and Larsen, P.R. 1982. Kinetic evidence suggesting two mechanisms for iodothyronine 5'- deiodination in rat cerebral cortex.** ***Proceedings of the National Academy of Science*** **79:5080-5084.**

37. **Silva, J.E., and Larsen, P.R. 1977. Pituitary nuclear 3,5,3'-triiodothyronine and thyrotropin secretion: an explanation for the effect of thyroxine.** ***Science*** **198:617-620.**

38. **Cheron, R.G., Kaplan, M.M., and Larsen, P.R. 1979. Physiological and pharmacological influences on thyroxine to 3,5,3'- triiodothyronine conversion and nuclear 3,5,3'-triiodothyronine binding in rat anterior pituitary.** ***Journal of Clinical Investigation*** **64:1402-1414.**

39. **Leonard, J.L. 1988. Dibutyryl cAMP induction of Type II 5'deiodinase activity in rat brain astrocytes in culture.** ***Biochem Biophys Res Commun*** **151:1164-1172.**

40. **Crantz, F.R., and Larsen, P.R. 1980. Rapid thyroxine to 3,5,3'-triiodothyronine conversion and nuclear 3,5,3'-triiodothyronine binding in rat cerebral cortex and cerebellum.** ***Journal of Clinical Investigation*** **65:935-938.**

41. **Silva, J.E., and Larsen, P.R. 1983. Adrenergic activation of triiodothyronine production in brown adipose tissue.** ***Nature*** **305:712-713.**

42. **Salvatore, D., Bartha, T., Harney, J.W., and Larsen, P.R. 1996. Molecular biological and biochemical characterization of the human type 2 selenodeiodinase.** ***Endocrinology*** **137:3308-3315.**

43. Bartha, T., Kim, S.W., Salvatore, D., Gereben, B., Tu, H.M., Harney, J.W., Rudas, P., and Larsen, P.R. 2000. Characterization of the 5'-flanking and 5'-untranslated regions of the cyclic adenosine 3',5'-monophosphate-responsive human type 2 iodothyronine deiodinase gene. *Endocrinology* 141:229-237.

44. Salvatore, D., Tu, H., Harney, J.W., and Larsen, P.R. 1996. Type 2 iodothyronine deiodinase is highly expressed in human thyroid. *Journal of Clinical Investigation* 98:962-968.

45. Botero, D., Gereben, B., Goncalves, C., de Jesus, L.A., Harney, J.W., and Bianco, A.C. 2002. Ubc6p and Ubc7p are required for normal and substrate-induced endoplasmic reticulum-associated degradation of the human selenoprotein type 2 iodothyronine monodeiodinase. *Mol Endocrinol* 16:1999-2007.

46. Kim, B.W., Zavacki, A.M., Curcio-Morelli, C., Dentice, M., Harney, J.W., Larsen, P.R., and Bianco, A.C. 2003. Endoplasmic reticulum-associated degradation of the human type 2 iodothyronine deiodinase (D2) is mediated via an association between mammalian UBC7 and the carboxyl region of D2. *Mol Endocrinol* 17:2603-2612.

47. Steinsapir, J., Harney, J., and Larsen, P.R. 1998. Type 2 iodothyronine deiodinase in rat pituitary tumor cells is inactivated in proteasomes. *Journal of Clinical Investigation* 102:1895-1899.

48. Steinsapir, J., Bianco, A.C., Buettner, C., Harney, J., and Larsen, P.R. 2000. Substrate-induced down-regulation of human type 2 deiodinase (hD2) is mediated through proteasomal degradation and requires interaction with the enzyme's active center. *Endocrinology* 141:1127-1135.

49. Gereben, B., Goncalves, C., Harney, J.W., Larsen, P.R., and Bianco, A.C. 2000. Selective proteolysis of human type 2 deiodinase: a novel ubiquitin- proteasomal mediated mechanism for regulation of hormone activation. *Molecular Endocrinology* 14:1697-1708.

50. Coux, O., Tanaka, K., and Goldberg, A.L. 1996. Structure and functions of the 20S and 26S proteasomes. *Annu Rev Biochem* 65:801-847.

51. Hershko, A., and Ciechanover, A. 1998. The ubiquitin system. *Annu Rev Biochem* 67:425-479.

52. Dentice, M., Bandyopadhyay, A., Gereben, B., Callebaut, I., Christoffolete, M.A., Kim, B.W., Nissim, S., Mornon, J.P., Zavacki, A.M., Zeold, A., et al. 2005. The Hedgehog-inducible ubiquitin ligase subunit WSB-1 modulates thyroid hormone activation and PTHrP secretion in the developing growth plate. *Nat Cell Biol* 7:698-705.

53. Hilton, D.J., Richardson, R.T., Alexander, W.S., Viney, E.M., Willson, T.A., Sprigg, N.S., Starr, R., Nicholson, S.E., Metcalf, D., and Nicola, N.A. 1998. Twenty proteins containing a C-terminal SOCS box form five structural classes. *Proc Natl Acad Sci U S A* 95:114-119.

54. Neer, E.J., Schmidt, C.J., Nambudripad, R., and Smith, T.F. 1994. The ancient regulatory-protein family of WD-repeat proteins. *Nature* 371:297-300.

55. Curcio-Morelli, C., Zavacki, A.M., Christofollete, M., Gereben, B., de Freitas, B.C., Harney, J.W., Li, Z., Wu, G., and Bianco, A.C. 2003. Deubiquitination of type 2 iodothyronine deiodinase by von Hippel-Lindau protein-interacting

deubiquitinating enzymes regulates thyroid hormone activation. *J Clin Invest* 112:189-196.

56. Huang, S.A., and Bianco, A.C. 2008. Reawakened interest in type III iodothyronine deiodinase in critical illness and injury. *Nat Clin Pract Endocrinol Metab* 4:148-155.

57. Hernandez, A., Park, J.P., Lyon, G.J., Mohandas, T.K., and St Germain, D.L. 1998. Localization of the type 3 iodothyronine deiodinase (DIO3) gene to human chromosome 14q32 and mouse chromosome 12F1. *Genomics* 53:119-121.

58. Charalambous, M., and Hernandez, A. Genomic imprinting of the type 3 thyroid hormone deiodinase gene: Regulation and developmental implications. *Biochim Biophys Acta*.

59. da Rocha, S.T., and Ferguson-Smith, A.C. 2004. Genomic imprinting. *Curr Biol* 14:R646-649.

60. Ferguson-Smith, A.C., and Surani, M.A. 2001. Imprinting and the epigenetic asymmetry between parental genomes. *Science* 293:1086-1089.

61. Reik, W., and Walter, J. 2001. Genomic imprinting: parental influence on the genome. *Nat Rev Genet* 2:21-32.

62. Hernandez, A., Fiering, S., Martinez, E., Galton, V.A., and St Germain, D. 2002. The gene locus encoding iodothyronine deiodinase type 3 (Dio3) is imprinted in the fetus and expresses antisense transcripts. *Endocrinology* 143:4483-4486.

63. Ueta, C.B., Oskouei, B.N., Olivares, E.L., Pinto, J.R., Correa, M.M., Simovic, G., Simonides, W.S., Hare, J.M., and Bianco, A.C. Absence of myocardial thyroid hormone inactivating deiodinase results in restrictive cardiomyopathy in mice. *Mol Endocrinol* 26:809-818.

64. Charalambous, M., da Rocha, S.T., and Ferguson-Smith, A.C. 2007. Genomic imprinting, growth control and the allocation of nutritional resources: consequences for postnatal life. *Curr Opin Endocrinol Diabetes Obes* 14:3-12.

65. Wilkinson, L.S., Davies, W., and Isles, A.R. 2007. Genomic imprinting effects on brain development and function. *Nat Rev Neurosci* 8:832-843.

66. Lin, S.P., Coan, P., da Rocha, S.T., Seitz, H., Cavaille, J., Teng, P.W., Takada, S., and Ferguson-Smith, A.C. 2007. Differential regulation of imprinting in the murine embryo and placenta by the Dlk1-Dio3 imprinting control region. *Development* 134:417-426.

67. Hernandez, A., Martinez, M.E., Fiering, S., Galton, V.A., and St Germain, D. 2006. Type 3 deiodinase is critical for the maturation and function of the thyroid axis. *J Clin Invest* 116:476-484.

68. Moon, Y.S., Smas, C.M., Lee, K., Villena, J.A., Kim, K.H., Yun, E.J., and Sul, H.S. 2002. Mice lacking paternally expressed Pref-1/Dlk1 display growth retardation and accelerated adiposity. *Mol Cell Biol* 22:5585-5592.

69. Tsai, C.E., Lin, S.P., Ito, M., Takagi, N., Takada, S., and Ferguson-Smith, A.C. 2002. Genomic imprinting contributes to thyroid hormone metabolism in the mouse embryo. *Curr Biol* 12:1221-1226.

70. Yevtodiyenko, A., Carr, M.S., Patel, N., and Schmidt, J.V. 2002. Analysis of candidate imprinted genes linked to Dlk1-Gtl2 using a congenic mouse line. *Mamm Genome* 13:633-638.

71. **da Rocha, S.T., Edwards, C.A., Ito, M., Ogata, T., and Ferguson-Smith, A.C. 2008. Genomic imprinting at the mammalian Dlk1-Dio3 domain. *Trends Genet* 24:306-316.**

72. **Tierling, S., Dalbert, S., Schoppenhorst, S., Tsai, C.E., Oliger, S., Ferguson-Smith, A.C., Paulsen, M., and Walter, J. 2006. High-resolution map and imprinting analysis of the Gtl2-Dnchc1 domain on mouse chromosome 12. *Genomics* 87:225-235.**

73. **Oppenheimer, J.H., Schwartz, H.L., Mariash, C.N., Kinlaw, W.B., Wong, N.C.W., and Freake, H.C. 1987. Advances in our understanding of thyroid hormone action at the cellular level. *Endocrine Reviews* 8:288-308.**

74. **Hennemann, G., Docter, R., Friesema, E.C., de Jong, M., Krenning, E.P., and Visser, T.J. 2001. Plasma membrane transport of thyroid hormones and its role in thyroid hormone metabolism and bioavailability. *Endocr Rev* 22:451-476.**

75. **Friesema, E.C., Grueters, A., Biebermann, H., Krude, H., von Moers, A., Reeser, M., Barrett, T.G., Mancilla, E.E., Svensson, J., Kester, M.H., et al. 2004. Association between mutations in a thyroid hormone transporter and severe X-linked psychomotor retardation. *Lancet* 364:1435-1437.**

76. **Dumitrescu, A.M., Liao, X.H., Weiss, R.E., Millen, K., and Refetoff, S. 2006. Tissue-specific thyroid hormone deprivation and excess in monocarboxylate transporter (mct) 8-deficient mice. *Endocrinology* 147:4036-4043.**

77. **Trajkovic, M., Visser, T.J., Mittag, J., Horn, S., Lukas, J., Darras, V.M., Raivich, G., Bauer, K., and Heuer, H. 2007. Abnormal thyroid hormone metabolism in mice lacking the monocarboxylate transporter 8. *J Clin Invest* 117:627-635.**

78. **Bianco, A.C., and Silva, J.E. 1987. Intracellular conversion of thyroxine to triiodothyronine is required for the optimal thermogenic function of brown adipose tissue. *Journal of Clinical Investigation* 79:295-300.**

79. **Simonides, W.S., Mulcahey, M.A., Redout, E.M., Muller, A., Zuidwijk, M.J., Visser, T.J., Wassen, F.W., Crescenzi, A., da-Silva, W.S., Harney, J., et al. 2008. Hypoxia-inducible factor induces local thyroid hormone inactivation during hypoxic-ischemic disease in rats. *J Clin Invest* 118:975-983.**

80. **Brent, G.A. 1994. The molecular basis of thyroid hormone action. *The New England Journal of Medicine* 331:847-853.**

81. **Zhang, J., and Lazar, M.A. 2000. The mechanism of action of thyroid hormones. *Annual Review of Physiology* 62:439-466.**

82. **Kaplan, M.M., and Yaskoski, K.A. 1981. Maturational patterns of iodothyronine phenolic and tyrosyl ring deiodinase activities in rat cerebrum, cerebellum, and hypothalamus. *J Clin Invest* 67:1208-1214.**

83. **Galton, V.A. 2005. The roles of the iodothyronine deiodinases in mammalian development. *Thyroid* 15:823-834.**

84. **Hall, J.A., Ribich, S., Christoffolete, M.A., Simovic, G., Correa-Medina, M., Patti, M.E., and Bianco, A.C. 2010. Absence of thyroid hormone activation during development underlies a permanent defect in adaptive thermogenesis. *Endocrinology* 151:4573-4582.**

85. **Bianco, A.C., Maia, A.L., da Silva, W.S., and Christoffolete, M.A. 2005. Adaptive activation of thyroid hormone and energy expenditure. *Biosci Rep* 25:191-208.**
86. **Silva, J.E. 2006. Thermogenic mechanisms and their hormonal regulation. *Physiological Review* 86:435-464.**
87. **Lowell, B.B., and Spiegelman, B.M. 2000. Towards a molecular understanding of adaptive thermogenesis. *Nature* 404:652-660.**
88. **Feldmann, H.M., Golozoubova, V., Cannon, B., and Nedergaard, J. 2009. UCP1 ablation induces obesity and abolishes diet-induced thermogenesis in mice exempt from thermal stress by living at thermoneutrality. *Cell Metab* 9:203-209.**
89. **Cannon, B., and Nedergaard, J. 2011. Nonshivering thermogenesis and its adequate measurement in metabolic studies. *J Exp Biol* 214:242-253.**
90. **Bachman, E.S., Dhillon, H., Zhang, C.Y., Cinti, S., Bianco, A.C., Kobilka, B.K., and Lowell, B.B. 2002. betaAR signaling required for diet-induced thermogenesis and obesity resistance. *Science* 297:843-845.**
91. **Ueta, C.B., Fernandes, G.W., Capelo, L.P., Fonseca, T.L., Maculan, F.D., Gouveia, C.H., Brum, P.C., Christoffolete, M.A., Aoki, M.S., Lancellotti, C.L., et al. beta1 Adrenergic receptor is key to cold- and diet-induced thermogenesis in mice. *J Endocrinol* 214:359-365.**
92. **Heaton, G.M., Wagenvoord, R.J., Kemp, A., Jr., and Nicholls, D.G. 1978. Brown-adipose-tissue mitochondria: photoaffinity labelling of the regulatory site of energy dissipation. *Eur J Biochem* 82:515-521.**
93. **Ricquier, D., Lin, C., and Klingenberg, M. 1982. Isolation of the GDP binding protein from brown adipose tissue mitochondria of several animals and amino acid composition study in rat. *Biochem Biophys Res Commun* 106:582-589.**
94. **Enerback, S., Jacobsson, A., Simpson, E.M., Guerra, C., Yamashita, H., Harper, M.E., and Kozak, L.P. 1997. Mice lacking mitochondrial uncoupling protein are cold-sensitive but not obese. *Nature* 387:90-94.**
95. **de Jesus, L.A., Carvalho, S.D., Ribeiro, M.O., Schneider, M., Kim, S.W., Harney, J.W., Larsen, P.R., and Bianco, A.C. 2001. The type 2 iodothyronine deiodinase is essential for adaptive thermogenesis in brown adipose tissue. *J Clin Invest* 108:1379-1385.**
96. **Bianco, A.C., Sheng, X.Y., and Silva, J.E. 1988. Triiodothyronine amplifies norepinephrine stimulation of uncoupling protein gene transcription by a mechanism not requiring protein synthesis. *J Biol Chem* 263:18168-18175.**
97. **Christoffolete, M.A., Linardi, C.C., de Jesus, L., Ebina, K.N., Carvalho, S.D., Ribeiro, M.O., Rabelo, R., Curcio, C., Martins, L., Kimura, E.T., et al. 2004. Mice with targeted disruption of the Dio2 gene have cold-induced overexpression of the uncoupling protein 1 gene but fail to increase brown adipose tissue lipogenesis and adaptive thermogenesis. *Diabetes* 53:577-584.**
98. **Rubio, A., Raasmaja, A., and Silva, J.E. 1995. Thyroid hormone and norepinephrine signaling in brown adipose tissue. II: Differential effects of thyroid hormone on beta 3-adrenergic receptors in brown and white adipose tissue. *Endocrinology* 136:3277-3284.**
99. **Rubio, A., Raasmaja, A., Maia, A.L., Kim, K.R., and Silva, J.E. 1995. Effects of thyroid hormone on norepinephrine signaling in brown adipose tissue. I. Beta 1-**

and beta 2-adrenergic receptors and cyclic adenosine 3',5'-monophosphate generation. *Endocrinology* 136:3267-3276.

100. Carvalho, S.D., Bianco, A.C., and Silva, J.E. 1996. Effects of hypothyroidism on brown adipose tissue adenylyl cyclase activity. *Endocrinology* 137:5519-5529.

101. Sellers, E.A., and You, S.S. 1950. Role of the thyroid in metabolic responses to a cold environment. *The American Journal of Physiology* 163:81-91.

102. Golozoubova, V., Hohtola, E., Matthias, A., Jacobsson, A., Cannon, B., and Nedergaard, J. 2001. Only UCP1 can mediate adaptive nonshivering thermogenesis in the cold. *Faseb J* 15:2048-2050.

103. Ueta, C.B., Olivares, E.L., and Bianco, A.C. Responsiveness to thyroid hormone and to ambient temperature underlies differences between brown adipose tissue and skeletal muscle thermogenesis in a mouse model of diet-induced obesity. *Endocrinology* 152:3571-3581.

104. Virtanen, K.A., Lidell, M.E., Orava, J., Heglind, M., Westergren, R., Niemi, T., Taittonen, M., Laine, J., Savisto, N.J., Enerback, S., et al. 2009. Functional brown adipose tissue in healthy adults. *N Engl J Med* 360:1518-1525.

105. Young, J.B., Saville, E., Rothwell, N.J., Stock, M.J., and Landsberg, L. 1982. Effect of diet and cold exposure on norepinephrine turnover in brown adipose tissue of the rat. *Journal of Clinical Investigation* 69:1061-1071.

106. Wolf, M., Weigert, A., and Kreymann, G. 1996. Body composition and energy expenditure in thyroidectomized patients during short-term hypothyroidism and thyrotropin-suppressive thyroxine therapy. *Eur J Endocrinol* 134:168-173.

107. Lonn, L., Stenlof, K., Ottosson, M., Lindroos, A.K., Nystrom, E., and Sjostrom, L. 1998. Body weight and body composition changes after treatment of hyperthyroidism. *J Clin Endocrinol Metab* 83:4269-4273.

108. Kyle, L.H., Ball, M.F., and Doolan, P.D. 1966. Effect of thyroid hormone on body composition in myxedema and obesity. *N Engl J Med* 275:12-17.

109. Curcio, C., Lopes, A.M., Ribeiro, M.O., Francoso, O.A., Jr., Carvalho, S.D., Lima, F.B., Bicudo, J.E., and Bianco, A.C. 1999. Development of compensatory thermogenesis in response to overfeeding in hypothyroid rats. *Endocrinology* 140:3438-3443.

110. Castillo, M., Hall, J.A., Correa-Medina, M., Ueta, C., Kang, H.W., Cohen, D.E., and Bianco, A.C. 2011. Disruption of thyroid hormone activation in type 2 deiodinase knockout mice causes obesity with glucose intolerance and liver steatosis only at thermoneutrality. *Diabetes* 60:1082-1089.

111. Klein, I. 1990. Thyroid hormone and the cardiovascular system. *Am J Med* 88:631-637.

112. Dillmann, W.H. 1990. Biochemical basis of thyroid hormone action in the heart. *Am J Med* 88:626-630.

113. Polikar, R., Burger, A.G., Scherrer, U., and Nicod, P. 1993. The thyroid and the heart. *Circulation* 87:1435-1441.

114. Park, K.W., Dai, H.B., Ojamaa, K., Lowenstein, E., Klein, I., and Sellke, F.W. 1997. The direct vasomotor effect of thyroid hormones on rat skeletal muscle resistance arteries. *Anesth Analg* 85:734-738.

115. Ojamaa, K., Klemperer, J.D., and Klein, I. 1996. Acute effects of thyroid hormone on vascular smooth muscle. *Thyroid* 6:505-512.

116. Resnick, L.M., and Laragh, J.H. 1982. PLasma renin activity in syndromes of thyroid hormone excess and deficiency. *Life Sci* 30:585-586.
117. Ojamaa, K., Klemperer, J.D., MacGilvray, S.S., Klein, I., and Samarel, A. 1996. Thyroid hormone and hemodynamic regulation of beta-myosin heavy chain promoter in the heart. *Endocrinology* 137:802-808.
118. Morkin, E. 1993. Regulation of myosin heavy chain genes in the heart. *Circulation* 87:1451-1460.
119. Magner, J.A., Clark, W., and Allenby, P. 1988. Congestive heart failure and sudden death in a young woman with thyrotoxicosis. *West J Med* 149:86-91.
120. Ladenson, P.W., Sherman, S.I., Baughman, K.L., Ray, P.E., and Feldman, A.M. 1992. Reversible alterations in myocardial gene expression in a young man with dilated cardiomyopathy and hypothyroidism. *Proc Natl Acad Sci U S A* 89:5251-5255.
121. Dillmann, W.H. 1990. Biochemical basis of thyroid hormone action in the heart. *The American Journal of Medicine* 88:626-630.
122. Kiss, E., Jakab, G., Kranias, E.G., and Edes, I. 1994. Thyroid hormone-induced alterations in phospholamban protein expression. Regulatory effects on sarcoplasmic reticulum Ca2+ transport and myocardial relaxation. *Circ Res* 75:245-251.
123. Carvalho-Bianco, S.D., Kim, B.W., Zhang, J.X., Harney, J.W., Ribeiro, R.S., Gereben, B., Bianco, A.C., Mende, U., and Larsen, P.R. 2004. Chronic cardiac-specific thyrotoxicosis increases myocardial beta-adrenergic responsiveness. *Molecular Endocrinology* 18:1840-1849.
124. Trivieri, M.G., Oudit, G.Y., Sah, R., Kerfant, B.G., Sun, H., Gramolini, A.O., Pan, Y., Wickenden, A.D., Croteau, W., Morreale de Escobar, G., et al. 2006. Cardiac-specific elevations in thyroid hormone enhance contractility and prevent pressure overload-induced cardiac dysfunction. *Proc Natl Acad Sci U S A* 103:6043-6048.
125. Wassen, F.W., Schiel, A.E., Kuiper, G.G., Kaptein, E., Bakker, O., Visser, T.J., and Simonides, W.S. 2002. Induction of thyroid hormone-degrading deiodinase in cardiac hypertrophy and failure. *Endocrinology* 143:2812-2815.
126. Olivares, E.L., Marassi, M.P., Fortunato, R.S., da Silva, A.C., Costa-e-Sousa, R.H., Araujo, I.G., Mattos, E.C., Masuda, M.O., Mulcahey, M.A., Huang, S.A., et al. 2007. Thyroid function disturbance and type 3 iodothyronine deiodinase induction after myocardial infarction in rats a time course study. *Endocrinology* 148:4786-4792.
127. Pol, C.J., Muller, A., Zuidwijk, M.J., van Deel, E.D., Kaptein, E., Saba, A., Marchini, M., Zucchi, R., Visser, T.J., Paulus, W.J., et al. 2011. Left-ventricular remodeling after myocardial infarction is associated with a cardiomyocyte-specific hypothyroid condition. *Endocrinology* 152:669-679.

Errata

Nos materiais e métodos do artigo **“Responsiveness to thyroid hormone and to ambient temperature underlies differences between brown adipose tissue and skeletal muscle thermogenesis in a mouse model of diet-induced obesity”**, foram expressas as porcentagens em calorias de: proteína (15,2%); carboidratos (42,8%) e gordura (42%) contidas na dieta hipercalórica em calorias. As porcentagens dos mesmos expressas por grama de dieta são: proteína (17,3%); carboidratos (48,6%) e gordura (21,2%).